TEL AVIV UNIVERSITY
Pursuing the Unknown

Dynamics in solid-state NMR via Recoupling of Anisotropic Interactions

Amir Goldbourt
School of Chemistry, Tel Aviv University

NMR meets biology
Gokarna, Karnataka, India

@GoldNMR lab

Last update 27-Jan-26

amirgo@tauex.tau.ac.il

Overview

- Hamiltonians in solid state NMR
- Static and MAS
- CSA recoupling methods
- Dipolar recoupling methods
- 2H quadrupolar lineshapes
- CODEX
- Relaxation - T1ρ, T1, T2 – consider coherent effects, MAS effects
- Chemical exchange (lithium motion in batteries, cations in inorganic materials …)
- Summary

General form of the **MR** Hamiltonian

$$H = \sum_{\lambda} H_{\lambda}\,; \qquad H_{\lambda \in Ze,Zn,cs,Q,ZFS} = \sum_{j} H_{\lambda_j}\,; \qquad H_{\lambda \in J,D,A} = \sum_{j}\sum_{i<j} H_{\lambda_{i,j}}$$

$$H = H_{Ze} + H_{ZFS} + H_A + H_{Zn} + H_J + H_{cs} + H_D + H_Q + H_{MW} + H_{RF}$$

Electron spin

H_{Ze}: *Electron Zeeman Hamiltonian ↔ electron spins with magnetic field (This includes spin-orbit coupling).*

H_{ZFS}: *Zero Field Splitting ↔ electron spin – electron spin (Fine structure in the EPR spectra)*

H_A: *Hyperfine Interaction ↔ electron spin – nuclear spin (Hyperfine structure in EPR spectra)*

H_{Je}: *J*

H_{De}:

H_{Zn}

Internal NMR Hamiltonian

H_J: *S*

H_{cs} : *Chemical shift Hamiltonian ↔ spins shielded by electrons ↔ ~kHz, isotropic(solution & solids) + anisotropic (solids)*

H_D : *Dipolar coupling Hamiltonian ↔ spin-spin via space ↔ ~kHz, anisotropic, solids*

H_Q : *Quadrupolar coupling Hamiltonian ↔ spins>1/2 with electric field gradients ↔ ~MHz, anisotropic, solids*

H_{MW} : *Microwave Frequency field ↔ electron spins with external AC magnetic field irradiation (typically in microwave and mm-waves (GHz))*

H_{RF} : *Radio Frequency field ↔ External magnetic field irradiation* ↔ $H_1 = \omega_1 I_x \cos(\omega_{rf} t)$

H_{cs} : ↔ *~kHz, isotropic(solution & solids) + anisotropic (solids)*

H_D ↔ *~kHz, anisotropic, solids*

H_Q ↔ *~MHz, anisotropic, solids*

Interactions as tensors

- The two types of interactions are spin ↔ spin and spin ↔ magnetic field
- Both can be represented by the following expressions in matrix form:

$$C_\lambda \begin{pmatrix} I_x & I_y & I_z \end{pmatrix} \begin{pmatrix} A_{xx} & A_{xy} & A_{xz} \\ A_{yx} & A_{yy} & A_{yz} \\ A_{zx} & A_{zy} & A_{zz} \end{pmatrix} \begin{pmatrix} K_x \\ K_y \\ K_z \end{pmatrix} = C_\lambda \vec{I} \cdot \hat{A} \cdot \vec{K}$$

- C_λ is a constant that represents the size of the interaction
- $\vec{I}$ is a vector of the three spin components
- $\hat{A}$ is the interaction tensor in a general frame of reference
- $\vec{K}$ is the magnetic field ($\vec{B}$), or a spin $\hat{S}$ (with similar or different γ).

Every tensor can be expressed in its Principal Axis System: $\hat{A}^{PAS} = R^{-1}\hat{A}R = \begin{pmatrix} A_{xx}^{PAS} & 0 & 0 \\ 0 & A_{yy}^{PAS} & 0 \\ 0 & 0 & A_{zz}^{PAS} \end{pmatrix}$

R is the diagonalization (rotation) matrix

(anti-symmetric elements off-diagonal can be ignored)

Interactions as tensors – principal axis system

$$\hat{A}^{PAS} = \begin{pmatrix} A_{xx}^{PAS} & 0 & 0 \\ 0 & A_{yy}^{PAS} & 0 \\ 0 & 0 & A_{zz}^{PAS} \end{pmatrix}$$

Tensors can be decomposed to
trace A_{iso}, anisotropy Δ_A, and asymmetry η_A.

Trace: $A_{iso} = \frac{1}{3}(A_{xx}^{PAS} + A_{yy}^{PAS} + A_{zz}^{PAS})$

Anisotropy: $\Delta_A = A_{aniso} = A_{zz}^{PAS} - A_{iso}$

Asymmetry: $\eta_A = (A_{yy}^{PAS} - A_{xx}^{PAS})/A_{aniso}$

Haeberlen convention

$$|A_{xx}^{PAS} - \sigma_{iso}| \leq |A_{yy}^{PAS} - \sigma_{iso}| \leq |A_{zz}^{PAS} - \sigma_{iso}|$$

$$\hat{A}^{PAS} = A_{iso}\begin{pmatrix} 1 & 0 & 0 \\ 0 & 1 & 0 \\ 0 & 0 & 1 \end{pmatrix} + \Delta_A \begin{pmatrix} -\frac{1}{2}(1+\eta_A) & 0 & 0 \\ 0 & -\frac{1}{2}(1-\eta_A) & 0 \\ 0 & 0 & 1 \end{pmatrix}$$

Chemical shift Hamiltonian – shielding tensor

- Chemical shielding results from induced magnetic fields.
- The interaction is between the spin I, the shielding tensor σ, and magnetic field B=(0,0,B_0)

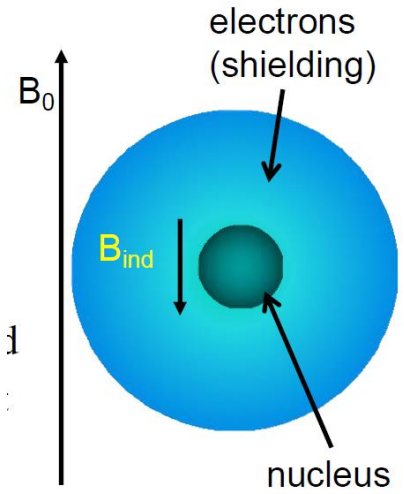

Image taken from the lecture notes of Konstantin Ivanov, 4th "NMR meets biology" meeting, Khajuraho, 2018

In the laboratory frame, the Shielding Hamiltonian is given by

$$H_\sigma = \gamma(I_x \quad I_y \quad I_z)\begin{pmatrix}\sigma_{xx}^L & \sigma_{xy}^L & \sigma_{xz}^L\\ \sigma_{yx}^L & \sigma_{yy}^L & \sigma_{yz}^L\\ \sigma_{zx}^L & \sigma_{zy}^L & \sigma_{zz}^L\end{pmatrix}\begin{pmatrix}0\\0\\B_0\end{pmatrix} = \gamma\vec{I}\cdot\hat{\sigma}^L\cdot\vec{B}$$

The chemical shielding tensor can also be expressed in its **Principal Axis System** (fixed in the molecule):

$$\hat{\sigma}^{PAS} = \begin{pmatrix}\sigma_{xx}^{PAS} & 0 & 0\\ 0 & \sigma_{yy}^{PAS} & 0\\ 0 & 0 & \sigma_{zz}^{PAS}\end{pmatrix} = R^{-1}\hat{\sigma}^L R$$

- R transforms from the LAB frame to the PAS frame

Chemical shielding tensor - definitions

The chemical shielding tensor can be expressed by the three principal components $\sigma_{xx}^{PAS}, \sigma_{yy}^{PAS}, \sigma_{zz}^{PAS}$

or

By its trace, anisotropy, and asymmetry:

Trace: $\sigma_{iso} = \frac{1}{3}(\sigma_{xx}^{PAS} + \sigma_{yy}^{PAS} + \sigma_{zz}^{PAS})$

Anisotropy: $\sigma_{aniso} = \sigma_{zz}^{PAS} - \sigma_{iso}$

Asymmetry: $\eta_\sigma = (\sigma_{yy}^{PAS} - \sigma_{xx}^{PAS})/\sigma_{aniso}$

Haeberlen convention

$$|\sigma_{xx}^{PAS} - \sigma_{iso}| \leq |\sigma_{yy}^{PAS} - \sigma_{iso}| \leq |\sigma_{zz}^{PAS} - \sigma_{iso}|$$

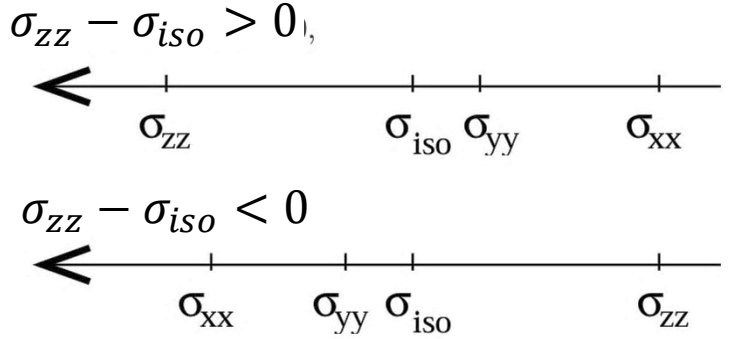

https://groups.chem.ubc.ca/straus/l2.pdf

The tensor can be described in its PAS as follows:

$$\hat{\sigma}^{PAS} = \sigma_{iso}\begin{pmatrix}1 & 0 & 0\\ 0 & 1 & 0\\ 0 & 0 & 1\end{pmatrix} + \sigma_{aniso}\begin{pmatrix}-\frac{1}{2}(1+\eta_\sigma) & 0 & 0\\ 0 & -\frac{1}{2}(1-\eta_\sigma) & 0\\ 0 & 0 & 1\end{pmatrix}$$

CS can be positive or negative

NMR Chemical shielding – Back to lab frame

- The two angles relating B to σ are θ (polar) and ϕ (azimuthal)
- The magnetic field has no preference to x or y

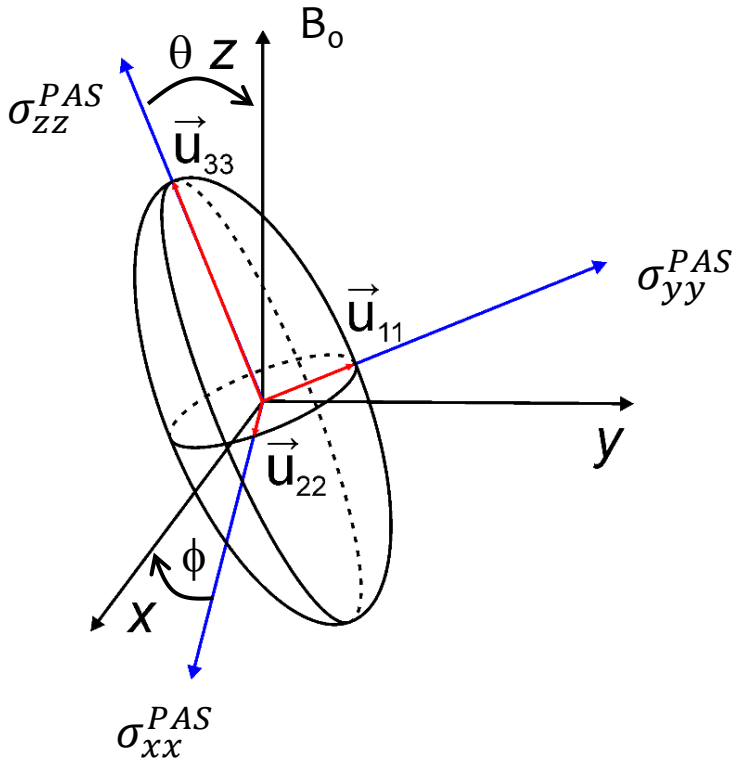

- Rotate around the z axis at angle ϕ
- Rotate around x axis at angle θ
- The result is three angluar-dependent terms, σ_{xz}^{LAB}, σ_{yz}^{LAB}, σ_{zz}^{LAB}

Using perturbation theory, or averaging over the Larmor Frequency, it can be shown that only σ_{zz}^{LAB} term is important ('Zeeman truncation' or 'Secular approximation')

$$\overline{H_{cs}^{(0)}} = \gamma\vec{I}\cdot\hat{\sigma}^{L}\cdot\vec{B} = \gamma(0,0,I_z)\cdot\hat{\sigma}^{L}\cdot\begin{pmatrix}0\\0\\B_0\end{pmatrix} = \gamma I_z\sigma_{zz}^{lab}B_0 = -\omega_0\sigma_{zz}^{lab}I_z$$

Chemical shielding Hamiltonian: lab frame

$$\hat{\sigma}^{PAS} = \begin{pmatrix} \sigma_{xx}^{PAS} & 0 & 0 \\ 0 & \sigma_{yy}^{PAS} & 0 \\ 0 & 0 & \sigma_{zz}^{PAS} \end{pmatrix} = R^{-1}\hat{\sigma}^{L}R$$

$$\hat{\sigma}^{Lab} = R\hat{\sigma}^{PAS}R^{-1}$$

$$\hat{\sigma}_{zz}^{Lab} = (0,0,1)\hat{\sigma}^{Lab}\begin{pmatrix}0\\0\\1\end{pmatrix} = (0,0,1)R\hat{\sigma}^{PAS}R^{-1}\begin{pmatrix}0\\0\\1\end{pmatrix}$$

$$= (sin\theta cos\phi, sin\theta sin\phi, cos\theta)\hat{\sigma}^{PAS}(sin\theta cos\phi, sin\theta sin\phi, cos\theta)^{\mathrm{T}}$$

$$= \sigma_{iso} - \sigma_{xx}^{PAS}\sin^2\theta\cos^2\phi + \sigma_{yy}^{PAS}\sin^2\theta\sin^2\phi + \sigma_{zz}^{PAS}\cos^2\theta$$

This can be expressed with the assymetry and anisotropy as follows:

$$\hat{\boldsymbol{\sigma}}_{\boldsymbol{zz}}^{\boldsymbol{Lab}}(\boldsymbol{\theta},\boldsymbol{\phi}) = \boldsymbol{\sigma_{iso}} + \frac{\mathbf{1}}{\mathbf{2}}\boldsymbol{\sigma_{aniso}}\{\mathbf{3}\cos^2\boldsymbol{\theta} - \mathbf{1} + \boldsymbol{\eta}\boldsymbol{sin}^2\boldsymbol{\theta}\,\boldsymbol{cos2\phi}\}$$

$$\boldsymbol{H_{cs}} = \boldsymbol{\gamma}\hat{\boldsymbol{\sigma}}_{\boldsymbol{zz}}^{\boldsymbol{Lab}}(\boldsymbol{\theta},\boldsymbol{\phi})\boldsymbol{B_0 I_z} = -\boldsymbol{\omega_0}\hat{\boldsymbol{\sigma}}_{\boldsymbol{zz}}^{\boldsymbol{Lab}}(\boldsymbol{\theta},\boldsymbol{\phi})\boldsymbol{I_z}$$

Shielding: Small reduction of Larmor frequency

Shielding lineshapes and molecular symmetry

$\sigma_{zz}=\sigma_{xx}=\sigma_{yy} \cong 0$

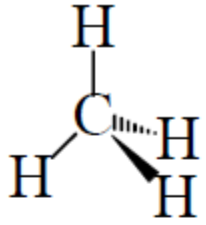

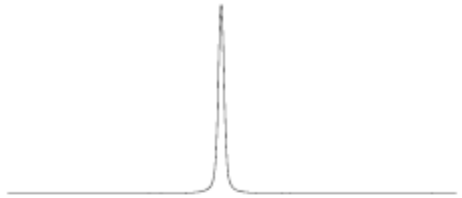

Spherical symmetry: shielding is similar in all directions, very small CSA.

$\delta \approx 0$

$\sigma_{xx} \neq \sigma_{yy}$

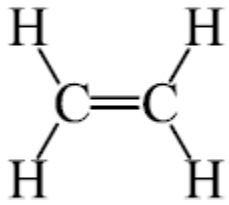

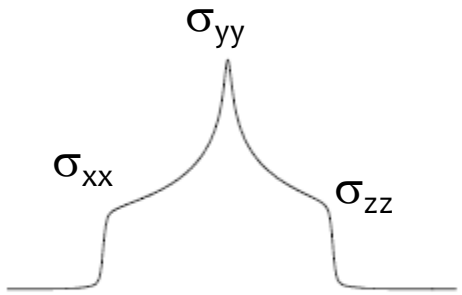

Non-axial symmetry: Shielding is different in three directions

$\eta = 1$

$\sigma_{xx}=\sigma_{yy}$

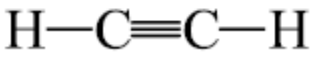

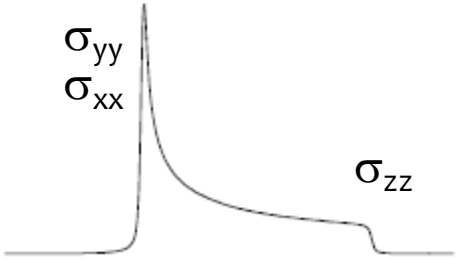

Axial symmetry: molecule is // to $\mathbf{B}_0$ maximum shielding; when molecule is $\perp$ to $\mathbf{B}_0$ maximum deshielding

$\eta = 0$

See also Schurko's lectures:
https://www.emory.edu/NMR/web_swu/SSNMR_redor/ssnmr_schurko

Chemical shift anisotropy (CSA)

Define the tensor using the ppm scale $\boldsymbol{\delta = (\sigma_{ref} - \sigma) \cdot 10^6}$

$$\hat{\delta}^{PAS} = \begin{pmatrix} \delta_{33}^{PAS} & 0 & 0 \\ 0 & \delta_{22}^{PAS} & 0 \\ 0 & 0 & \delta_{11}^{PAS} \end{pmatrix}$$

$$\boldsymbol{H_{cs} = H_{iso} + H_{CSA}}$$
$$\boldsymbol{= \delta_{iso} I_z + \frac{1}{2} \delta_{aniso} \{3 \cos^2 \theta - 1 + \eta sin^2 \theta \, cos2\phi\}}$$

Chemical shift conventions

Standard Convention

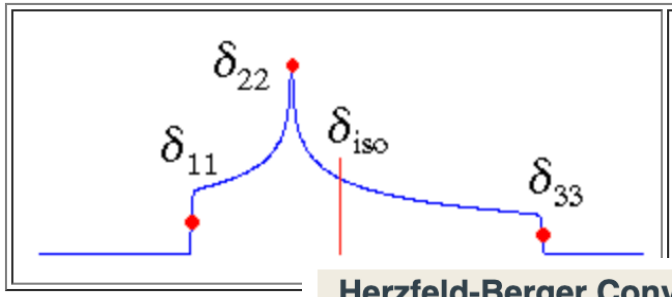

Principal Components:	$\delta_{11} \geq \delta_{22} \geq \delta_{33}$
Isotropic Value:	$\delta_{iso} = (\delta_{11}+\delta_{22}+\delta_{33})/3$

Herzfeld-Berger Convention

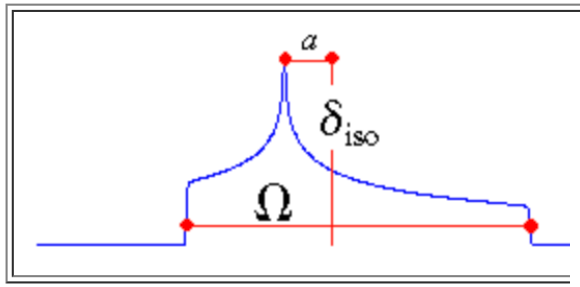

Isotropic Value:	$\delta_{iso} = (\delta_{11}+\delta_{22}+\delta_{33})/3$
Span:	$\Omega \approx \delta_{11}-\delta_{33}$ $(\Omega \geq 0)$
Skew:	$\kappa = 3(\delta_{22}-\delta_{iso})/\Omega$; $(-1 \leq \kappa \leq +1)$

Haeberlen Convention

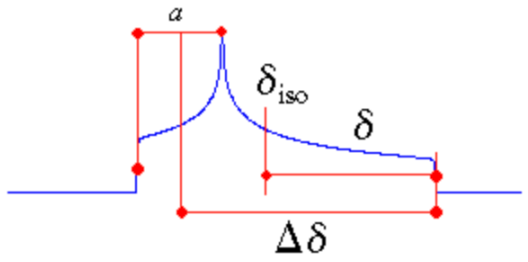

Principal Components:	$\lvert\delta_{zz}-\delta_{iso}\rvert \geq \lvert\delta_{xx}-\delta_{iso}\rvert \geq \lvert\delta_{yy}-\delta_{iso}\rvert$
Isotropic Value:	$\delta_{iso} = (\delta_{11}+\delta_{22}+\delta_{33})/3$
Reduced Anisotropy:	$\delta = \delta_{zz}-\delta_{iso}$
Anisotropy:	$\Delta\delta = \delta_{zz}-(\delta_{xx}+\delta_{yy})/2 = 3\delta/2$
Asymmetry:	$\eta = (\delta_{yy}-\delta_{xx})/\delta$; $(0 \leq \eta \leq +1)$

http://anorganik.uni-tuebingen.de/klaus/nmr/index.php?p=conventions/csa/csa

The values at the discontinuities of the CSA tensor static powder lineshape

$\delta_{aniso}=\delta_{33}-\delta_{iso}=-20$ ppm
$\eta=0.7$
$\delta_{iso}=0$ ppm

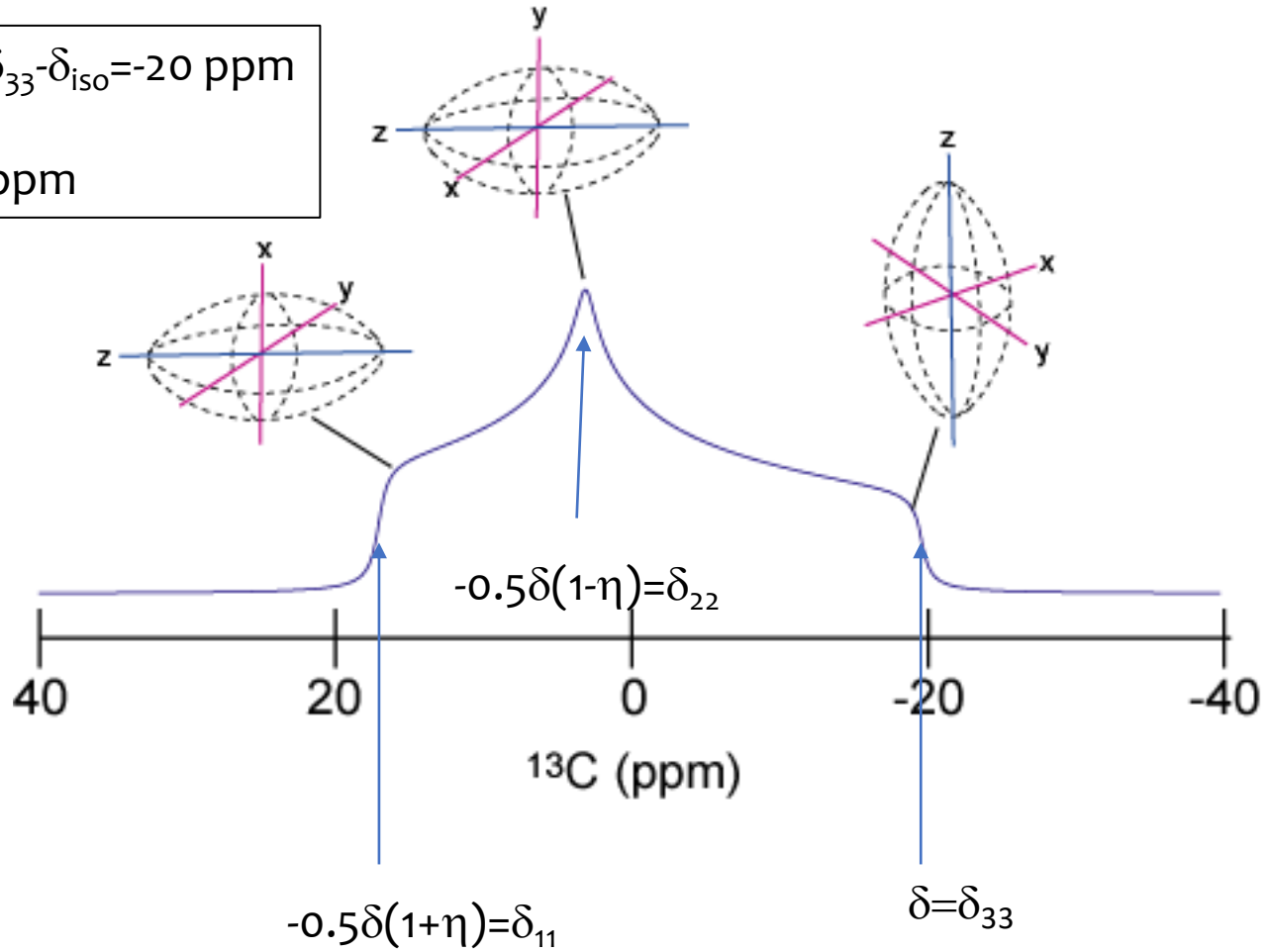

$$\hat{\delta}^{PAS} = \delta_{iso}\begin{pmatrix}1 & 0 & 0\\ 0 & 1 & 0\\ 0 & 0 & 1\end{pmatrix}$$

$$+\delta_{aniso}\begin{pmatrix}-\frac{1}{2}(1+\eta_\sigma) & 0 & 0\\ 0 & -\frac{1}{2}(1-\eta_\sigma) & 0\\ 0 & 0 & 1\end{pmatrix}$$

Discovery of chemical shifts 1950, ^{19}F & ^{14}N NMR!

(1.05T, 45 MHz ^{1}H)

Dependence of the F^{19} Nuclear Resonance Position on Chemical Compound*

W. C. Dickinson
Research Laboratory of Electronics, Massachusetts Institute of Technology, Cambridge, Massachusetts
January 9, 1950

MOST unexpectedly, it has been found that for F^{19} the value of the applied magnetic field H_0 for nuclear magnetic resonance at a fixed radiofrequency depends on the chemical compound containing the fluorine nucleus. The assumption has

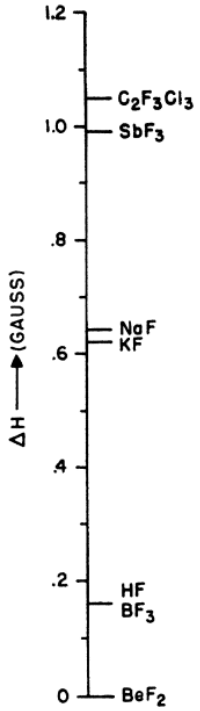

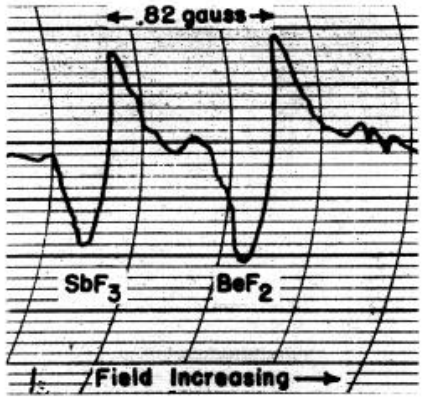

FIG. 2. The nuclear resonances of F^{19} in a single sample containing a half and half mixture of SbF_3 and BeF_2 (saturated aqueous solutions). The applied resonance magnetic field is about 7000 gauss at a radiofrequency of 28.0 megacycles.

Phys. Rev. 77, p736 (Jan 9)

The Dependence of a Nuclear Magnetic Resonance Frequency upon Chemical Compound*

W. G. Proctor and F. C. Yu
Department of Physics, Stanford University, Stanford, California
January 18, 1950

IN the course of measurements on N^{14}, mentioned in the previous letter, we made the surprising observation that its frequency of resonance, in liquid samples, depended strongly upon the chemical compound in which it was contained.[1,2] This effect is strikingly demonstrated by the appearance of two resonances, separated by 1.6 kc in the neighborhood of 3300 kc, corresponding to a field of 10,500 gauss, using a solution of NH_4NO_3 in 2.0-molar $MnSO_4$ as a sample. These resonances presumably arise from the NH_4^+ and NO_3^- complexes, since samples of $NH_4C_2H_3O_2$ and HNO_3 separately give rise to two different resonances whose frequencies approximate those from the above sample. The separation is four times greater than the line widths measured between points of maximum slope.

We have observed, within a resolution of 0.1 kc, that the N^{14} resonances from the ion NH_4^+ from the compounds NH_4NO_3, $NH_4C_2H_3O_2$, and MH_4Cl coincide at one frequency, while those from the ion NO_3^- from the compounds NH_4NO_3, HNO_3, and $Cu(NO_3)_2$ coincide at another frequency. Measuring the N^{14} resonances from other molecules relative to that arising from the ion NO_3^- from HNO_3 or NH_4NO_3, we have obtained the results given in Table I. All such frequency shifts have been in the direction of lower frequency.

The separations of resonances from four pairs of compounds were also measured at 6700 gauss, corresponding to a frequency of 2100 kc, to determine whether or not the frequency separations were independent of the field intensity. They are apparently proportional to it, for the ratios of the separations are in agreement with the ratio 6700/10,500=0.64, within our experimental resolution. (See Table II.)

We further made the observation that the separation of the two resonances arising from NH_4NO_3 was dependent on the concentration of the paramagnetic salt $MnCl_2$ added to it. A 7.5-molar solution of this salt without $MnCl_2$ shows two resonances separated by 1.0 kc, as given in Table I, but with 1.0- and 2.0-molar concentrations of $MnCl_2$ the separations become 1.4 kc and 1.6 kc, respectively.

We shall continue to investigate this phenomenon because of its direct significance for the interpretation of nuclear magnetic resonance frequencies in terms of nuclear moments, as well as to obtain an insight into its origin. With the largest observed line shift amounting to about 5 parts in 10^4, this effect is almost twice as large as the total diamagnetic correction calculated for the atom. These calculations, however, do not hold for the polyatomic molecules which we have studied and appreciable modification of the diamagnetism, as well as terms due to induced paramagnetism (high frequency matrix elements) can be expected, particularly in cases where three out of seven electrons may be strongly influenced by the chemical bond. The fact that the shifts are of the same order of magnitude as the diamagnetic correction and exhibit likewise proportionality to the applied field suggests a similar origin, although we have not been able to explain satisfactorily the observed magnitude of the effect. Until it is clearly understood, the accuracy of magnetic moments determined under certain chemical conditions remains somewhat in doubt.

We should like to express our appreciation to Professor Felix Bloch for stimulating discussions about this work.

* Assisted by the Joint Program of the AEC and the ONR.
[1] W. C. Dickinson, at M. I. T., has also observed similar shifts for F^{19} in different compounds. We are grateful to Professor F. Bitter for communicating this information to us.
[2] W. D. Knight, Phys. Rev. **76**, 1259 (1949), has observed a large frequency difference between the nuclear magnetic resonance frequency of a metal and its salt. The satisfactory explanation which he has given for this difference does not apply, however, to our case.

TABLE I. Frequency shifts relative to the resonance from the ion NO_3^- at 10,500 gauss.

Compound observed	Frequency shift (kc)
NH_4^+ from NH_4NO_3, $NH_4C_2H_3O_2$, NH_4Cl	−1.0
Liquid NH_3, containing 0.6-molar $Cr(NO_3)_3$; NH_4OH	−1.2
$(NH_2)_2CO$	−1.0
KCN	−0.2

TABLE II. Resonance frequency separations with different compounds and field intensities.

Compounds compared	Separation (kc) at 10,500 gauss	Separation (kc) at 6700 gauss	Ratio
NH_4^+ and NO_3^- from 7.5-molar NH_4NO_3 in 2.0-molar $MnSO_4$	1.6	0.9	0.58
HNO_3 and $NH_4C_2H_3O_2$	1.0	0.7	0.70
HNO_3 and $(NH_2)_2CO$	1.0	0.6	0.60
NH_3, containing 0.6-molar $Cr(NO_3)_3$ and NO_3^-, from NH_4NO_3	1.2	0.7	0.58

Phys. Rev. 77, p717 (Jan 18)

Chemical shift vs. off-resonance

Off-resonance

$2\pi\Delta\nu = \Delta\omega$

Determined by the irradiation frequency ω_{rf}

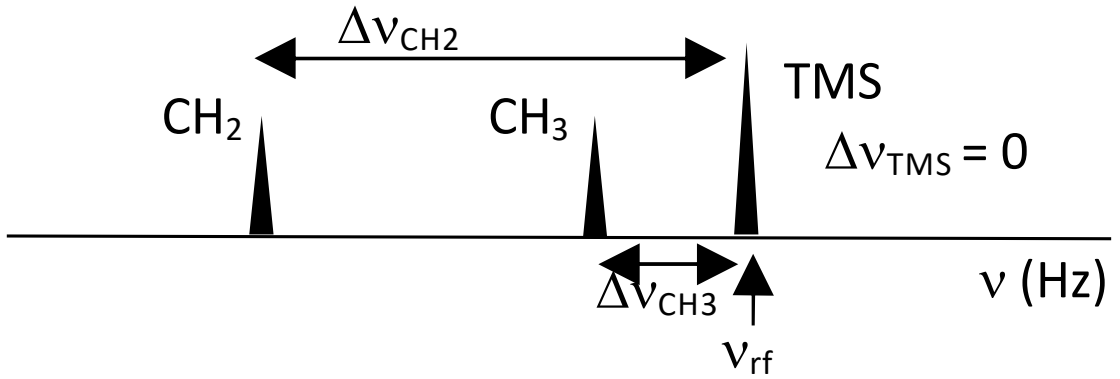

Chemical shift

$\delta = \omega_{ref} - \omega$

Determined by reference compound, indepdent of ω_{rf}

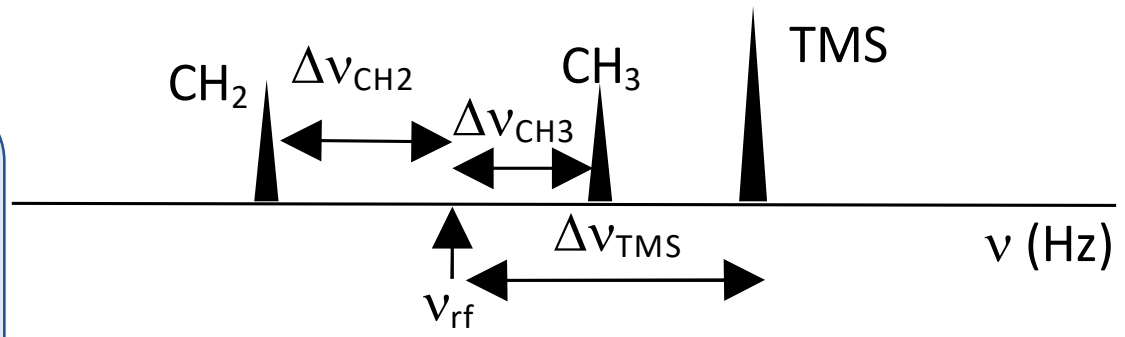

Same chemical shift value δ_x, different off-resonance values $\Delta\omega_x$

In the rotating frame, $\mathbf{H_z + H_{cs}} = \boldsymbol{\Delta\omega I_z} - \frac{1}{2}\boldsymbol{\omega_0\sigma_{aniso}}\{\mathbf{3\cos^2\theta - 1 + \eta sin^2\theta\, cos2\phi}\}\boldsymbol{I_z}$

Dynamics

Averaged CSA lineshapes

Physical rotation of a single crystal

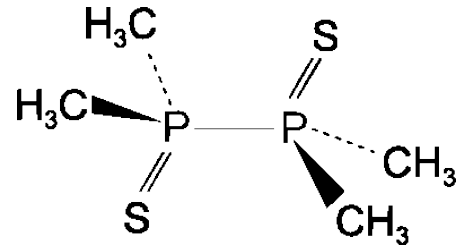

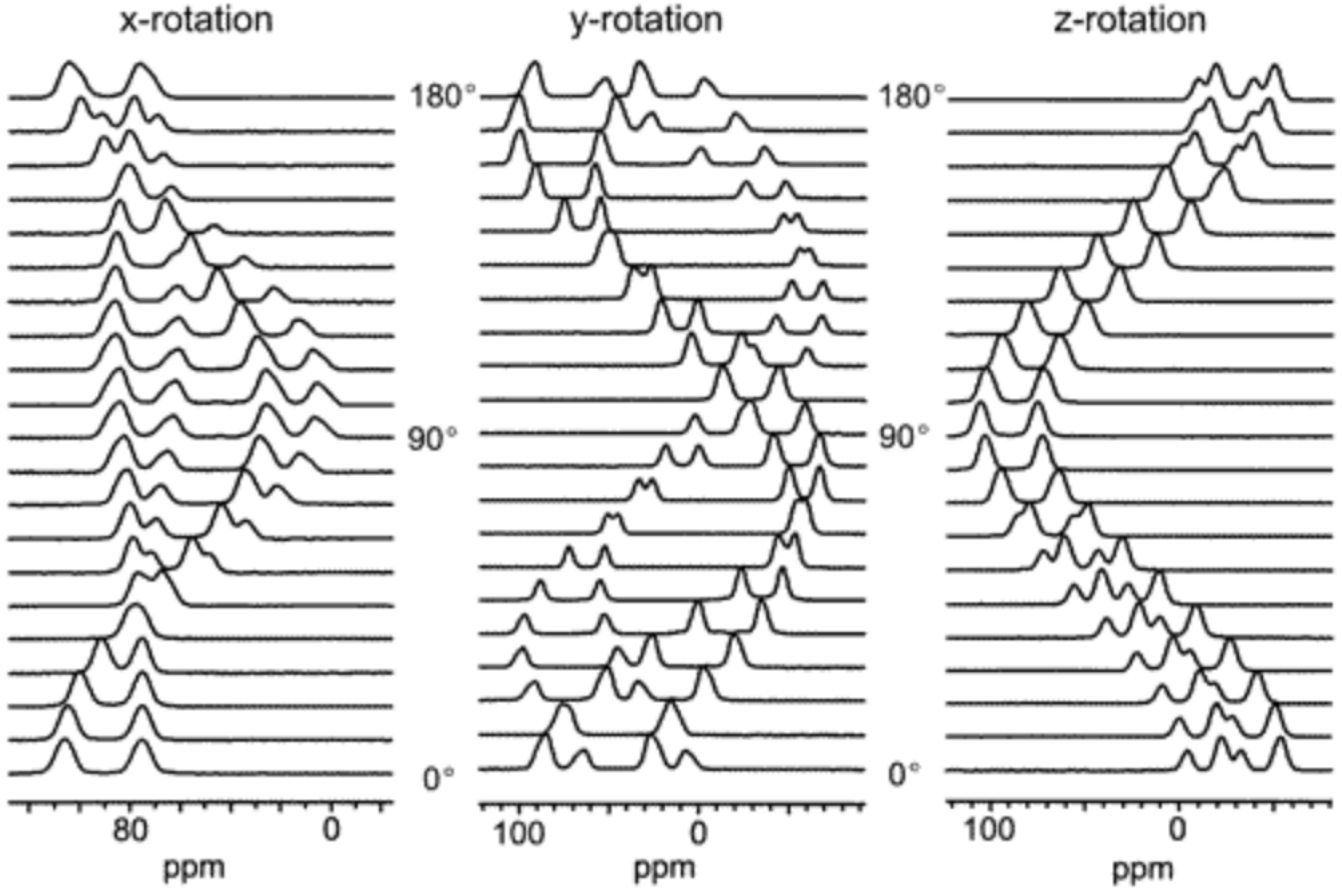

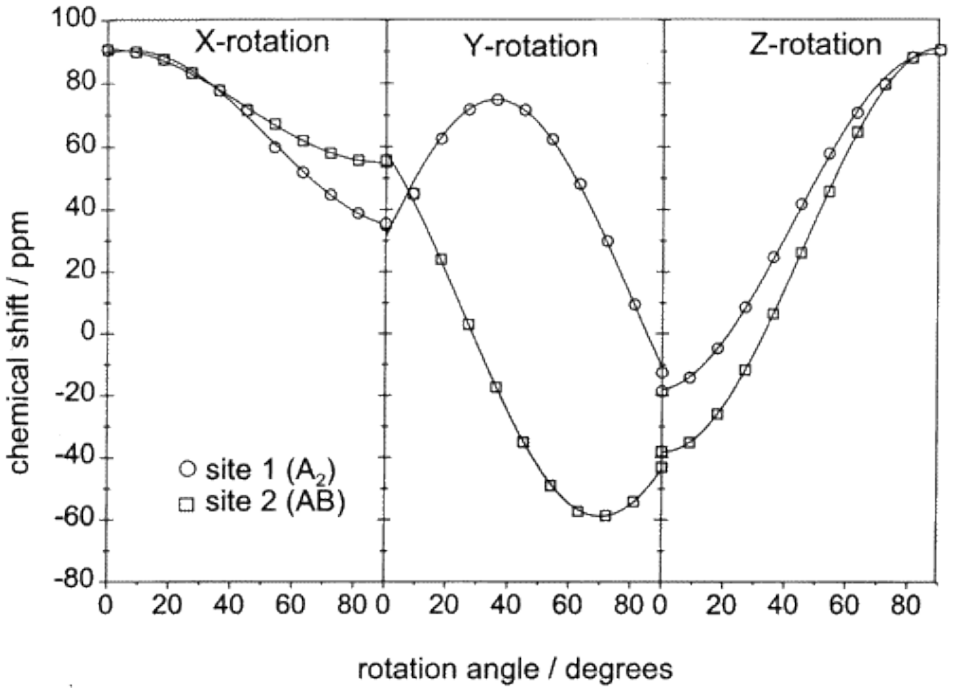

Phosphorus-31 CP NMR spectra of a single crystal of TMPS for rotations of the crystal holder about its *X*, *Y*, and *Z* axes, acquired at 4.7 T.

J. Phys. Chem. A 2000, 104, 19, 4598–4605
https://doi.org/10.1021/jp9944839

Mechanical rotation of a powder: Magic angle spinning

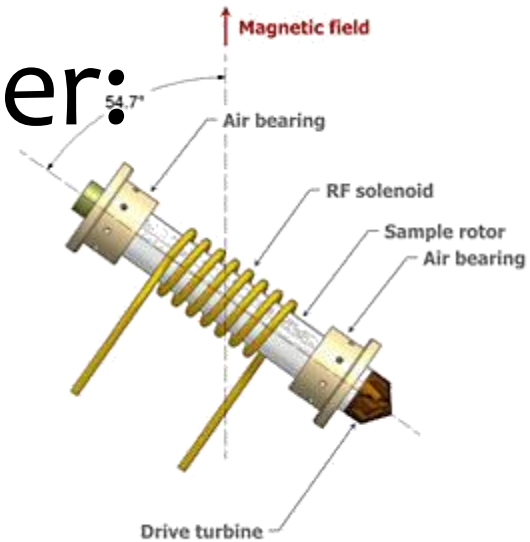

At least two transformations from PAS:

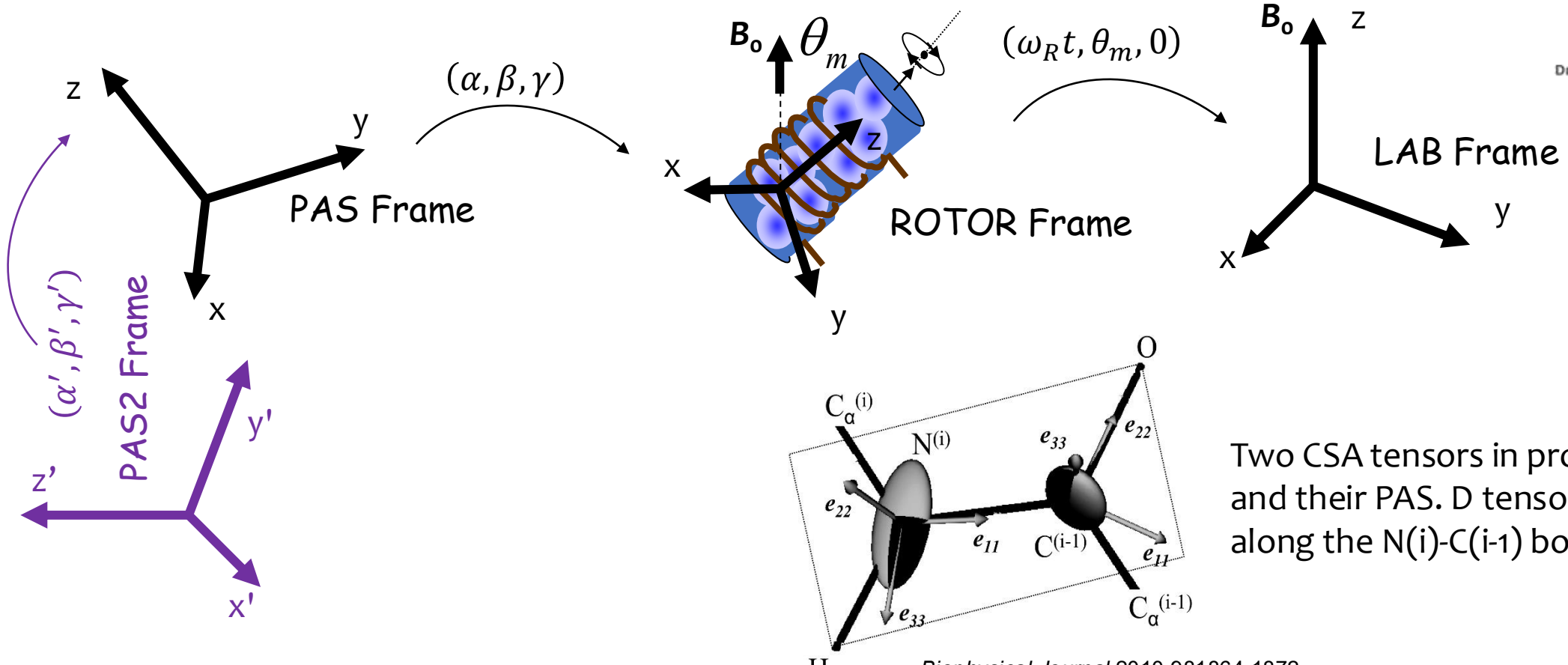

Two CSA tensors in protein backbone and their PAS. D tensor oriented along the N(i)-C(i-1) bond

Biophysical Journal 2010 981864-1872

CSA interaction under MAS ($\theta = 54.7°$)

$$H_{CSA} = \sigma_{aniso} * P_2(\theta)$$

$$= \sigma_{aniso}\left(A_1\cos(\omega_R t+\gamma)+A_2\cos(2\omega_R t+2\gamma)+B_1\sin(\omega_R t+\gamma)+B_2\sin(2\omega_R t+2\gamma)\right)I_z$$

$$\delta \equiv \sigma_{aniso} = \sigma_{zz} - \sigma_{iso}$$

$$A_1 = \tfrac{\sqrt{2}}{2}\delta\sin 2\beta\left(1+\tfrac{\eta}{3}\cos 2\alpha\right)$$

$$A_2 = \tfrac{1}{2}\delta\left(\cos^2\beta - 1 + \tfrac{\eta}{3}\cos^2\beta\cos 2\alpha\right)$$

$$B_1 = -\tfrac{\sqrt{2}}{3}\delta\eta\sin 2\beta\sin 2\alpha$$

$$B_2 = -\tfrac{1}{3}\delta\eta\cos\beta\sin 2\alpha$$

CSA averaged by spinning

Glycine ^{13}C spectrum, MAS θ=54.7°

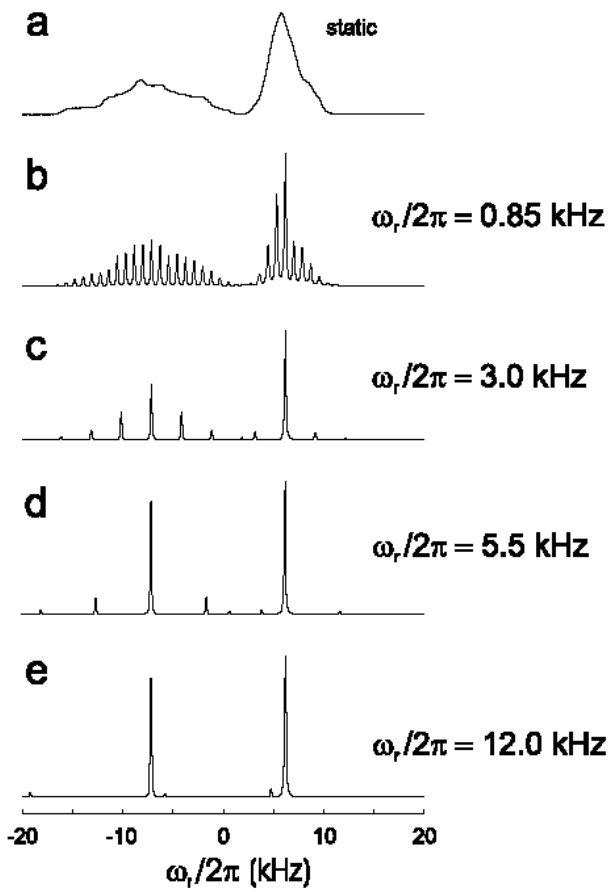

Faster averaging, spectrum becomes isotropic

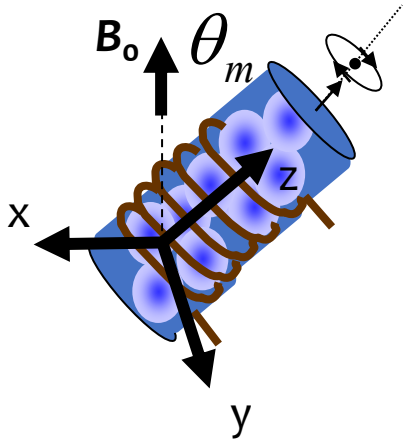

^{31}P spectrum, fast VAS, $\theta \neq 54.7°$

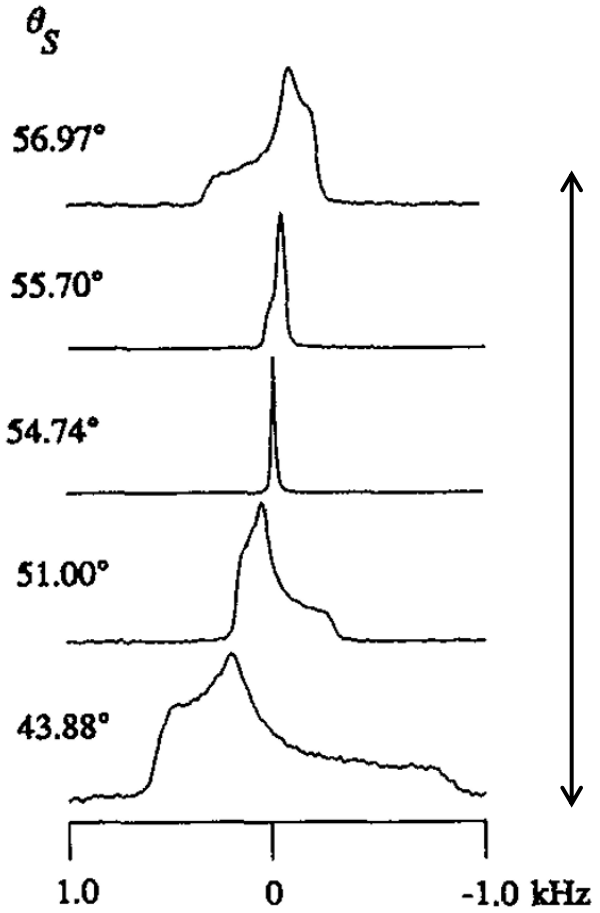

Averaging around a different angle generates different scaled lineshapes

Wu, Wasylishen; J. Chem. Phys. 100, 4828–4834 (1994) https://doi.org/10.1063/1.467203

Magic angle spinning – biological samples

- Two-dimensional 13C-13C isotropic spectra of a protein
- Spinning sidebands stretches are marked
- Complete averaging creates high-resolution spectra

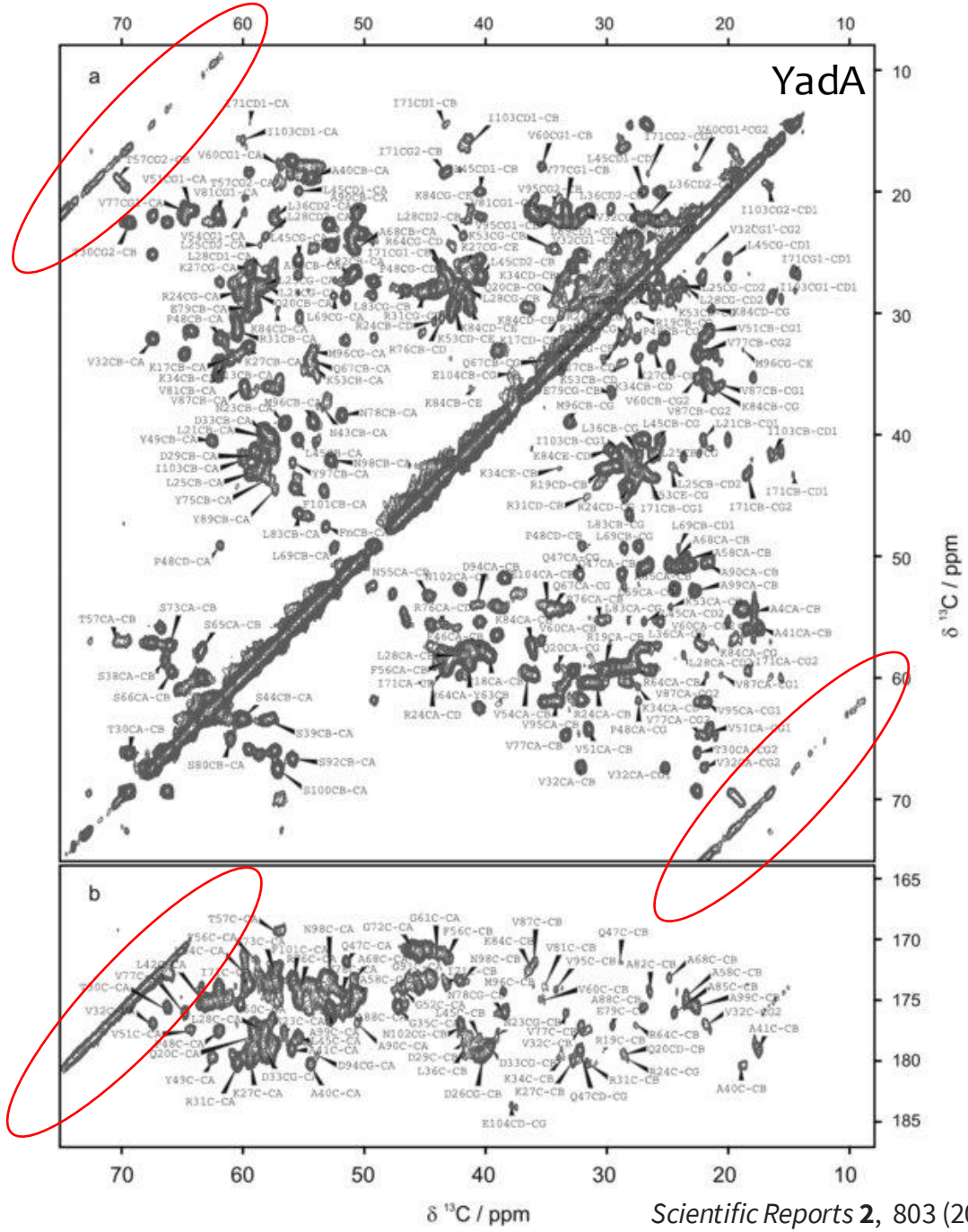

Scientific Reports **2**, 803 (2012)

Natural motions - dynamics

- Methyl group rotation
- Vector bond rotation
- Ring flips
- Chemical Exchange
- Domain motions

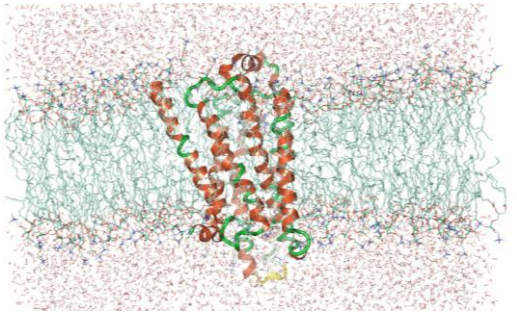

https://cresset-group.com/science/science-resources/membrane-protein-molecular-dynamics/

Time scales

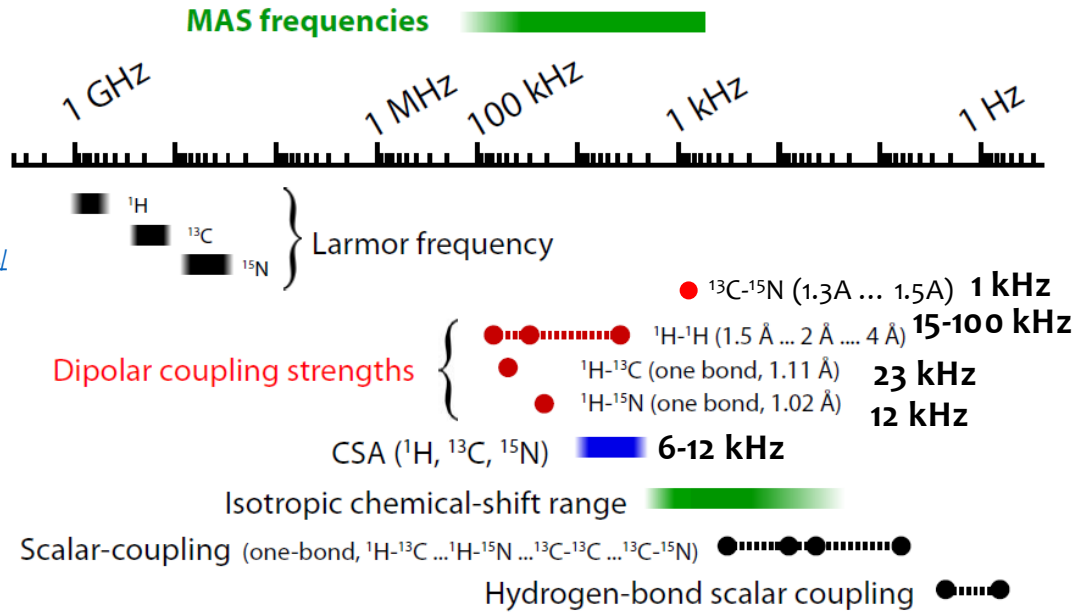

Schanda & Ernst, Progress in Nuclear Magnetic Resonance Spectroscopy 96 (2016) 1–46

- Each is associated with a different type of motion, and a different time scale
- All have some axis of motion with a typical angle with respect to molecular frame

Information from recoupling

Given an averaged tensor, and a motional model, we can get the amplitudes of motion when it is fast enough such that $k >> \omega$

Tensor motions can be viewed with MD

For dynamic residues, **CSA reorients on the ns timescale,** much faster than δ_{aniso}

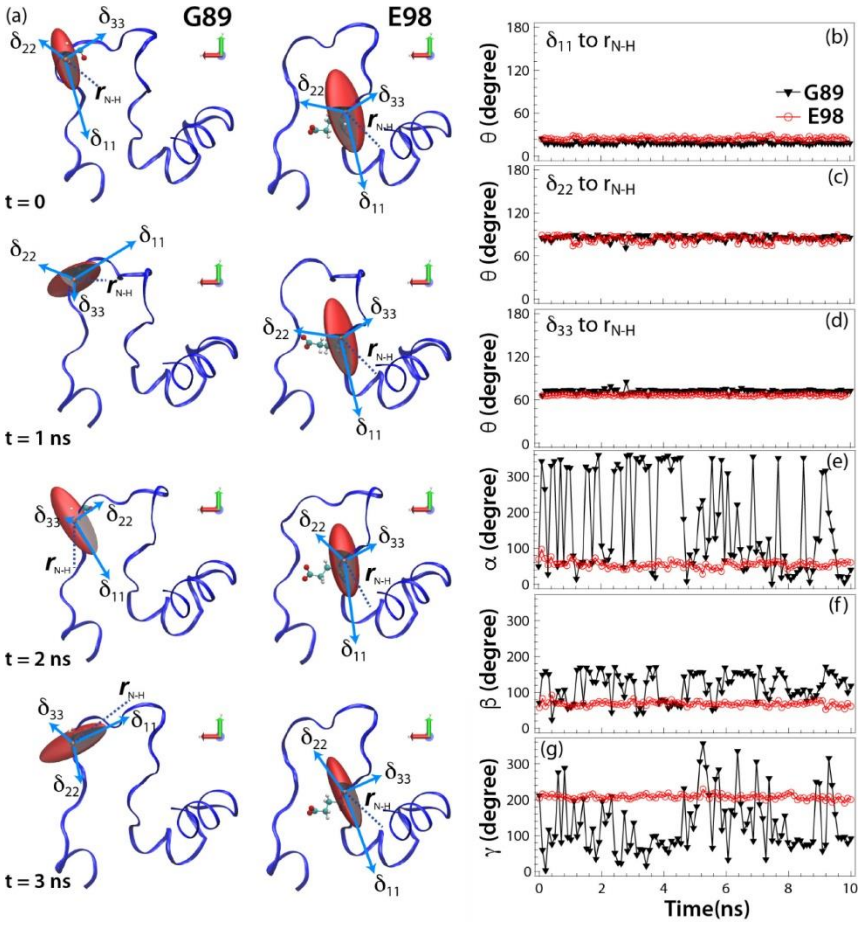

HIV capsid protein

NMR done on tubular assemblies

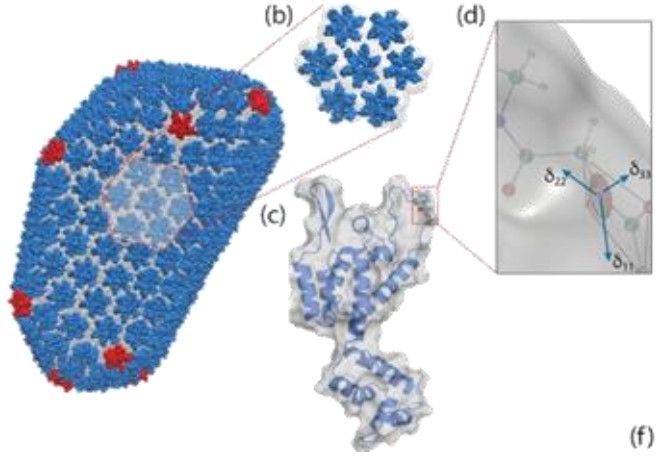

(a) Amplitudes and orientations of backbone ^{15}NH CSA tensors for G89 (left) and E98 (right) in HIV-1 CA protein with respect to the molecular frame, for the individual structures along the MD trajectory at *t* = 0, 1, 2, and 3 ns (from top to bottom, respectively).
(b–d) Plots of the relative angles between the principal components of the ^{15}N CSA tensor, δ_{ii}, and the N–H bond, r_{N-H}.
(e-g) Euler angles for the backbone ^{15}NH CSA tensors in the molecular frame. Calculated by QM/MM (at the DFT level)

Polenova & coworkers

J. Am. Chem. Soc. 2016, 138, 42, 14066−14075

https://doi.org/10.1021/jacs.6b08744

CSA lineshapes under (hopping) motion

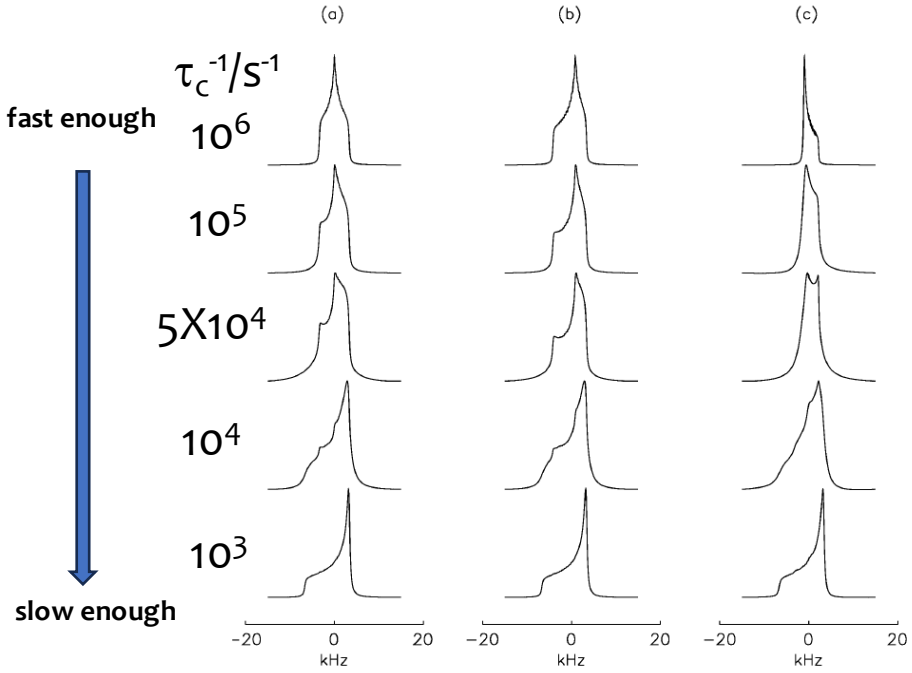

Two-site jump, 109.5°

Two-site jump, 120°

Three-site jump, 70.5°

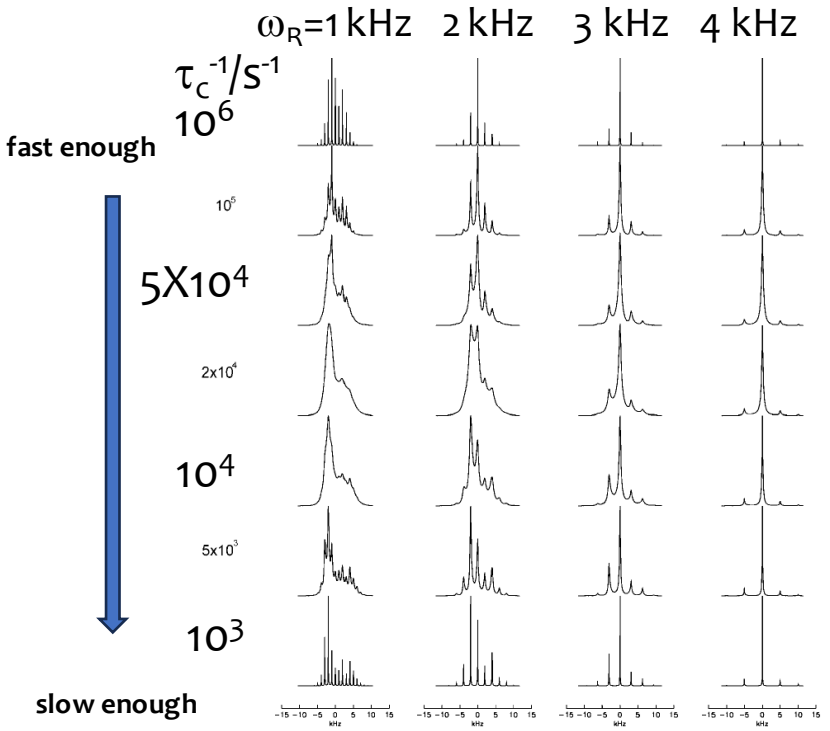

MAS, $\omega_{csa}=10^4$ Hz
Two-site jump, 120°

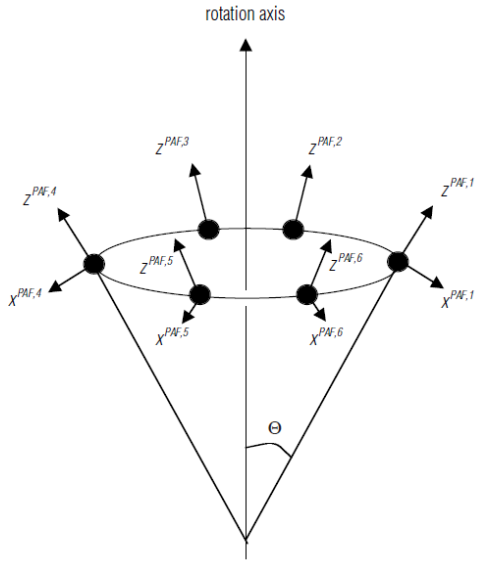

Solid state NMR spectroscopy: Principles and applications. Edited by Melinda Duer

CSA recoupling in a rigid protein – GB1

10926 J. Phys. Chem. B 2006, 110, 10926−10936

Determinations of ^{15}N Chemical Shift Anisotropy Magnitudes in a Uniformly ^{15}N,^{13}C-Labeled Microcrystalline Protein by Three-Dimensional Magic-Angle Spinning Nuclear Magnetic Resonance Spectroscopy

Benjamin J. Wylie, W. Trent Franks, and Chad M. Rienstra*

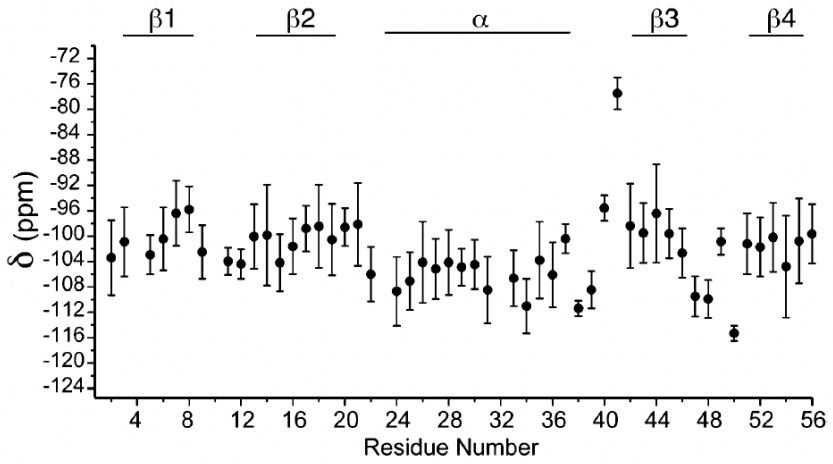

structure[a]	δ[b]
all[c]	−103.5 ± 5.6 ppm
helix[a]	−106.2 ± 2.3 ppm
sheet[a]	−100.5 ± 2.4 ppm
other[d]	−103.9 ± 3.1 ppm

ssnmr structure of GB1

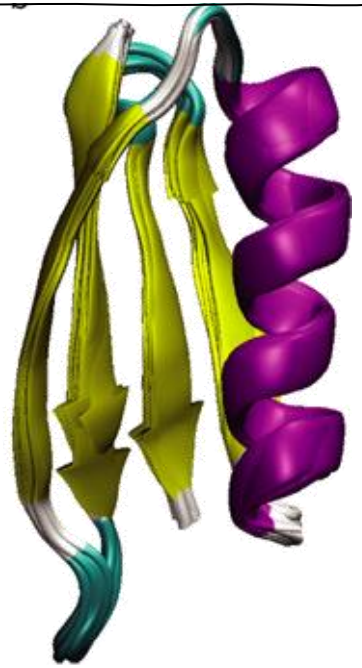

N-acetyl-D-valine (NAV)

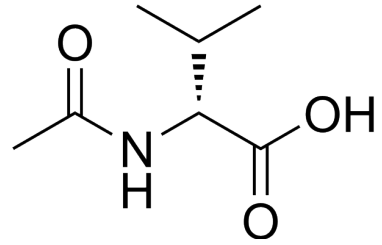

δ=-107.5+-5.1 ppm and η=0.28+-0.16.

Measuring CSA

- Under MAS, CSA reduces to spinning sidebands
- Slow spinning can be used to fit CSA (simulations, Herzfeld Berger)
- Recoupling technique under fast MAS

J. Chem. Phys. 73(12),

pulsed
- SUPER (Schmidt-Rohr, https://dx.doi.org/10.1006/jmre.2002.2503)
- xCSA (Gan, https://dx.doi.org/10.1016/j.jmr.2011.09.015)

cw
- ROCSA (original: Chan & Tycko, https://doi.org/10.1063/1.1565109) {C-seq}
- RNCSA (Hou, Polenova, http://dx.doi.org/10.1063/1.4754149) {R-seq}

A question – what is the 2D spectrum obtained from the following pulse sequence?

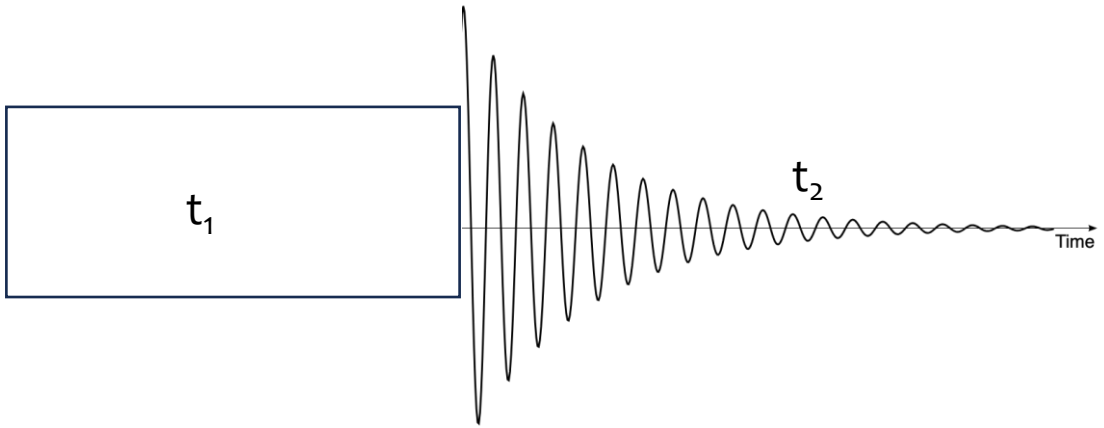

ROCSA (recoupling of chemical shift anisotropy)

Jerry C. C. Chan and Robert Tycko[a)]
Laboratory of Chemical Physics, National Institute of Diabetes and Digestive and Kidney Diseases, National Institutes of Health, Bethesda, Maryland 20892-0520

J. Chem. Phys., Vol. 118, No. 18, 8 May 2003

Recoupling

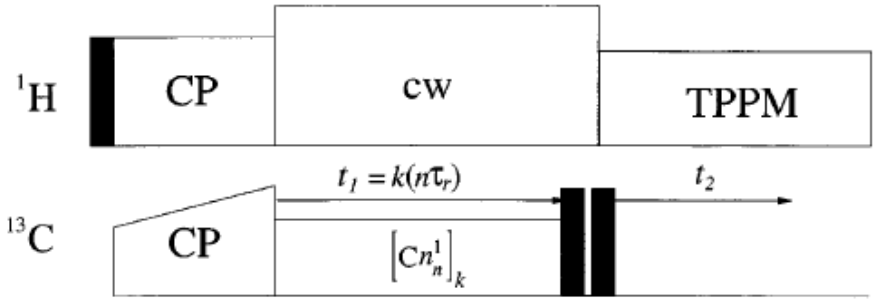

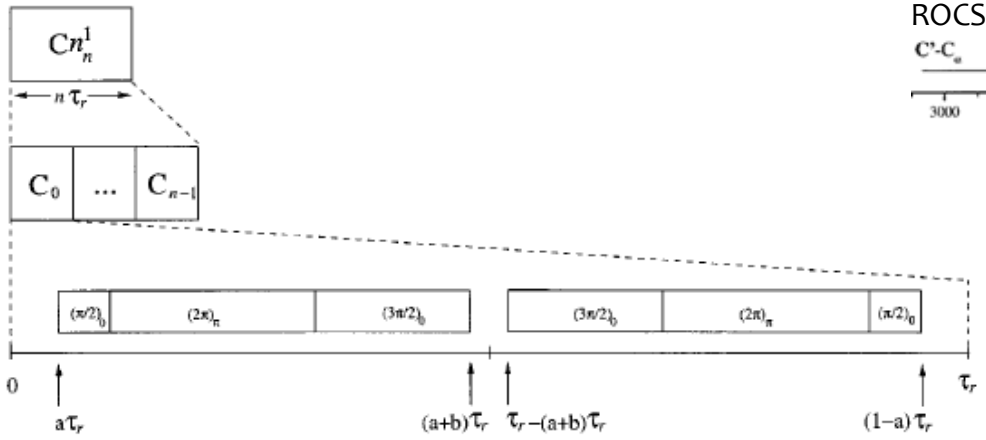

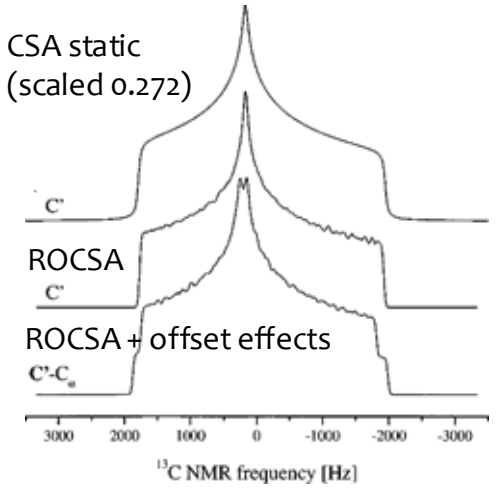

2D experiment.
Indirect dimension: Cn_n^1 recoupling
Direct dimension: chemical shift

Cn_n^1: k cycles of nTr, ϕ=2πq/n
Each element is made of two composite 360 pulses and a delay. RF is 4.28XVr.
Homonuclear recoupled (0.05)
Heteronuclear – recoupled (need decoupling)

Recouples A1, A2 elements of the Hamiltonian – both cos(wr*t) and cos(2wr*t) – allows sign discrimination

Combining ROCSA in multi-dimensional experiments

Wiley … Rienstra

J. AM. CHEM. SOC. 2005, *127*, 11946−11947

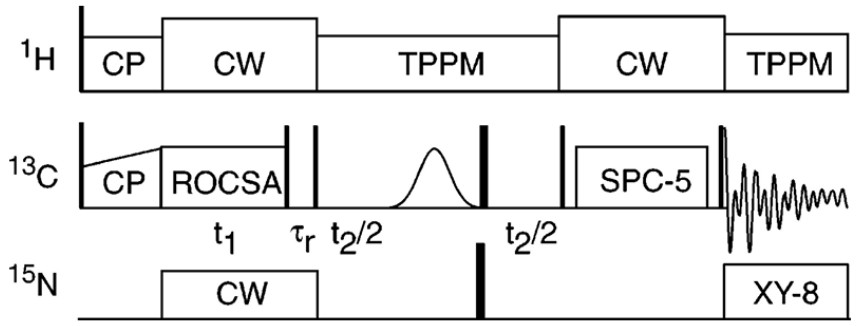

Figure 1. ROCSA−C−C 3D recoupling pulse sequence. ROCSA was applied under CW decoupling on ^{15}N and ^{1}H. A soft (Gaussian) pulse was placed in the middle of the t_2 evolution period to remove the influence of the scalar (CO−Cα and CO−Cβ) couplings. Narrow and wide rectangles represent $\pi/2$ and π pulses. Full experimental details, including phase cycles, are provided in the Supporting Information.

Wiley … Rienstra

J. Phys. Chem. B **2006,** *110,* 10926−10936

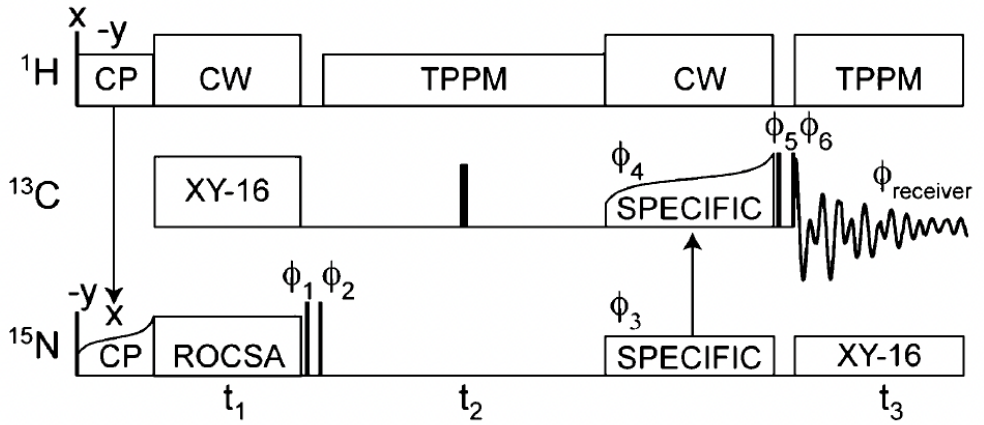

Figure 1. Pulse sequence diagram of [^{15}N]−^{15}N−^{13}C 3D ROCSA. The ROCSA element was inserted before the indirect ^{15}N chemical shift evolution period of a ^{15}N−^{13}C 2D experiment. ROCSA was applied under CW decoupling on ^{1}H (∼120 kHz) and rotor-synchronized XY π-pulse decoupling on ^{13}C. An eight-step phase cycle was used: $\phi_1 = (-y, -y, -y, -y, -y, -y, -y, -y)$, $\phi_2 = (y, y, -x, -x, -y, -y, x, x)$, $\phi_3 = (x, -x, y, -y, -x, x, -y, y)$, $\phi_4 = (x, x, -x, -x, x, x, -x, -x)$, $\phi_5 = (-y, -y, y, y, -y, -y, y, y)$, $\phi_6 = (x, x, y, y, -x, -x, -y, -y)$, $\phi_{receiver} = (x, -x, y, -y, -x, x, -y, y)$. Hypercomplex sampling was achieved in the t_1 (ROCSA) dimension by adding the States−TPPI phase to ϕ_1. The TPPI phase list was added to ϕ_3 to provide quadrature detection in t_2.

ROCSA – cont.

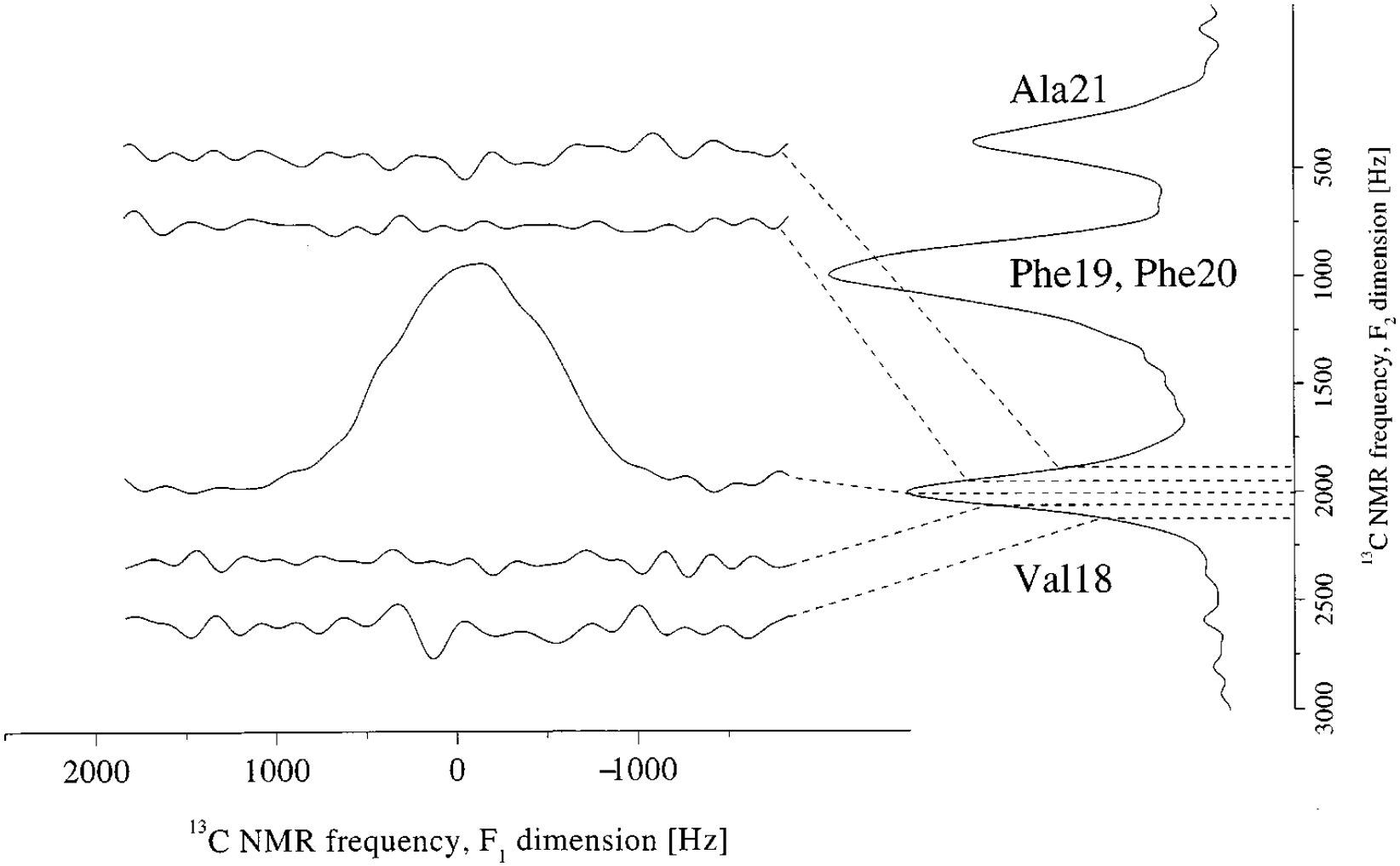
Ala21
Phe19, Phe20
Val18
2000
1000
0
–1000
^{13}C NMR frequency, F_1 dimension [Hz]
500
1000
1500
2000
2500
3000
^{13}C NMR frequency, F_2 dimension [Hz]

ROCSA – results amino acids

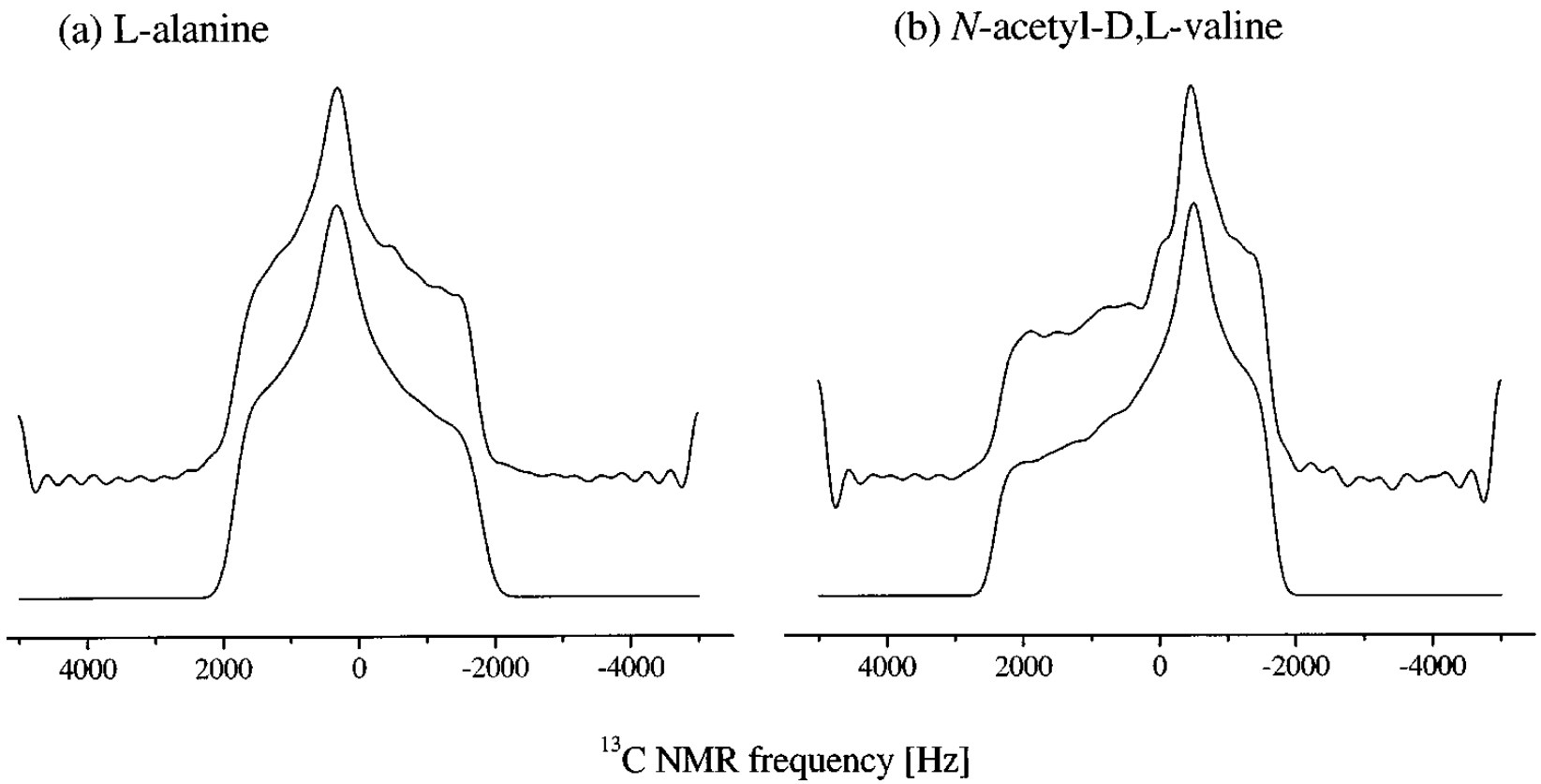

SUPER

A Robust Technique for Two-Dimensional Separation of Undistorted Chemical-Shift Anisotropy Powder Patterns in Magic-Angle-Spinning NMR

S-F. Liu, J-D. Mao, and K. Schmidt-Rohr[1]

Journal of Magnetic Resonance 155, 15–28 (2002)

- Recouples a scaled static lineshape
- Scaling factor – up to 0.2
- Sensitive to homonuclear couplings
- Requires RF=12.12Vr – suitable for slow spinning

Compound name/carbon site	σ_{11} (ppm)	σ_{22} (ppm)	σ_{33} (ppm)	σ_{iso} (ppm)
Glycine	244	181	104	176.4
Glycine literature	**247**	**182**	**103**	**177**
L-Alanine	242	184	108	177.9
l-Alanine literature	**243**	**184**	**107**	**178**
Poly(ethylene terephthalate) (PET)	250	130	115	165.3

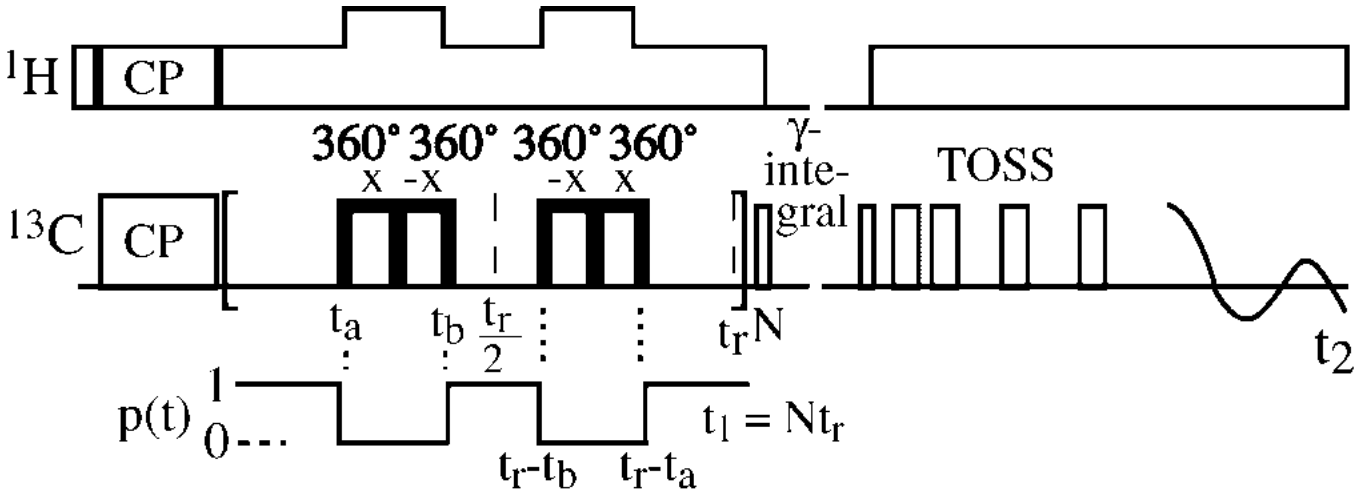

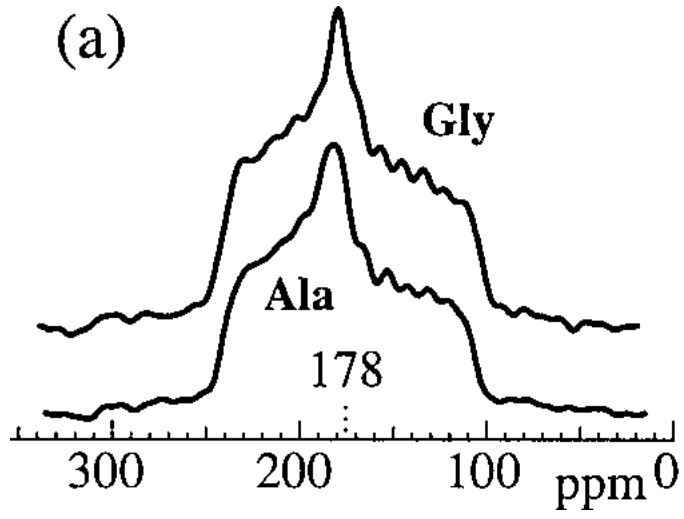

CSA from spinning sidebands

750 MHz
13C': -83.5ppm helix, -77.7ppm sheet
15N: -115ppm helix, -106ppm sheet

Chemical-Shift Anisotropy Measurements of Amide and Carbonyl Resonances in a Microcrystalline Protein with Slow Magic-Angle Spinning NMR Spectroscopy

Benjamin J. Wylie, Lindsay J. Sperling, Heather L. Frericks, Gautam J. Shah, W. Trent Franks, and Chad M. Rienstra*

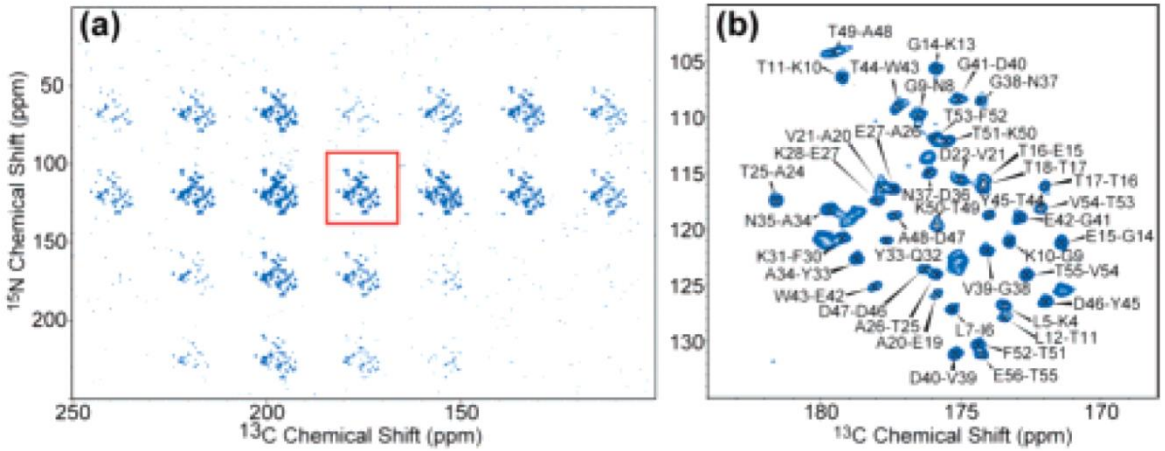

Figure 1. Slow 2D magic-angle spinning (MAS) $^{15}N-^{13}C$ correlation spectrum of GB1, 750 MHz ^{1}H frequency: (a) full bandwidth 2D plane of N−C′ sideband manifolds at 4 kHz MAS; (b) centerband manifold with resonance assignments indicated.

D40N-V39C'

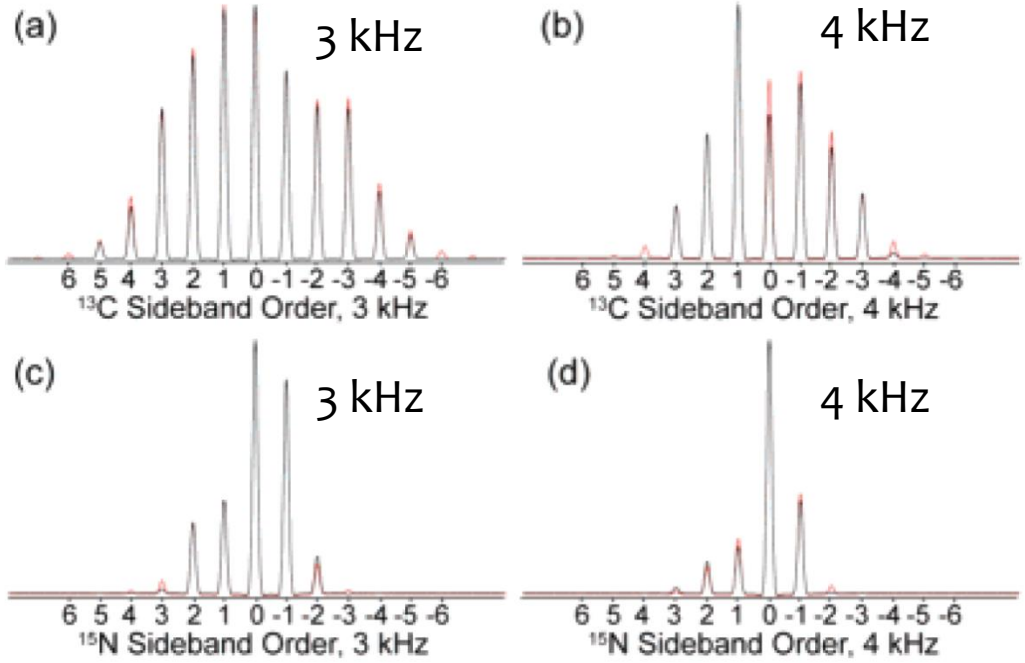

THE JOURNAL OF CHEMICAL PHYSICS **137**, 134201 (2012)

RNCSA

Recoupling of chemical shift anisotropy by R-symmetry sequences in magic angle spinning NMR spectroscopy

Guangjin Hou,[1,2] In-Ja L. Byeon,[2,3] Jinwoo Ahn,[2,3] Angela M. Gronenborn,[2,3] and Tatyana Polenova[1,2,a)]

- R-sequence based recoupling
- Can recouple the terms with $\pm 1\omega_r$ frequencies, or $\pm 2\omega_r$ freq.
- 1*wr will have larger scaling factors – but also homonuclear
- 2*wr suppresses homonuclear, good for uniform labeling
- Result is loss of sign of the CSA

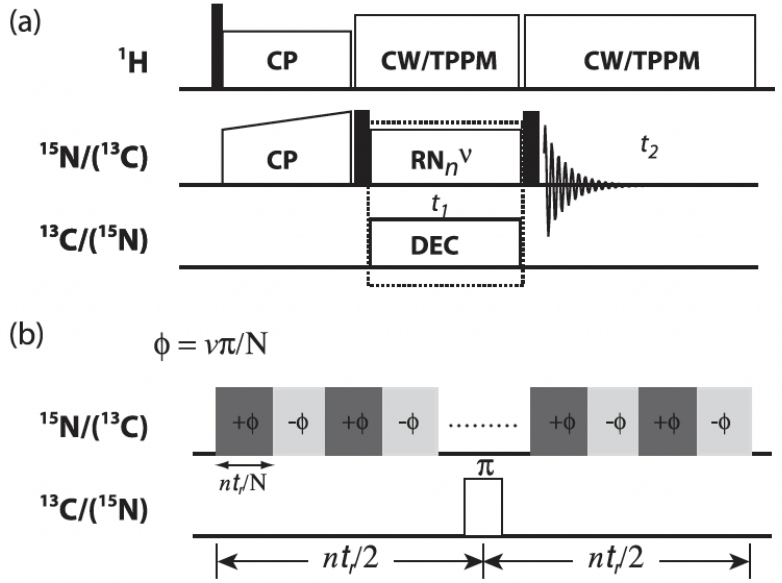

NAV lineshapes for various R-seq.

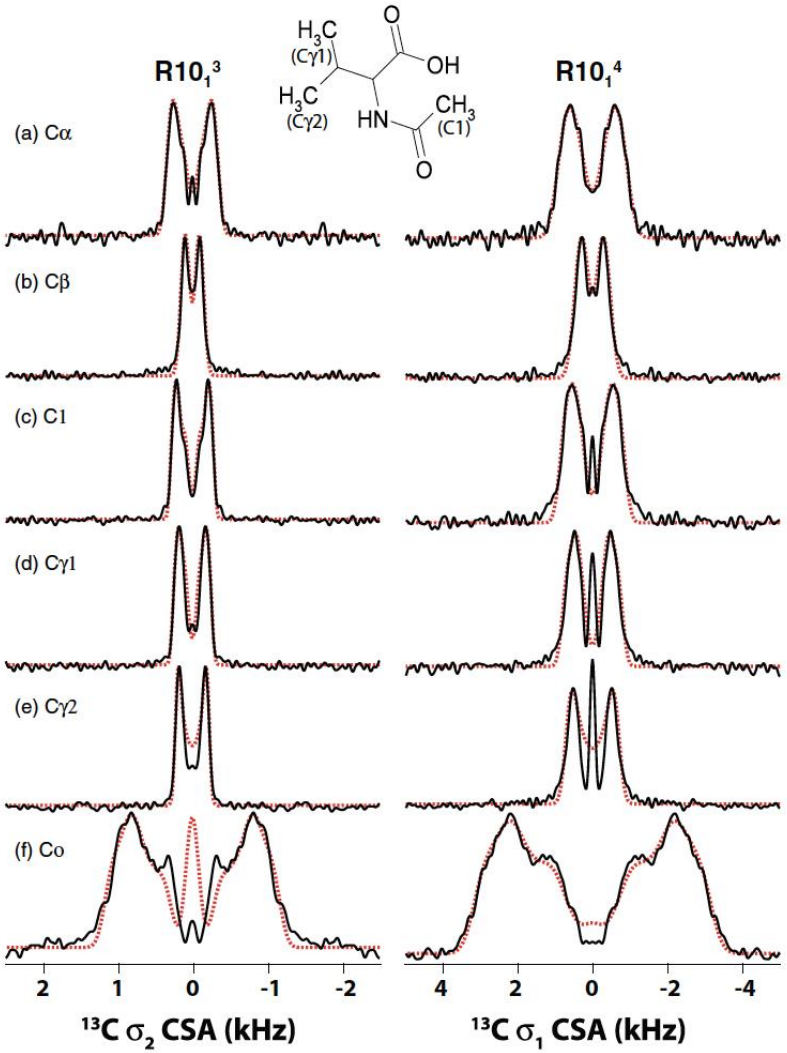

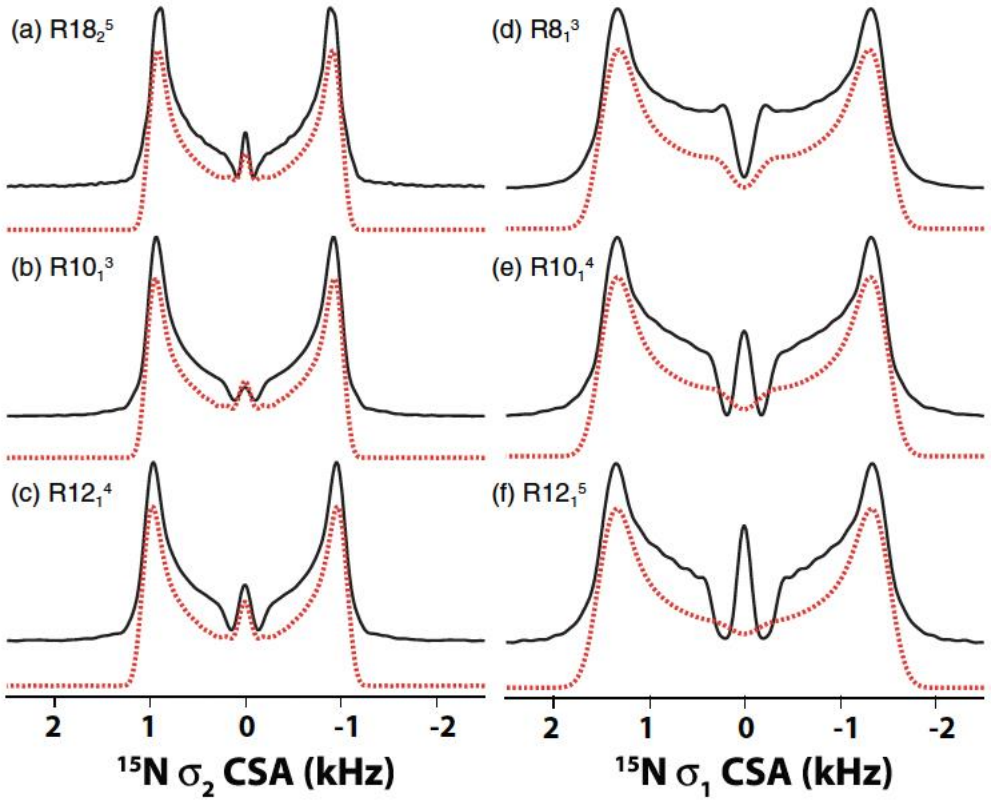

RNCSA - Scaling factors

RN_n^v :
N pulses of π_ϕ-$\pi_{-\phi}$
n rotor periods
$\phi=\pi v/N$
$\omega_{RF}/\omega_R=N/2n$

$R10_1^3$ (spin 12khz):
10 pulses, 1 TR
$\phi=3\pi/10=54$ deg
$\omega_{RF}=5\omega_R=60$ kHz

$R18_2^5$ (spin 12khz):
18 pulses, 2 TR
$\phi=5\pi/18=50$ deg
$\omega_{RF}=4.5\omega_R=54$ kHz

Table S1. Summary of γ-Encoded R-Symmetry Sequences Suitable for Recoupling of the CSA Interaction. N is from 10 to 20, $N/2n$ is from 1.0 to 8.0.

Symmetry numbers			Scaling factors for $\sum H^{CSA}(l, m, \lambda, \mu)$		Scaling factors for $\sum H^{DD}(l, m, \lambda, \mu)$	ω_{rf}/ω_r
N	n	V	$m=\pm1$	$m=\pm2$		
6	1	1	0	0.2865	0.2250	3
6	1	2	0.4385	0	0.2421	3
8	1	2	0	0.3000	0.1039	4
8	1	3	0.4436	0	0.2078	4
10	1	3	0	0.3066	0	5
10	1	4	0.4460	0	0.2110	5
10	2	1	0	0.2733	0	2.5
10	2	3	0.4335	0	0.1950	2.5
10	3	1	0	0.2236	0	1.667
10	3	2	0.4134	0	0.1706	1.667
12	1	4	0	0.3100	0	6
12	1	5	0.4472	0	0.2127	6
14	1	5	0	0.3123	0	7
14	1	6	0.4481	0	0.2137	7
14	2	3	0	0.2946	0	3.5
14	2	5	0.4417	0	0.2054	3.5
14	3	1	0	0.2669	0	2.333
14	3	4	0.4311	0	0.1921	2.333
14	4	1	0	0.2314	0	1.75
14	5	3	0	0.1907	0	1.4
14	6	5	0	0.1472	0	1.167
16	1	6	0	0.3137	0	8
16	1	7	0.4486	0	0.2142	8
16	3	2	0	0.2785	0	2.667
16	3	5	0.4356	0	0.1976	2.667
16	5	2	0	0.2165	0	1.6
16	5	3	0.4105	0	0.1671	1.6
16	7	1	0.3746	0	0.1285	1.143
16	7	6	0	0.1425	0	1.143
18	2	5	0	0.3038	0	4.5
18	4	1	0	0.2634	0	2.25
18	5	1	0	0.2356	0	1.8
18	7	5	0	0.1718	0	1.286
18	8	7	0	0.1384	0	1.125
20	3	4	0	0.2924	0	3.333
20	7	4	0	0.1949	0	1.429
20	9	8	0	0.1351	0	1.111

$\pm1\omega_r$ $\pm2\omega_r$

2D $^{15}N_{CSA}$-$^{15}N_{iso}$ RNCSA recoupling (fd phage)

Real FT of the CSA dimension creates perfectly symmetric spectrum

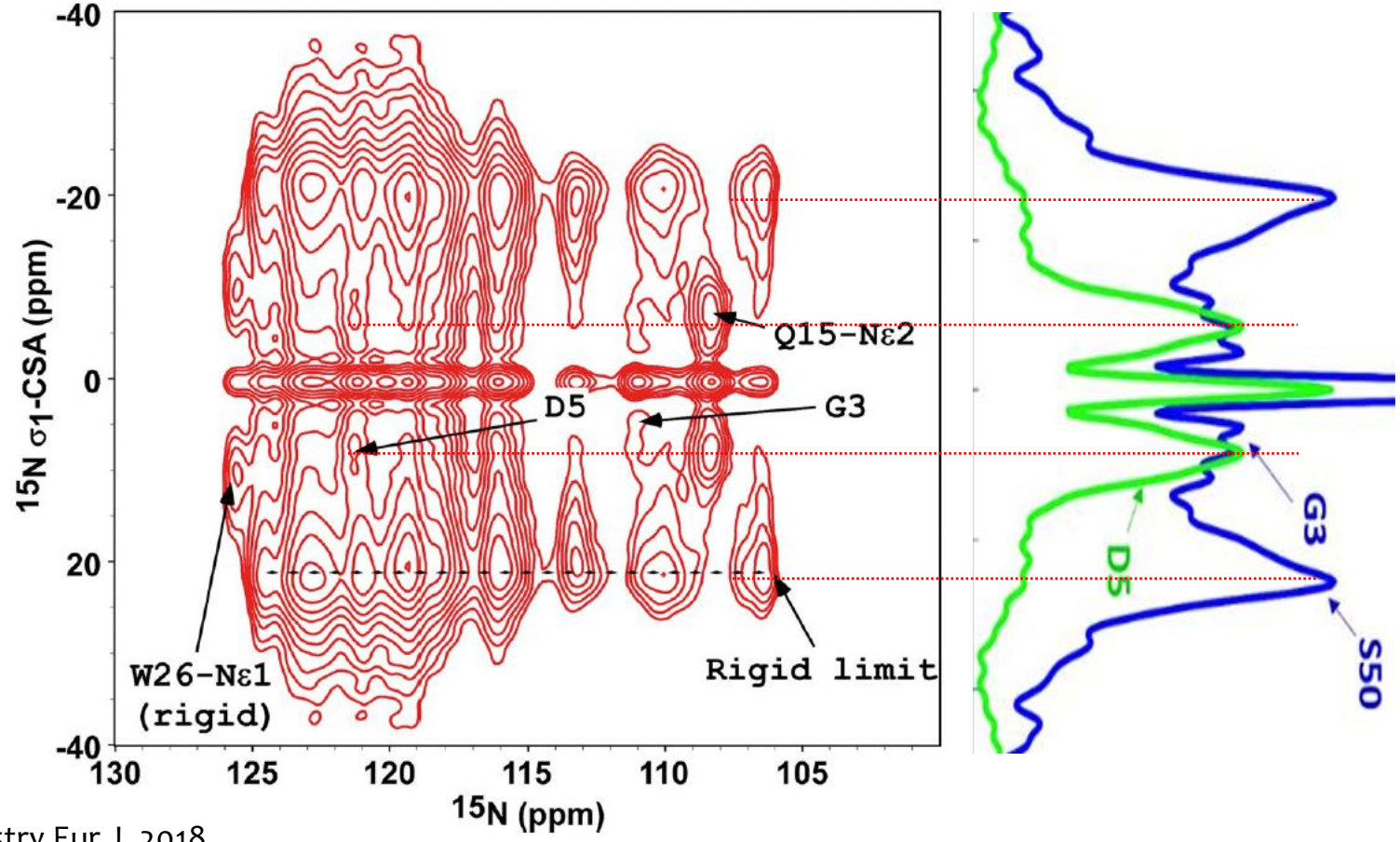

T. Aharoni, AG, Chemistry Eur J, 2018

RNCSA recoupling and dynamics

- In order to resolve lineshapes we need 3D experiments
- Two isotropic (chemical shift dimensions), one CSA dimension
- Examples: C-C resolved ----- N-C resolved

13C(CSA)-13C(iso)-13C(iso)

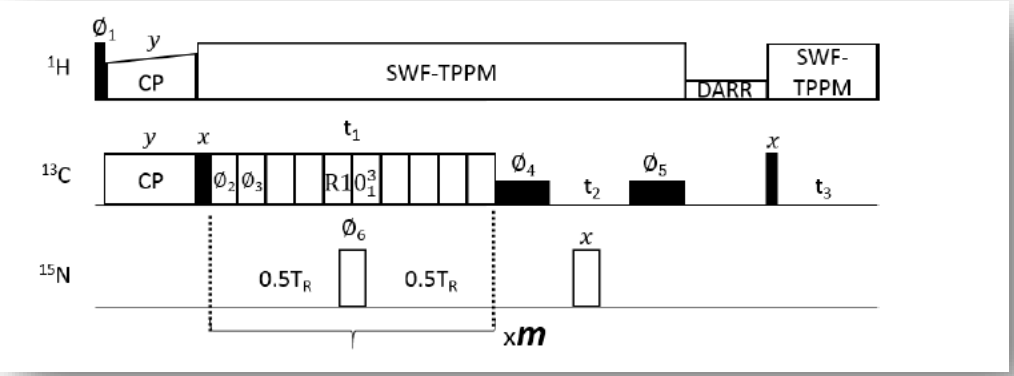

15N(CSA)-15N(iso)-13C(iso)

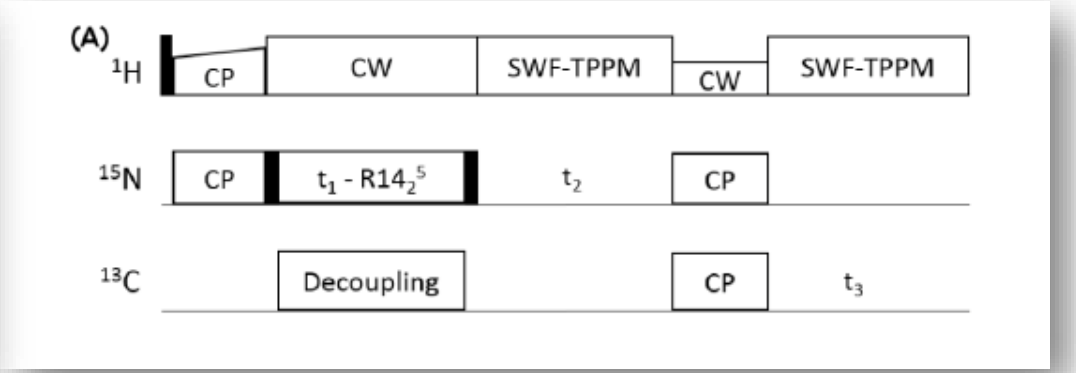

CSA recoupling – bacteriophage fd

$15N\left(R14_2^5\right) - 15N - 13C$

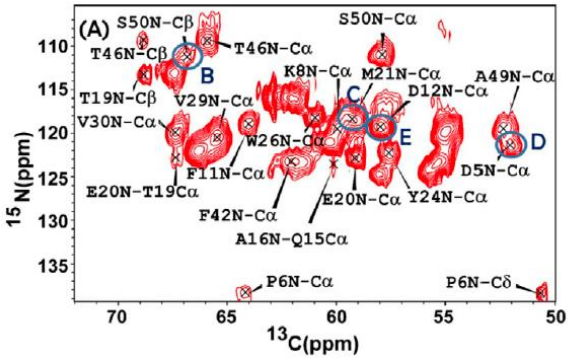

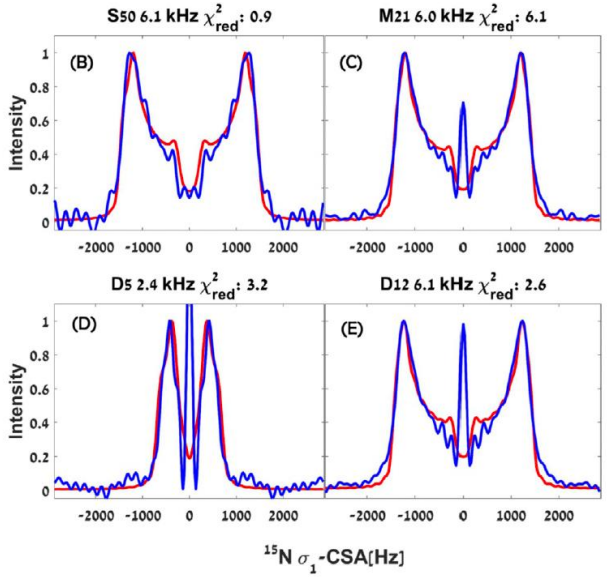

$13C\left(R10_1^3\right) - 13C - 13C$

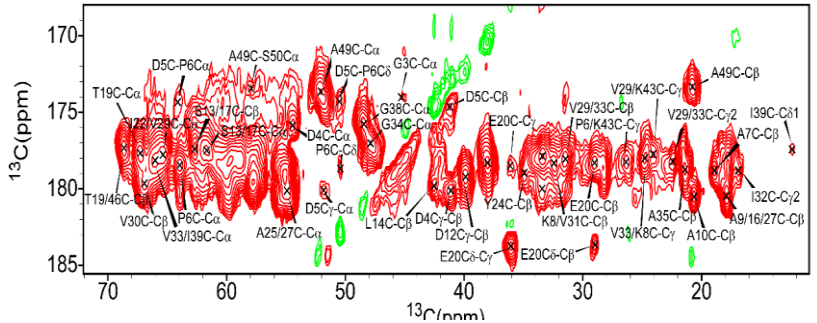

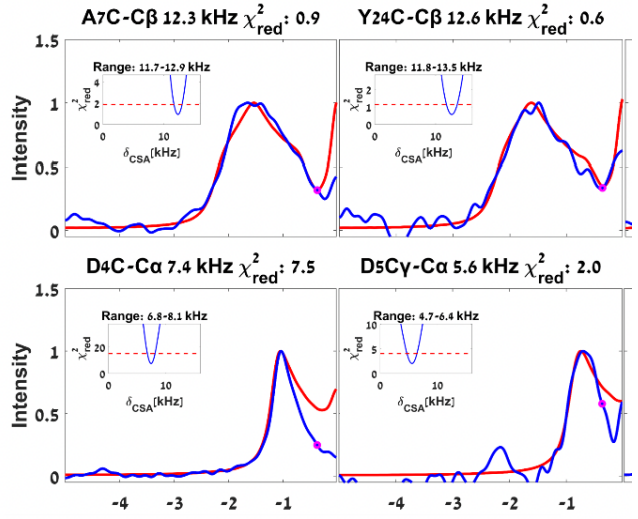

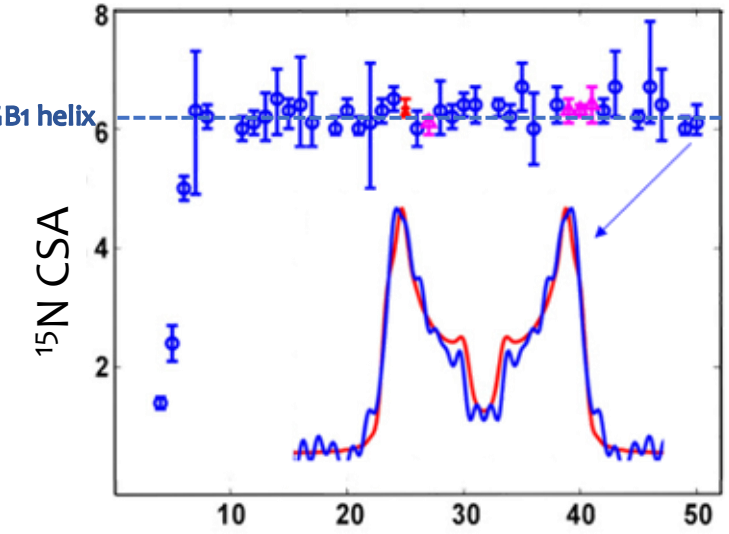

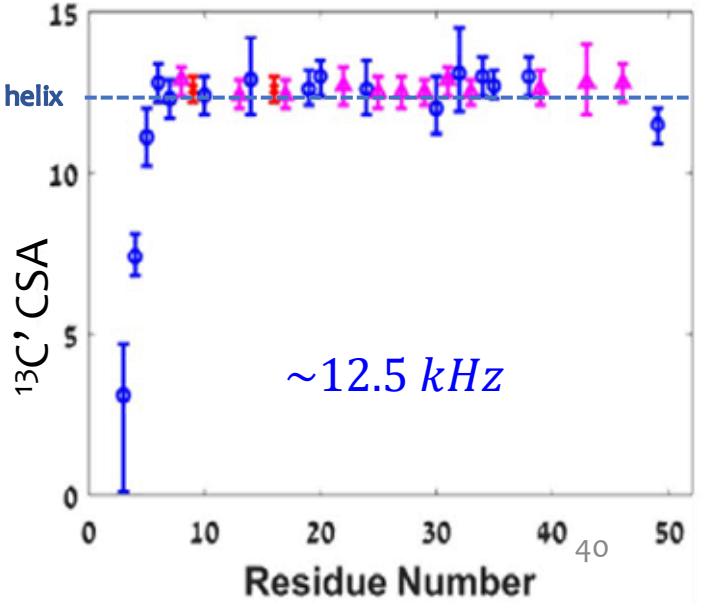

CSA-based dynamics in HIV capsid tubular assemblies – 15N CSA + MD

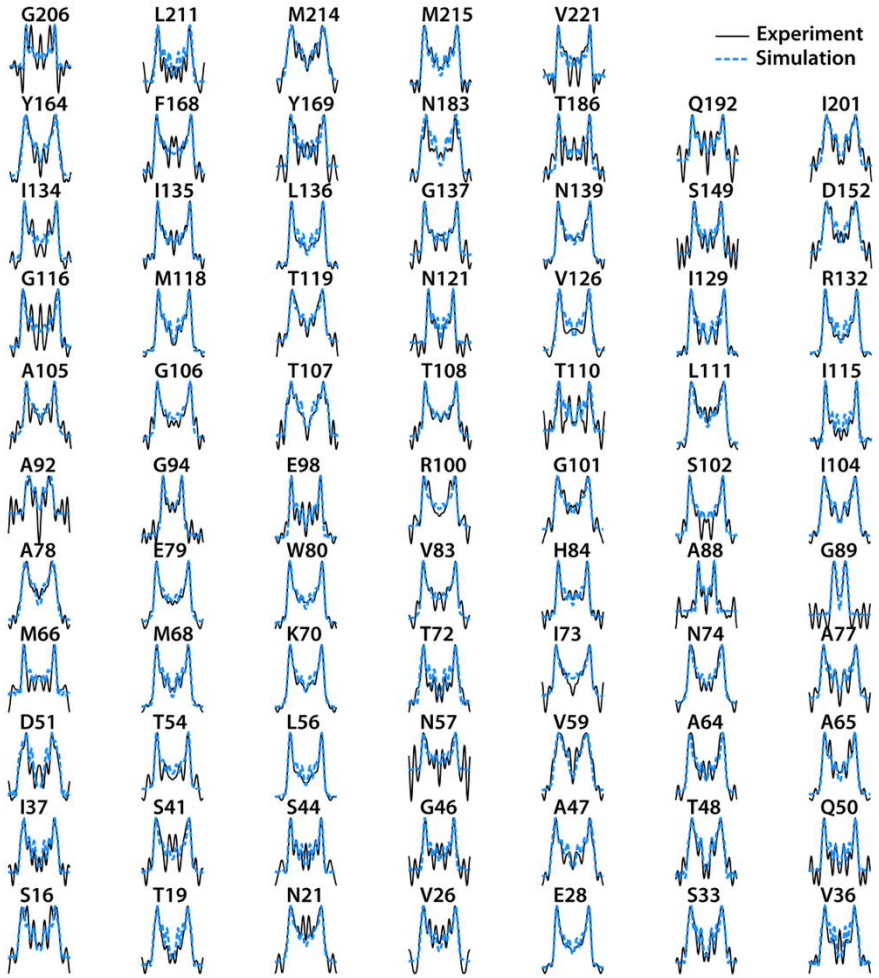

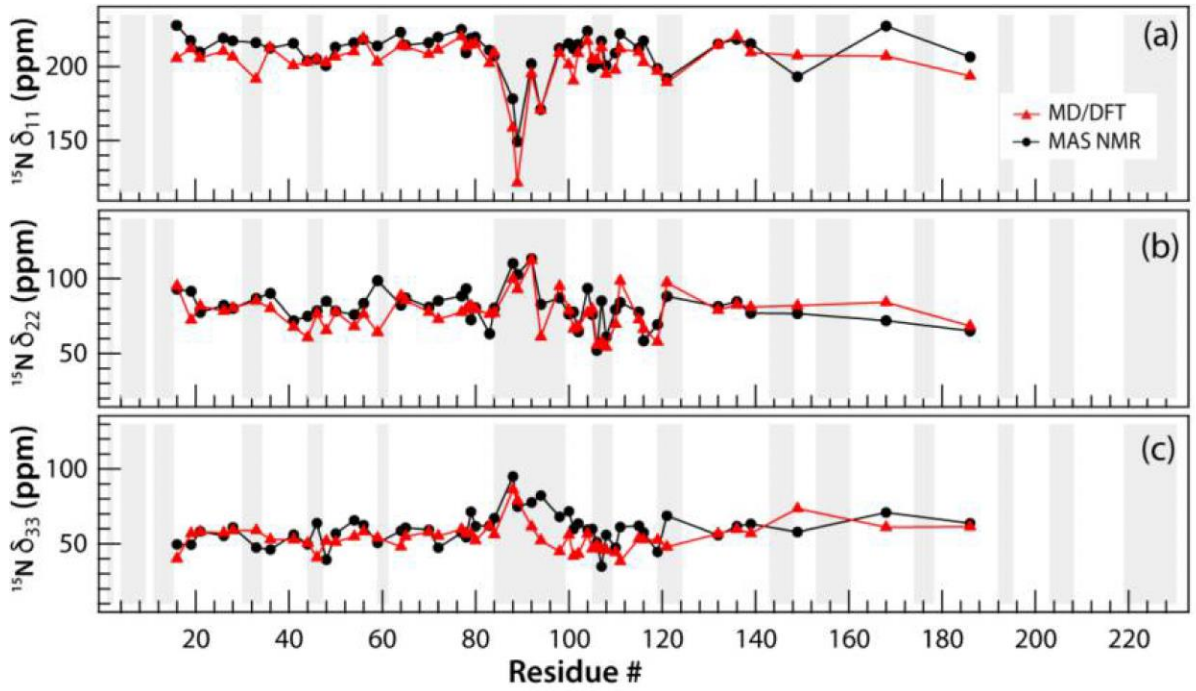

J. Chem. Phys. **153**, 104201 (2020); doi: 10.1063/5.0020682

CSA recoupling - Ubiquitin

Fritzsching, … McDermott

Method: fROCSA – variation on ROCSA – control on scaling factor

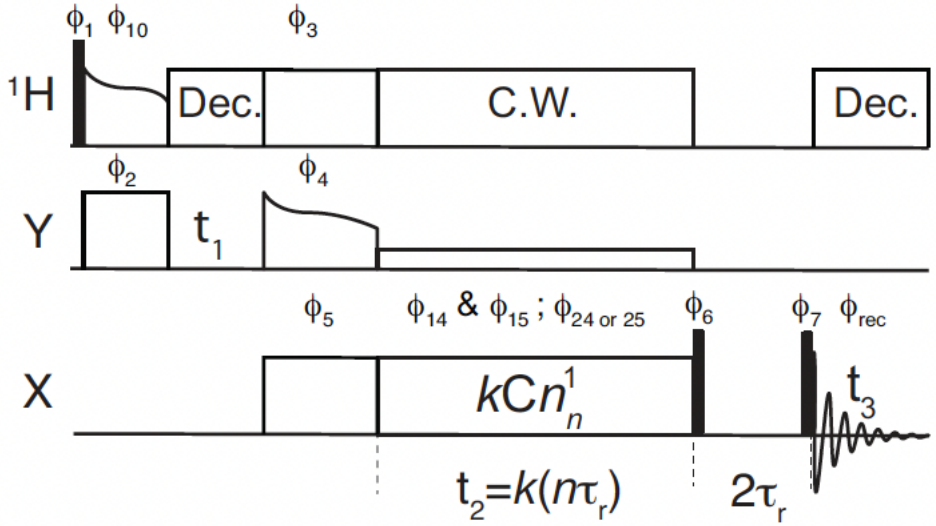

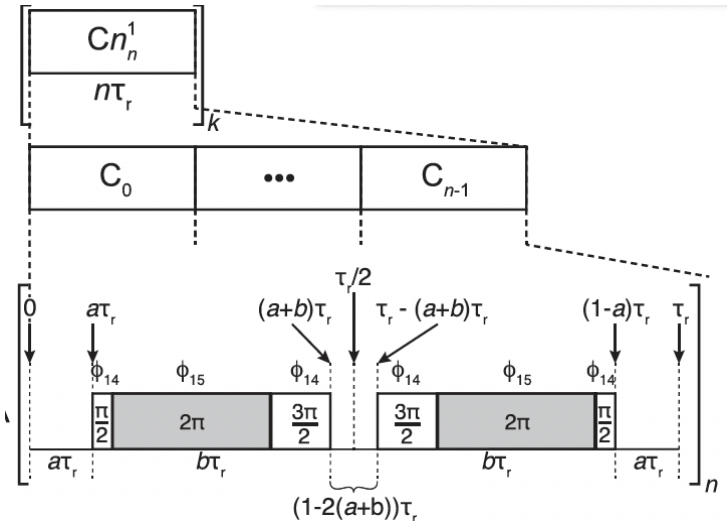

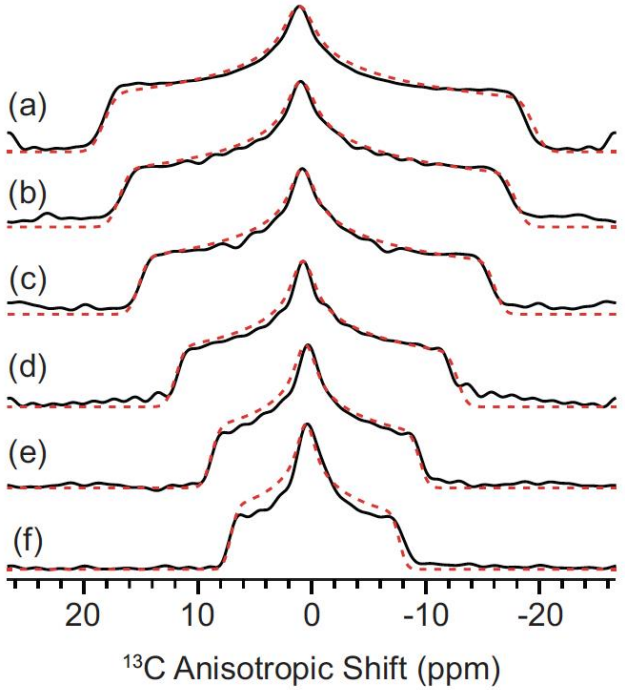

CSA recoupling – Ubiquitin - Results

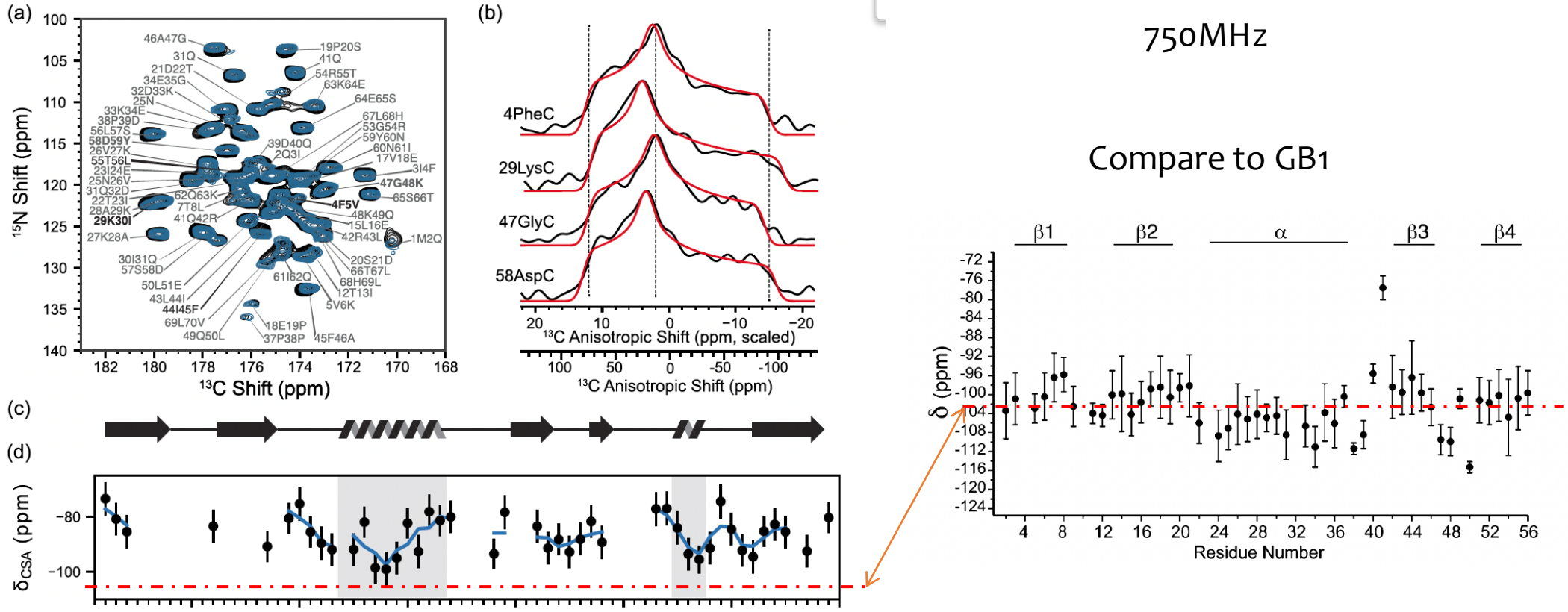

Increased dynamics in Ubiquitin!

CSA recoupling & dynamics - summary

- Various methods
- Should be combined with sufficiently resolved isotropic spectra
- Scaling factors vary
- RF requirement can be important
- Different sensitivity to RF inhomogeniety
- Different sensitivity to OFFSET
- Should consider 13C-13C and 13C-15N couplings
- No clear “RIGID LIMIT” – values vary according to secondary struct.

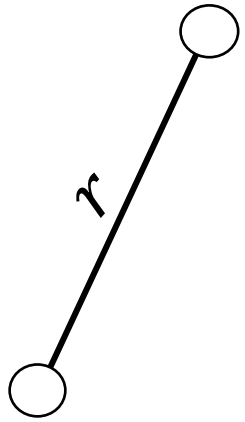

Dipolar coupling

$$d = \hbar\left(\frac{\mu_0}{4\pi}\right)\frac{\gamma_I\gamma_S}{r^3}$$

A simple calculation of the dipolar coupling constant in Hz:

$$\boldsymbol{d = 66.26\gamma_I\gamma_s r^{-3}}$$

- Distance **r** in Å
- γ in MHz·T^{-1}
- 66.26 = h^{35}

Advantage:
RIGID LIMIT is known – it is the static distance

A reference dipolar coupling between two ^{1}H spins separated by 1.00Å is calculated as follows:

$$\omega_{ij} = -\frac{\mu_0\hbar\gamma_i\gamma_j}{4\pi r_{ij}^3} \quad (1)$$

$$= -\frac{(4\pi\cdot 10^{-7}\,\frac{\mathrm{T\cdot m}}{\mathrm{A}})(1.05457\cdot 10^{-34}\,\frac{\mathrm{J\cdot s}}{\mathrm{rad}})(267.513\cdot 10^{6}\,\frac{\mathrm{rad}}{\mathrm{s\cdot T}})(267.513\cdot 10^{6}\,\frac{\mathrm{rad}}{\mathrm{s\cdot T}})}{4\pi\cdot(1.00\cdot 10^{-10}\,\mathrm{m})^3} \quad (2)$$

$$= -754.7\,\frac{\mathrm{krad}}{\mathrm{s}} \quad (3)$$

$$\nu_{ij} = -120.1\mathrm{kHz} \quad (4)$$

I made use of the fact that $1\mathrm{T} = 1\,\frac{\mathrm{kg}}{\mathrm{s^2\cdot A}} = 1\,\frac{\mathrm{J}}{\mathrm{A\cdot m^2}}$

From: Dipolar Couplings in Solid-State and Solution NMR (lorieau.com)

Dipolar interaction Hamiltonian

Classical definition:

$$E = \left\{ \frac{\mu_I \cdot \mu_S}{r^3} - 3\frac{(\mu_I \cdot r_I)(\mu_S \cdot r_S)}{r^5} \right\} \frac{\mu_0}{4\pi}$$

Quantum definition:

$$\hat{H}_D = \hbar \left(\frac{\gamma_I \gamma_S}{r^3} \right) \frac{\mu_0}{4\pi} \left\{ I \cdot S - \frac{3}{r^2} (I \cdot r_I)(S \cdot r_S) \right\}$$

$$\hat{H}_D = d\vec{I} \cdot \hat{D}^L \cdot \vec{S}$$

$$d = \hbar \left(\frac{\mu_0}{4\pi} \right) \frac{\gamma_I \gamma_S}{r^3}$$

A simple calculation of the dipolar coupling constant in Hz:

$$\boldsymbol{d = 66.26 \gamma_I \gamma_s r^{-3}}$$

- Distance **r** in Å
- γ in MHz·T^{-1}
- 66.26 = h^{35}

The dipolar interaction is **traceless,** and proportional to the inverse cube of the **distance**

Nice explanation how to calculated d: Dipolar Couplings in Solid-State and Solution NMR (lorieau.com)

Dipolar interaction Hamiltonian

$$H_D^{IS}(lab) = \hat{I} \cdot \hat{D}^L \cdot \hat{S} = \hat{I} \cdot R^{-1} \hat{D}^{PAS} R \cdot \hat{S} \qquad \hat{D}^{PAS} = \begin{pmatrix} d & 0 & 0 \\ 0 & d & 0 \\ 0 & 0 & -2d \end{pmatrix}$$

Full form of the dipolar interaction ('alphabets'):

$$\hat{H}_D = d[A + B + C + D + E + F]$$

$$A = 2I_z S_z \tfrac{1}{2}(3\cos^2\theta - 1)$$

$$B = -\tfrac{1}{2}[I_+ S_- + I_- S_+] \tfrac{1}{2}(3\cos^2\theta - 1)$$

$$C = \tfrac{3}{2}[I_z S_+ + I_+ S_z] sin\theta cos\theta e^{-i\phi}$$

$$D = \tfrac{3}{2}[I_z S_- + I_- S_z] sin\theta cos\theta e^{+i\phi}$$

$$E = \tfrac{3}{4}[I_+ S_+] \sin^2\theta \, e^{-2i\phi}$$

$$F = \tfrac{3}{4}[I_- S_-] \sin^2\theta \, e^{+2i\phi}$$

Zeeman truncation:

Heteronuclear case ($\gamma_I \neq \gamma_S$)

$$\hat{H}_D^{het} = d \cdot A$$

$$\boldsymbol{\hat{H}_D^{het} = d \cdot 2I_z S_z \cdot \tfrac{1}{2}(3\cos^2\theta - 1)}$$

Homonuclear case ($\gamma_I = \gamma_S$)

$$\hat{H}_D^{hom} = d \cdot [A + B]$$

$$\hat{H}_D^{hom} = d \cdot (3\cos^2\theta - 1)\left[I_z S_z - \tfrac{1}{2}(I_x S_x + I_y S_y)\right]$$

$$\boldsymbol{\hat{H}_D^{hom} = d \cdot \tfrac{1}{2}(3\cos^2\theta - 1)[3I_z S_z - \hat{I} \cdot \hat{S}]}$$

Dipolar spectrum

In solution – average over all orientations:

$$\int_0^{\pi} \frac{1}{2}(1 - 3cos^2\theta)sin\theta d\theta = 0$$

Result: No coherent contribution

In solids:

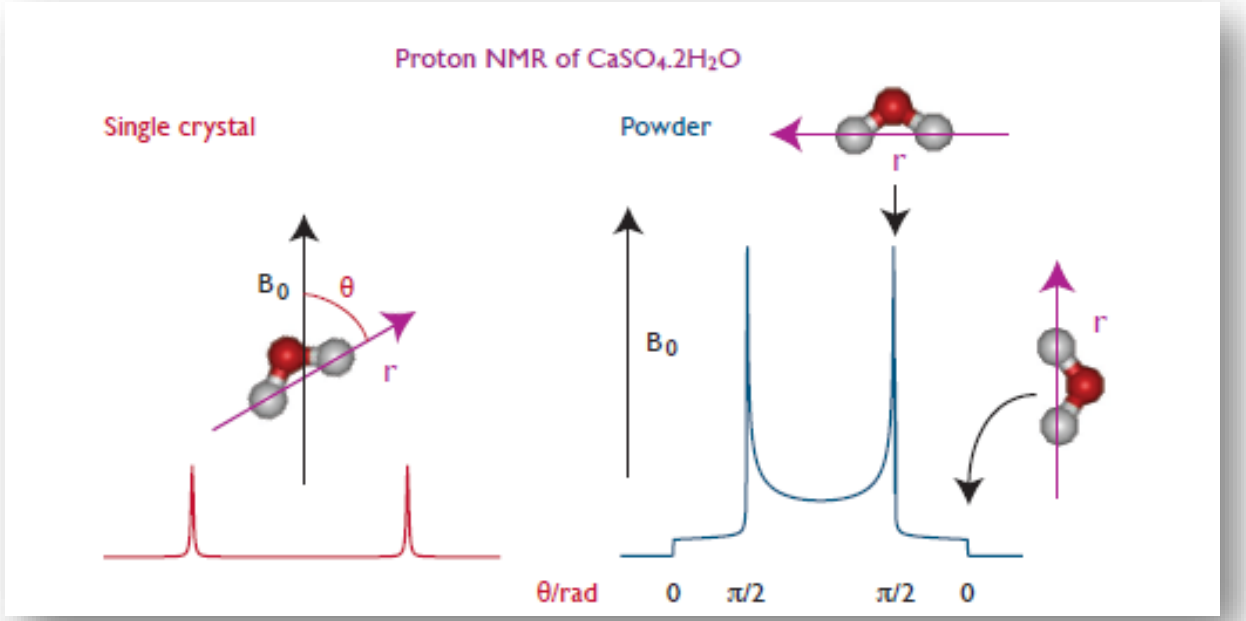


THE JOURNAL OF CHEMICAL PHYSICS VOLUME 16, NUMBER 4 APRIL, 1948

Nuclear Resonance Absorption in Hydrated Crystals: Fine Structure of the Proton Line

G. E. PAKE*

Lyman Laboratory of Physics, Harvard University, Cambridge, Massachusetts

(Received December 2, 1947)

Typical Distances and couplings in proteins

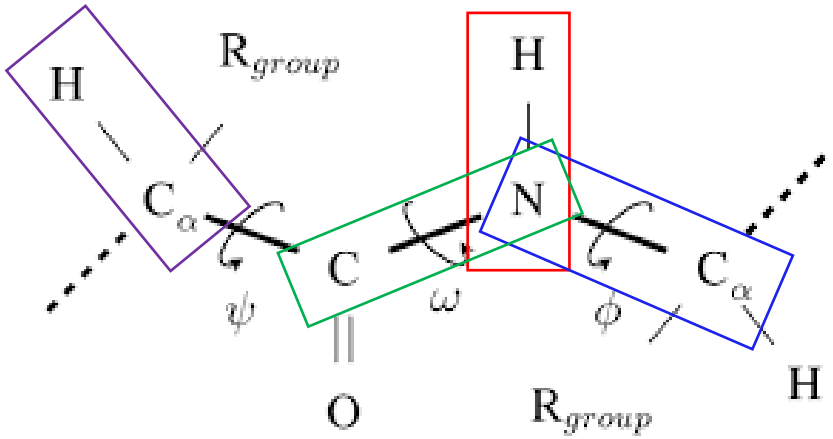

H-Cα, 1.09A, 20 kHz

H-N, 1.02A, 11.5 kHz

N-C', 1.32A, 1.5 kHz

N-Cα, 1.46A, 1.0 kHz

$$d = \hbar\left(\frac{\mu_0}{4\pi}\right)\frac{\gamma_I\gamma_S}{r^3}$$

$$= 66.26\frac{\gamma_I\left[\frac{MHz}{T}\right]\gamma_S\left[\frac{MHz}{T}\right]}{r^3[\dot{A}]}$$

Order parameter, dynamics averaging

$$S = \frac{D_{measured}}{D_{calculated}}$$

$S = 1: Rigid$
$S = 0: Isotropic$

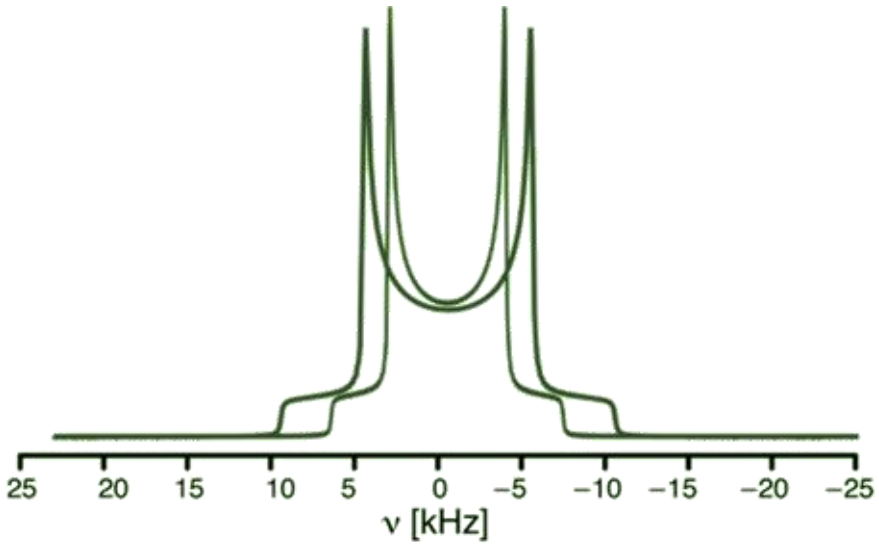

Diffusion/jump **on** a cone

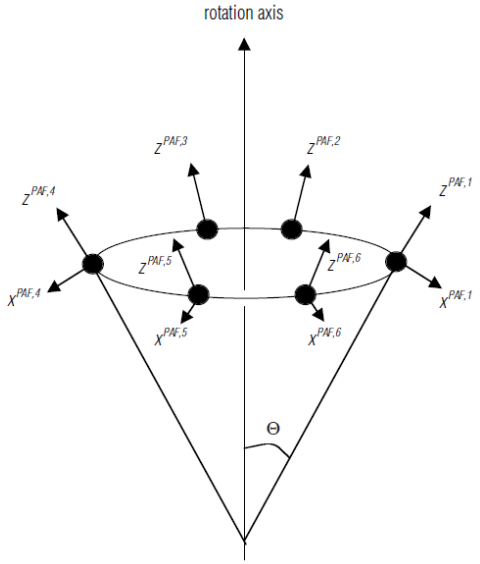

$$S = \frac{1}{2}(3\cos^2\beta - 1)$$

Diffusion **in** a cone

$$S = \cos(\alpha)(1 + \cos(\alpha))/2$$

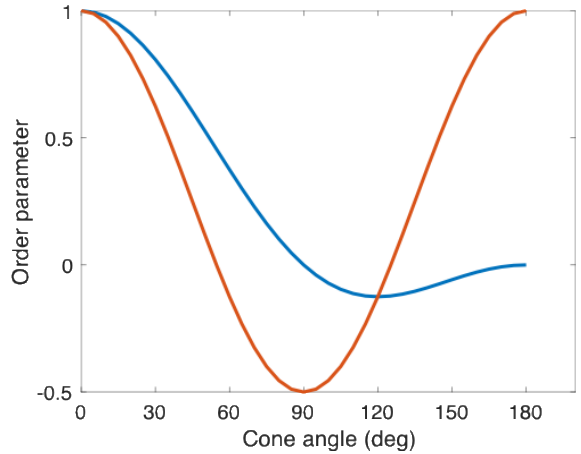

Dipolar interaction under MAS

$$H_D^{LAB} = d \cdot \{A_1 \cos(\omega_R t + \gamma) + A_2 \cos(2\omega_R t + 2\gamma)\}(3I_z S_z - I \cdot S)$$

$$A_1 = \frac{\sqrt{2}}{2}\delta \sin 2\beta\left(1 + \frac{\eta}{3}\cos 2\alpha\right)$$

$$A_2 = \frac{1}{2}\delta\left(\cos^2\beta - 1 + \frac{\eta}{3}\cos^2\beta \cos 2\alpha\right)$$

$$\omega_D(t) = d \sum_{m=-2,2} g_m^Q e^{im(\omega_R t + \gamma)}$$

Dipolar recoupling - multiple techniques

- REDOR
- DIPSHIFT
- Lee-Goldburg Cross-polarization
- Cross-polarization (with variable contact – CPVC) – high spinning
- PARS/wPARS (symmetry-based)
-
-

DIPSHIFT – measuring H-C, H-N couplings

Intermediate motions as studied by solid-state separated local field NMR experiments

J. Chem. Phys. **128**, 104505 (2008)

Eduardo Ribeiro deAzevedo,[1,a] Kay Saalwachter,[2] Ovidiu Pascui,[2] André A. de Souza,[1] Tito J. Bonagamba,[1] and Detlef Reichert[2]

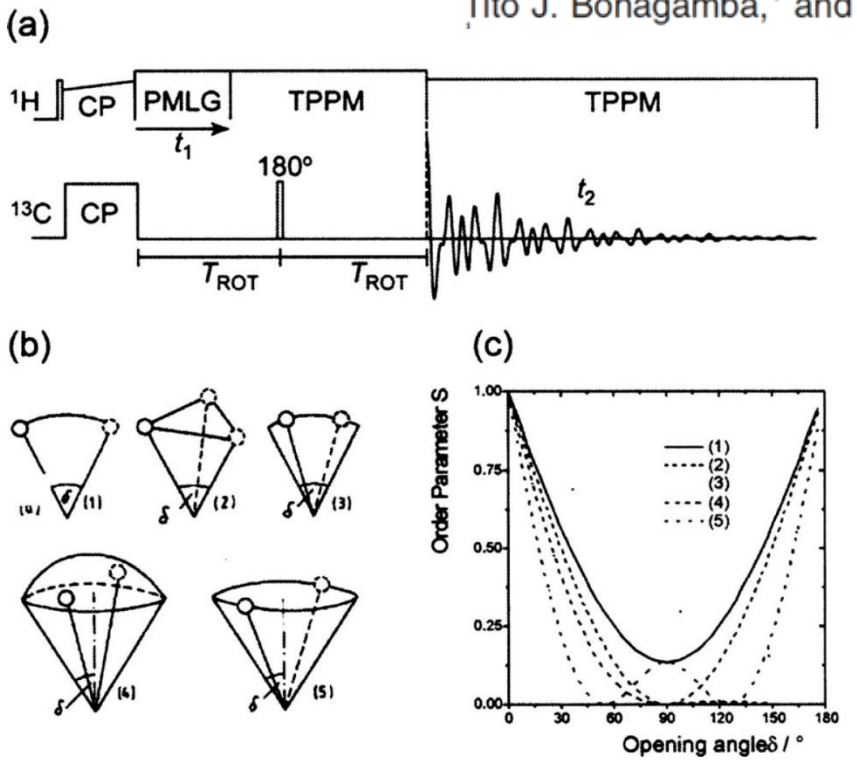

FIG. 1. (a) DIPSHIFT pulse sequence. (b) Depiction of some selected motional geometries, and (c) the behavior of the corresponding order parameters as a function of the motional amplitude (opening angle).

23 kHz, 64 deg

Fast (k>d) motion

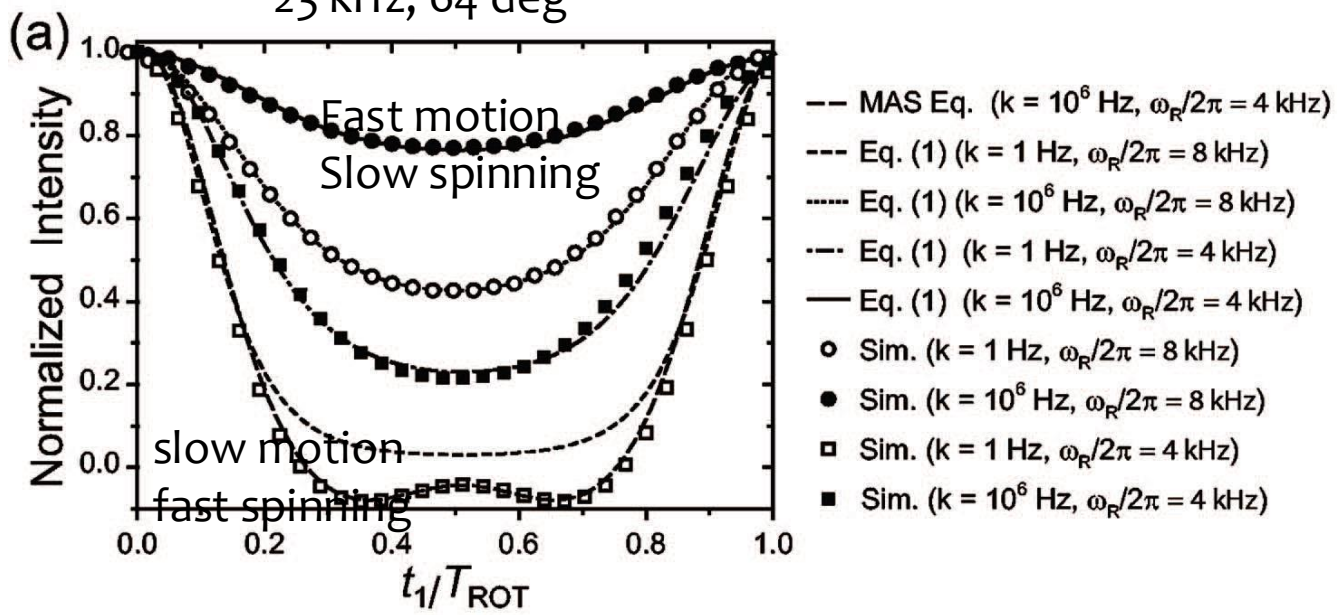

Original SLF experiments: Munowitch & Griffin, JACS 103, 2529, 1981; JCP 76, 2848, 1982

DIPSHIFT: A note about time scales

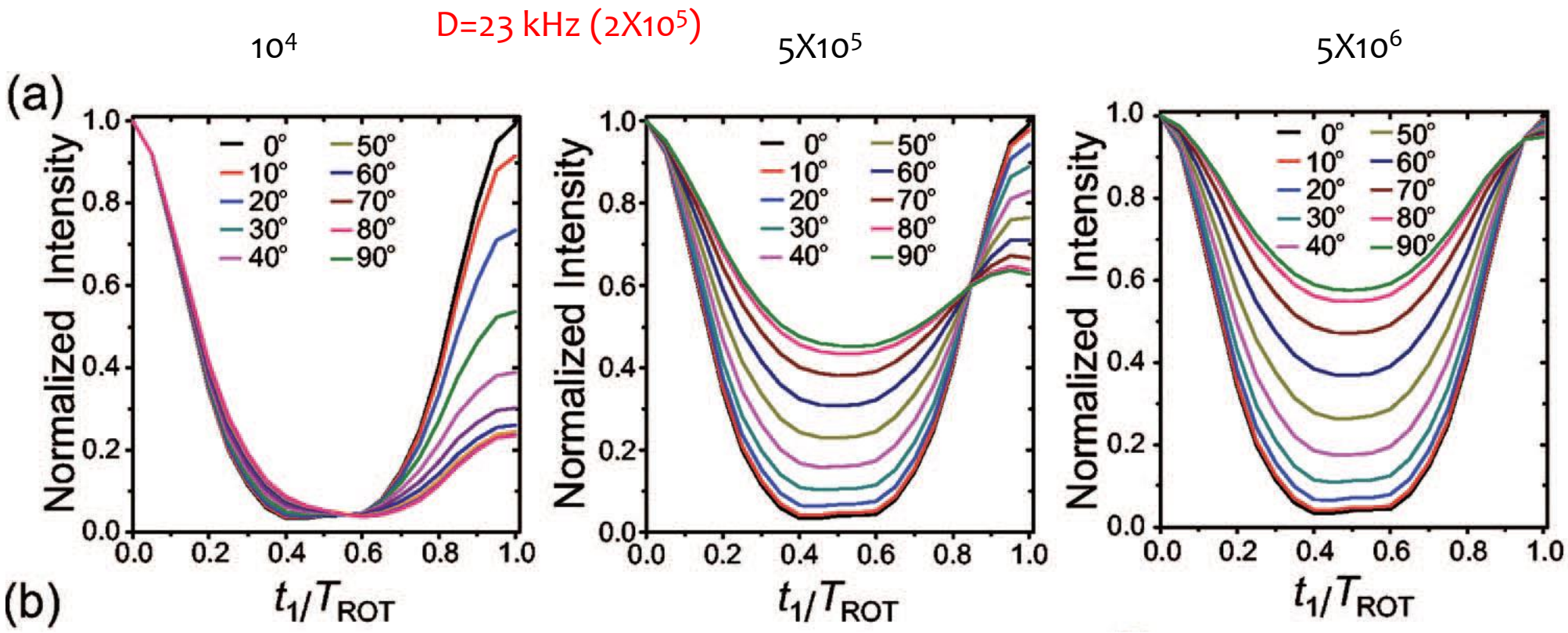

Slow motion, T2 dominates

Fast motion, cone angle dominates

recoupled dipshift: Hong, … Schmidt-Rohr, JMR 129, 85, 1997

DIPSHIFT versions in biological systems

Site-Resolved Backbone and Side-Chain Intermediate Dynamics in a Carbohydrate-Binding Module Protein Studied by Magic-Angle Spinning NMR Spectroscopy

Hadar Ivanir-Dabora,[a] Evgeny Nimerovsky,[a] P. K. Madhu,*[b, c] and Amir Goldbourt*[a]

Improved dipolar recoupling with 2 π pulses (see REDOR below)

Chem. Eur. J. **2015**, *21*, 10778 – 10785

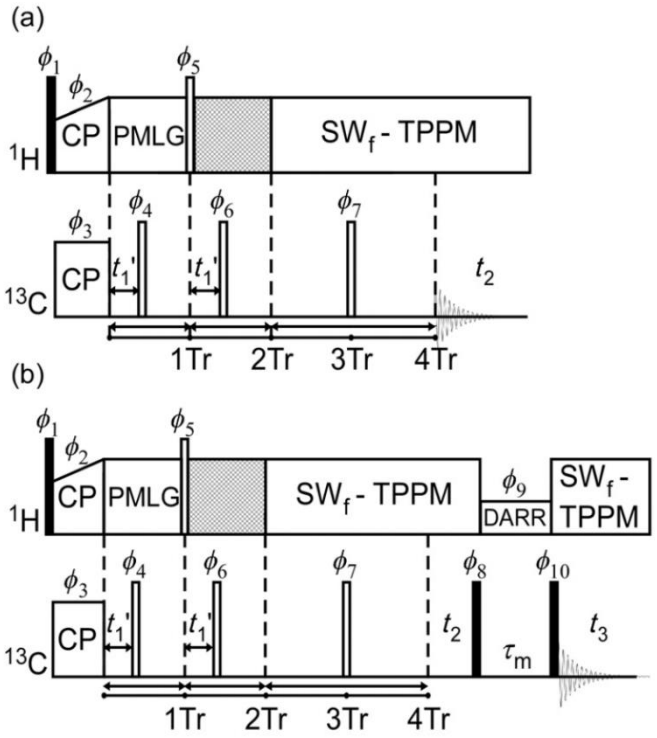

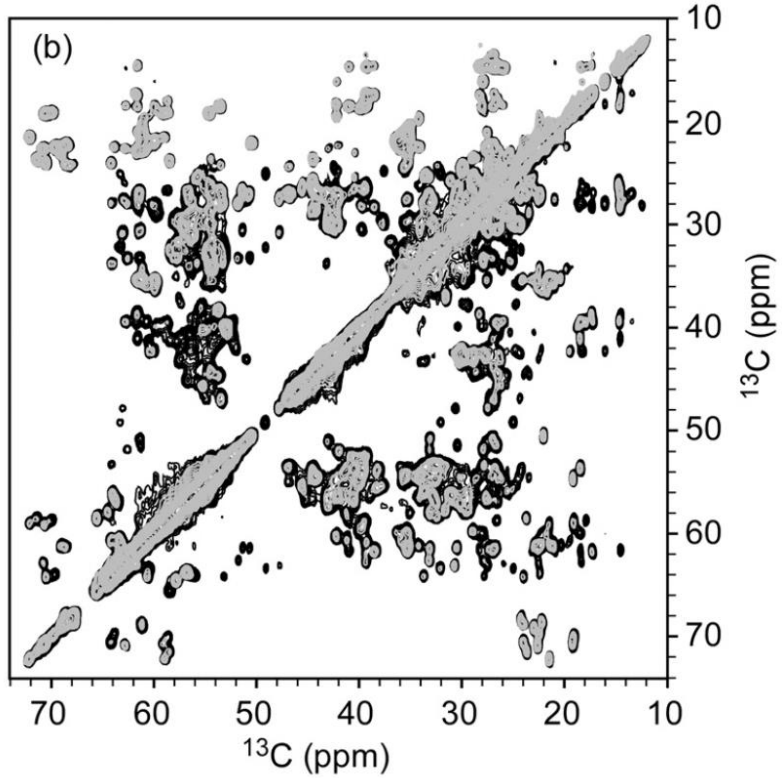

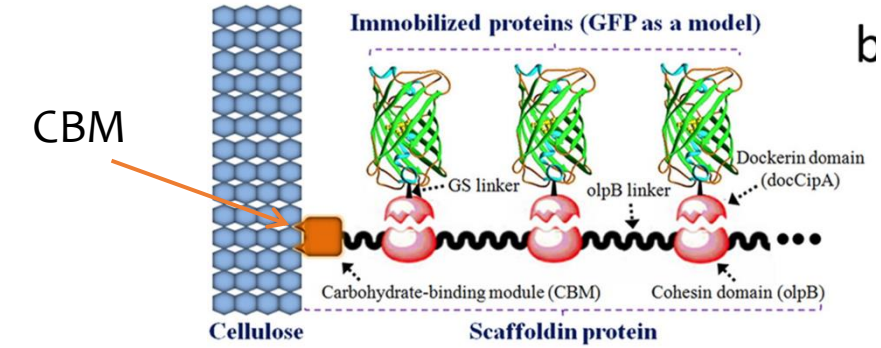

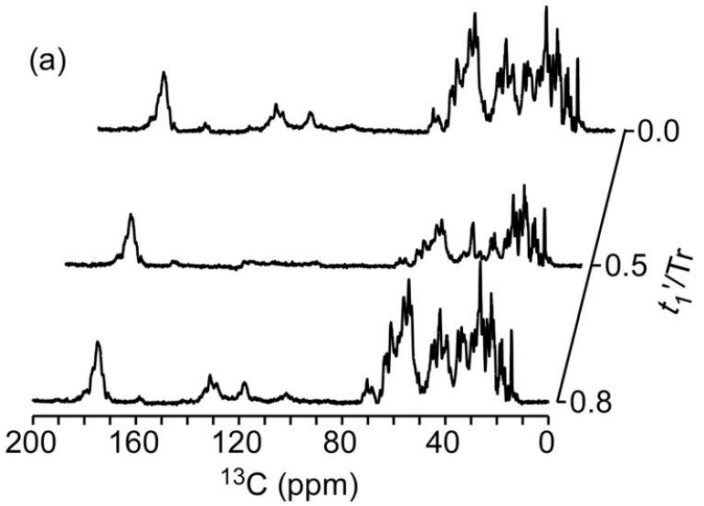

CBM protein – cont.

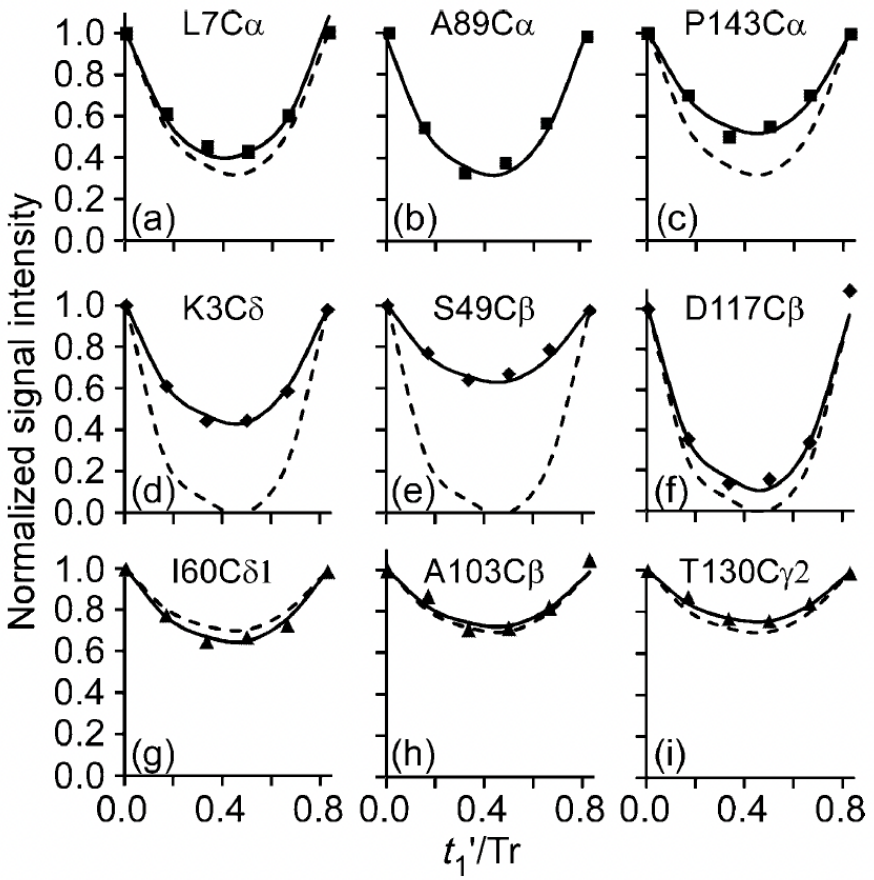

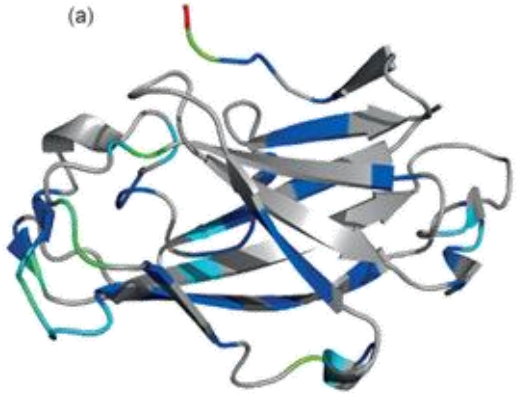

Table 1. Assignment, effective ^{1}H-^{13}C dipolar coupling (D_{eff}), order parameters, R^2 values, and secondary structure details for the curves shown in Figure 3.

Curve	Assignment[51]	D_{eff} [kHz]	Order parameter	R^2	Secondary structure[a]
a	L7Cα	18.0 ± 1.0	0.90 ± 0.05	0.010	β-sheet
b	A89Cα	20.0 ± 1.0	1.00 ± 0.05	0.006	β-turn
c	P143Cα	16.0 ± 1.0	0.80 ± 0.05	0.004	C-terminus
d	K3Cδ	17.6 ± 1.4	0.65 ± 0.05	0.002	β-sheet
e	S49Cβ	13.5 ± 1.4	0.50 ± 0.05	0.003	loop
f	D117Cβ	24.3 ± 1.4	0.90 ± 0.05	0.017	loop
g	I60Cδ1	10.8 ± 0.2	0.30 ± 0.02	0.001	loop
h	A103Cβ	11.4 ± 0.2	0.31 ± 0.02	0.008	β-turn
i	T130Cγ2	13.2 ± 0.2	0.36 ± 0.02	0.002	β-sheet

RN-DIPSHIFT

Hou, … Polenova

J. Am. Chem. Soc. 2011, 133, 18646–18655

Homonuclear decoupling with R-sym

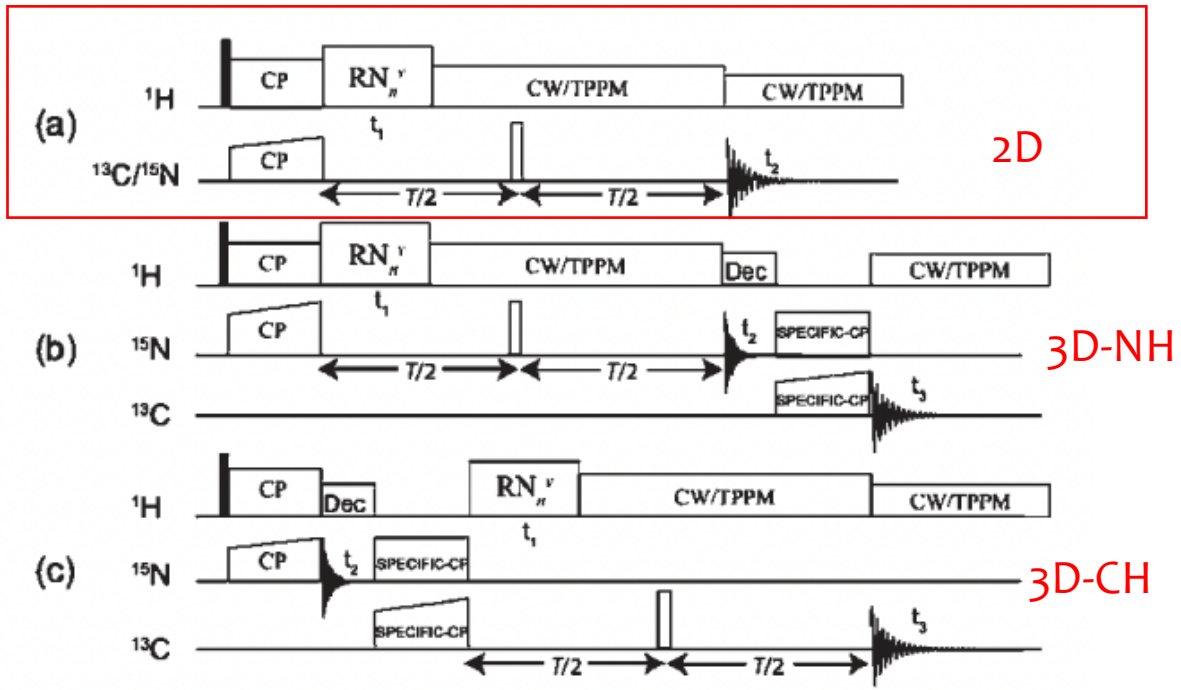

C-terminal domain of HIV-1 capsid protein :Tyrosine-labeled

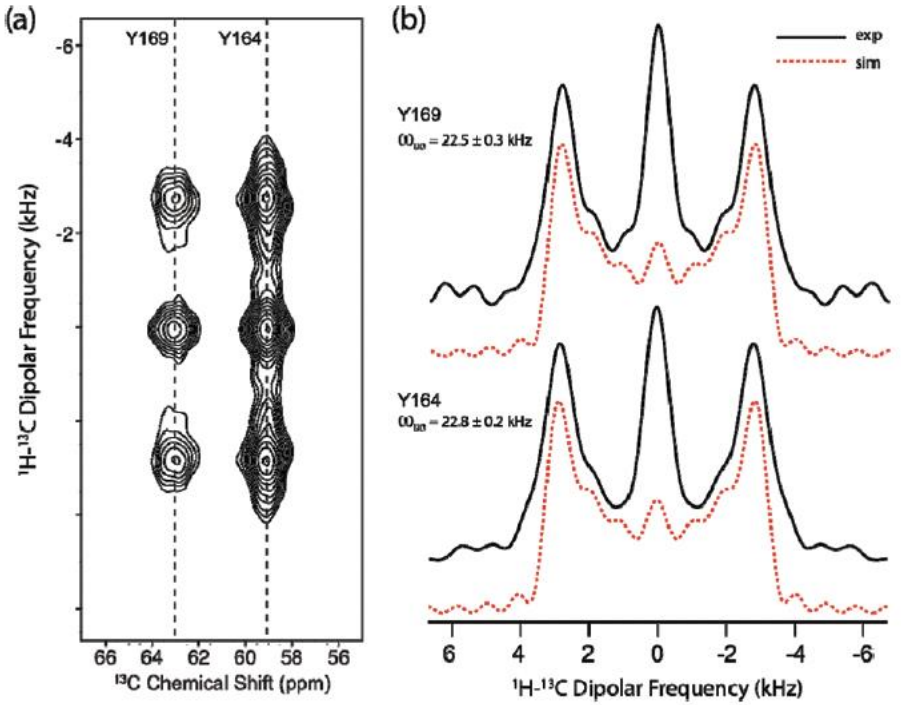

Figure 3. (a) Two-dimensional ^{1}H−^{13}C R16$_3^2$-based DIPSHIFT spectrum of [U-^{13}C,^{15}N]-Tyr HIV-1 C-terminal domain (CTD) of CA protein recorded at the MAS frequency of 40 kHz. The pulse

RN-DIPSHIFT

Hou, … Polenova

J. Am. Chem. Soc. 2011, 133, 18646–18655

Homonuclear decoupling with R-sym

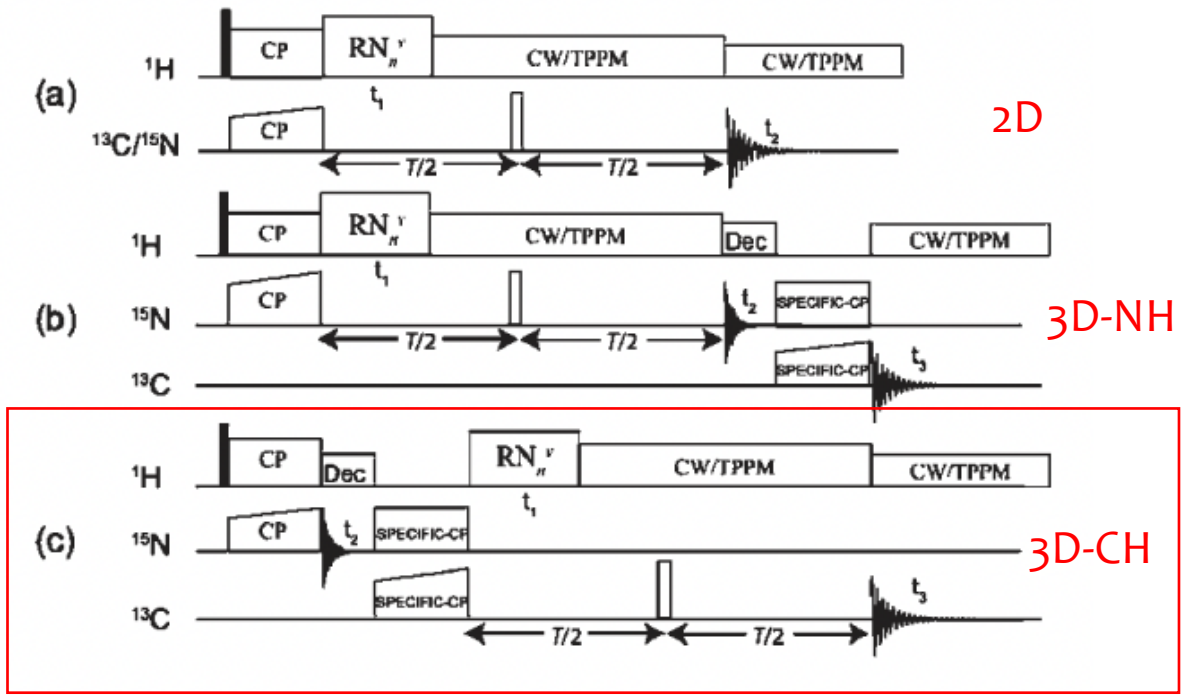

N-H dipolar coupling
Resolved on N-C spectrum

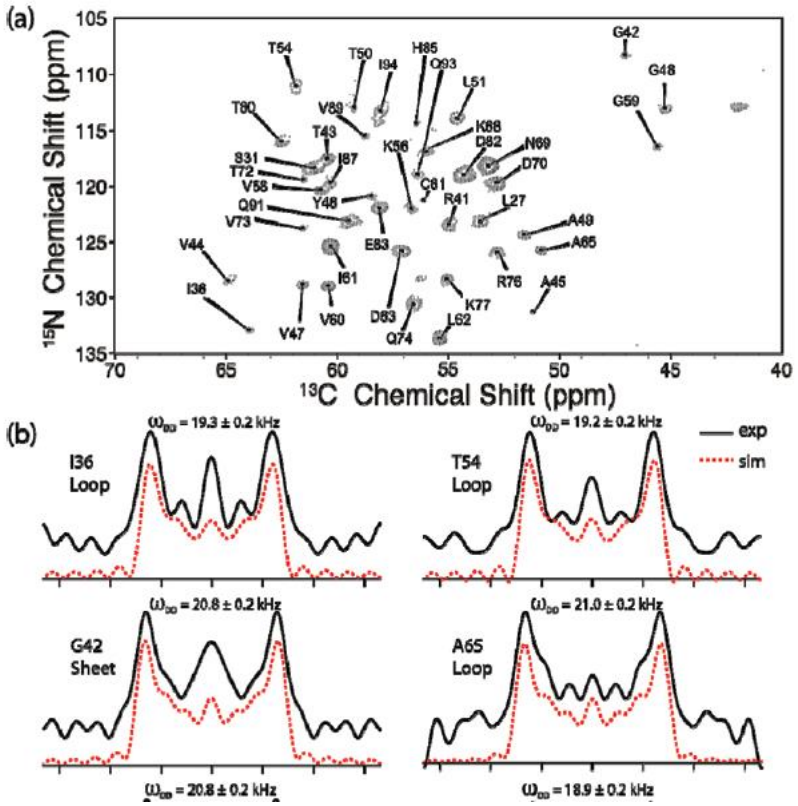

System: CAP-Gly domain of dynactin

(associated with microtubule function)

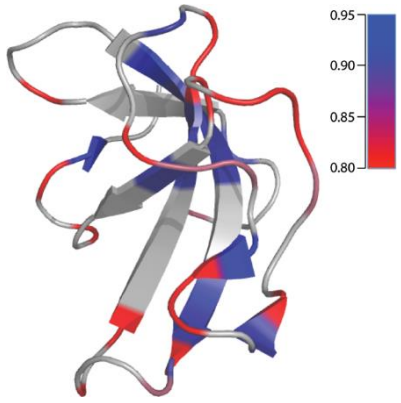

PARS-DIPSHIFT : supress ^{1}H CSA

Hou, … Polenova

J. Am. Chem. Soc. 2011, 133, 18646–18655

Homonuclear decoupling with R-sym

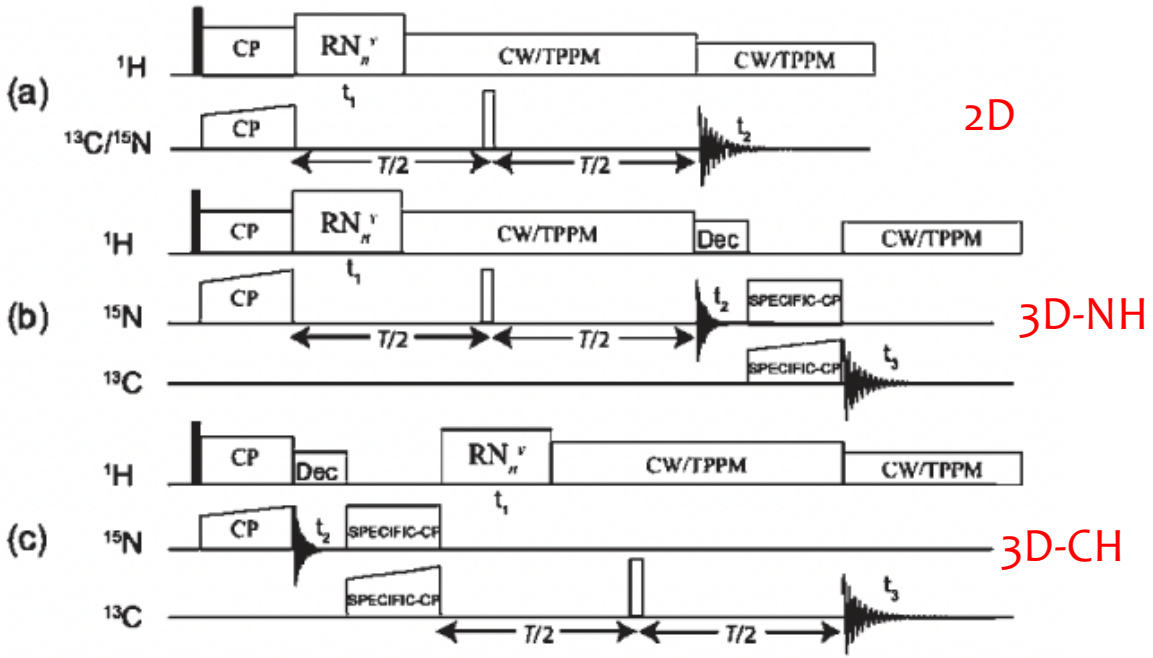

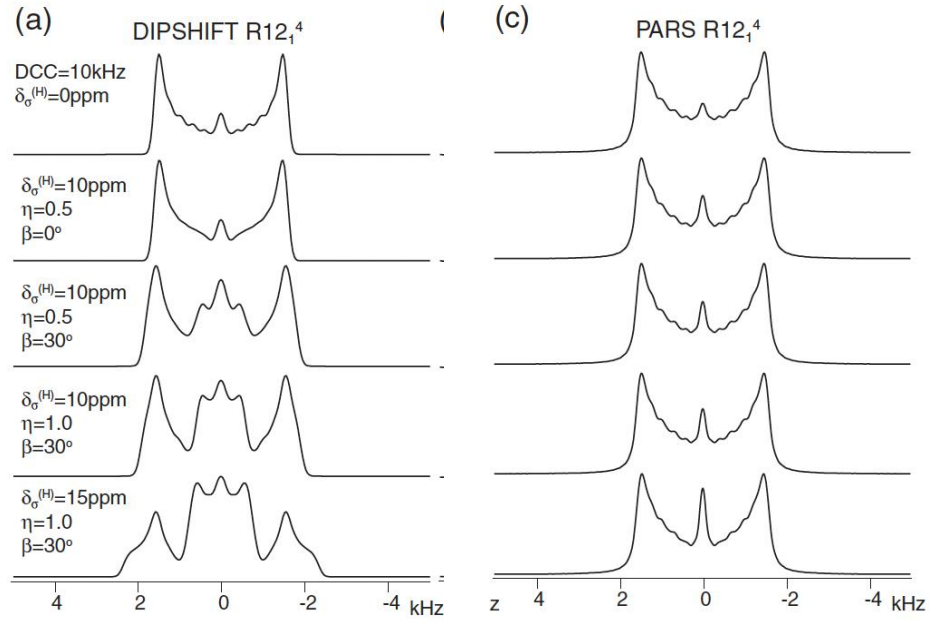

: J. Chem. Phys. **141**, 104202 (2014)

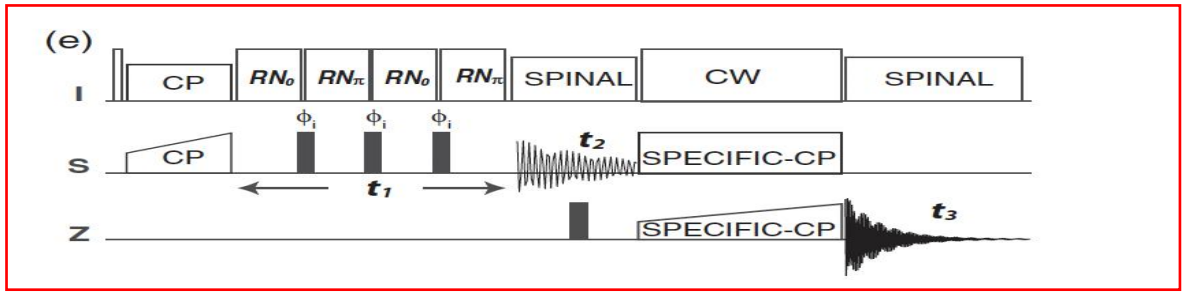

Results – LC8 protein

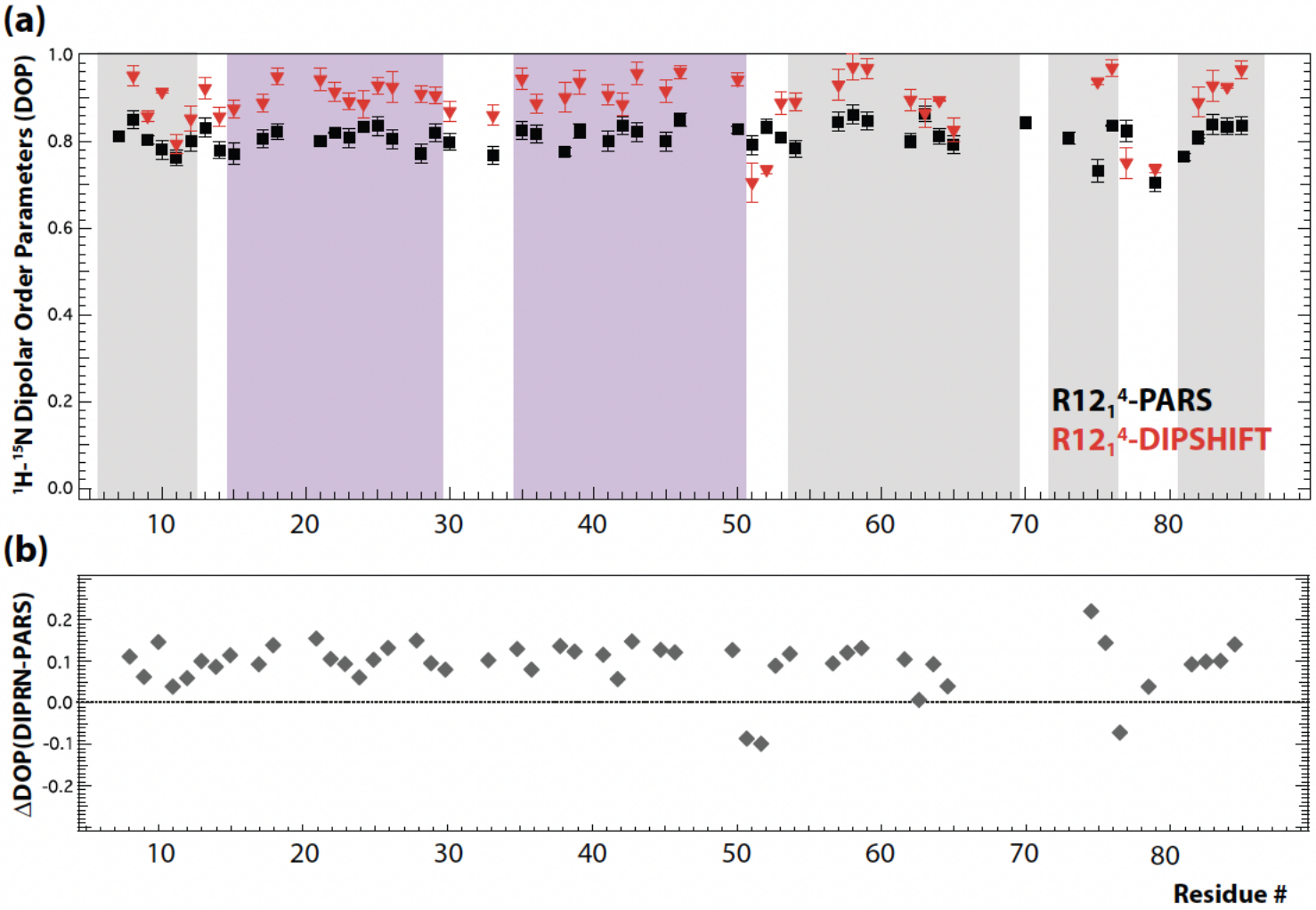

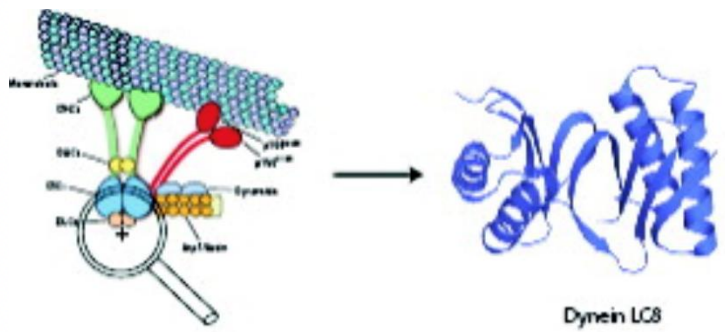

Microtubulin binding protein

NH and CH coupling via Cross-polarization

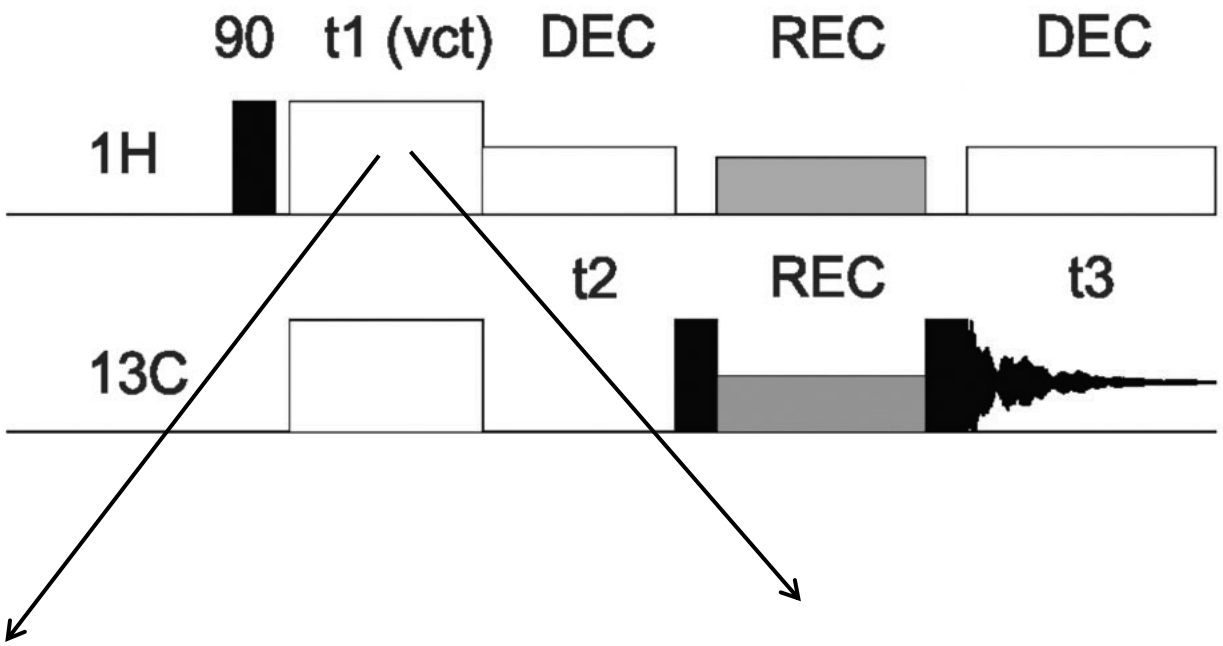

LGCP - moderate spinning
H-H coupling removed by multiple-pulse technique

CP - fast enough spinning
H-H coupling removed by spinning

(note: DIPSHIFT relies on uncomplete averaging)

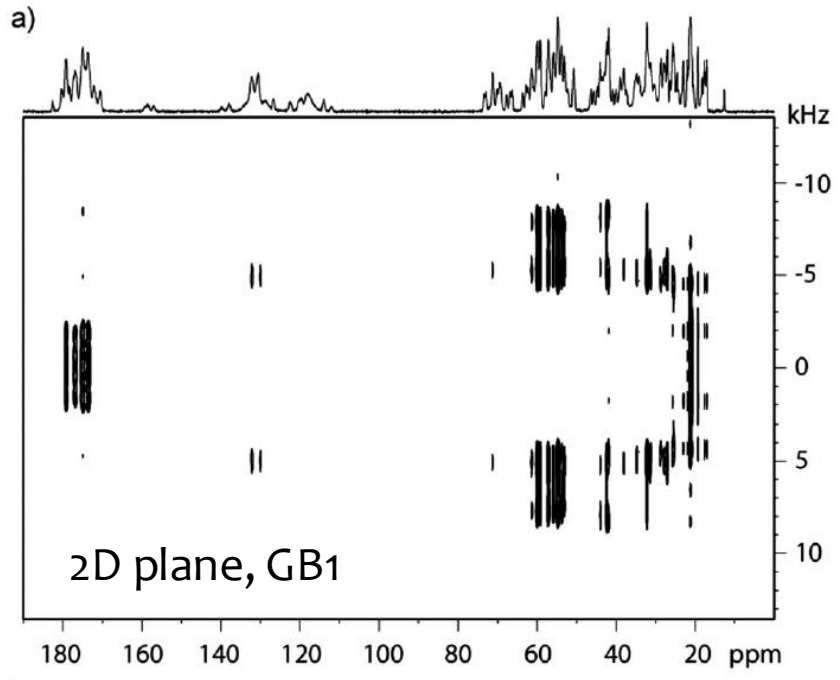

Paluch et al. PCCP 17, 28789, 2015

Examples – LGCP

Justin Lorieau and Ann E. McDermott*

Magn. Reson. Chem. 2006; **44**: 334–347

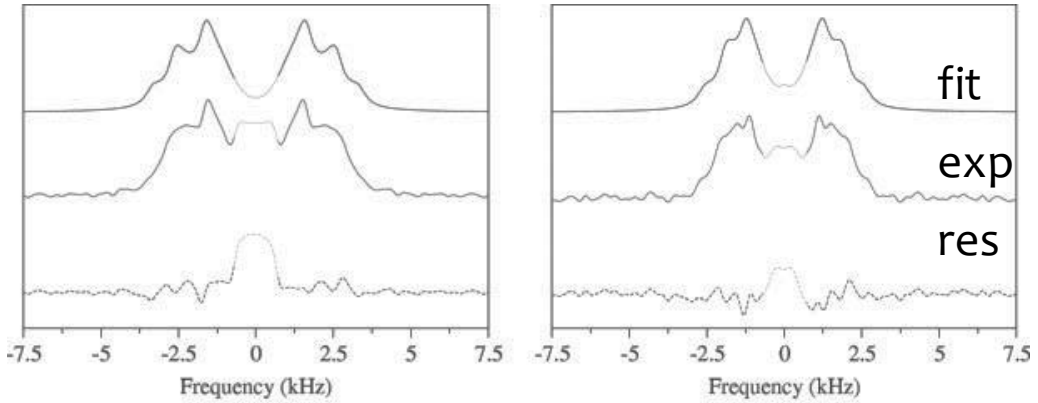

Rotamer 1:
D=5.5 kHz, S=0.23

Rotamer 2:
D=4.0 kHz, S=0.17

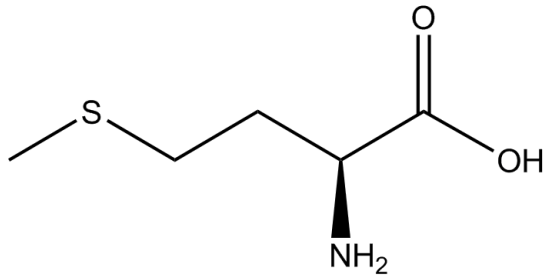

Oldfield, Biochemistry 22, p1917, 1982

^{2}H Quadrupolar NMR spectra of CD_3 Met:
Below zero: S=0.33; above zero: more motion

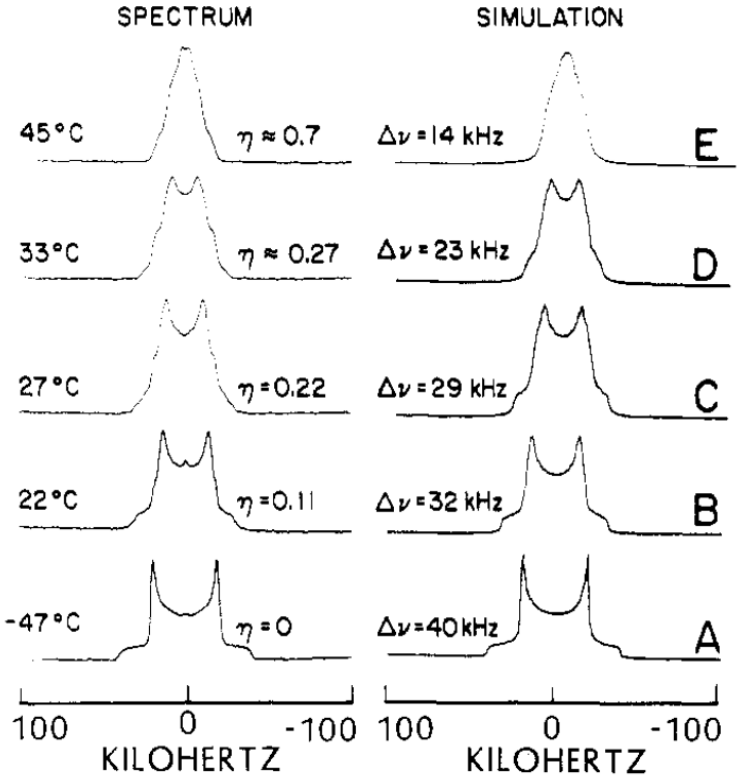

FIGURE 1: Deuterium NMR spectra obtained by using the quadrupole echo Fourier-transform method at 55.3 MHz (corresponding to a magnetic field strength of 8.45 T) of L-[ϵ-$^2H_3$]methionine, in the crystalline solid state as a function of temperature (left) together with some computer simulations (right) of the experimental spectra. The

LGCP-based dynamics in Pf1 phage

Conformational dynamics of an intact virus: Order parameters for the coat protein of Pf1 bacteriophage

Justin L. Lorieau*, Loren A. Day†, and Ann E. McDermott*‡

10366–10371 | PNAS | July 29, 2008 | vol. 105 | no. 30

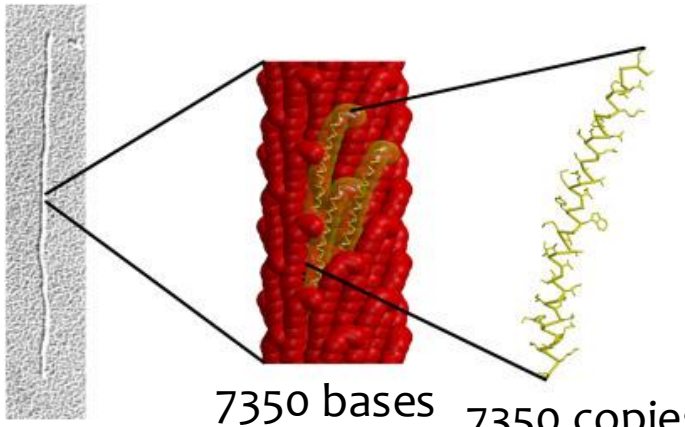

1μmX7nm

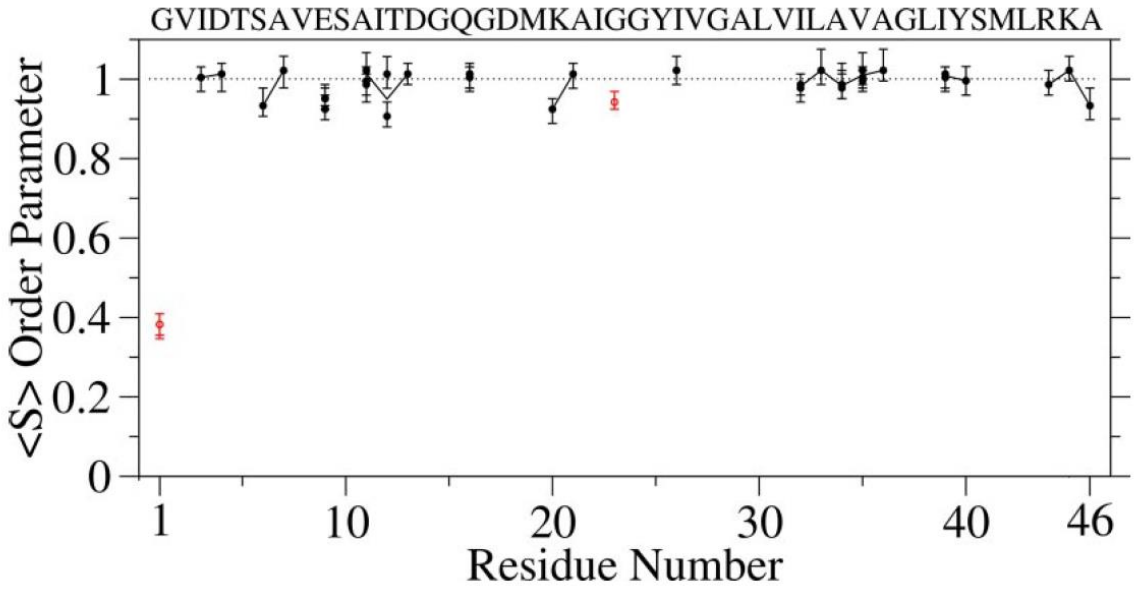

Table 1. Average solid-state NMR order parameters by side-chain position for the Pf1 virus

Spin system	Average	Minimum/maximum
$(^{13}C^{1}H)\alpha$	0.99 ± 0.04	0.91/1.02
$(^{13}C^{1}H)\beta$	0.88 ± 0.10	0.72/1.00
$(^{13}C^{1}H_2)\beta$	0.78 ± 0.17	0.60/1.00
$(^{13}C^{1}H_2)\gamma$	0.52 ± 0.17	0.28/0.81

LGCP-based dynamics in Pf1 phage

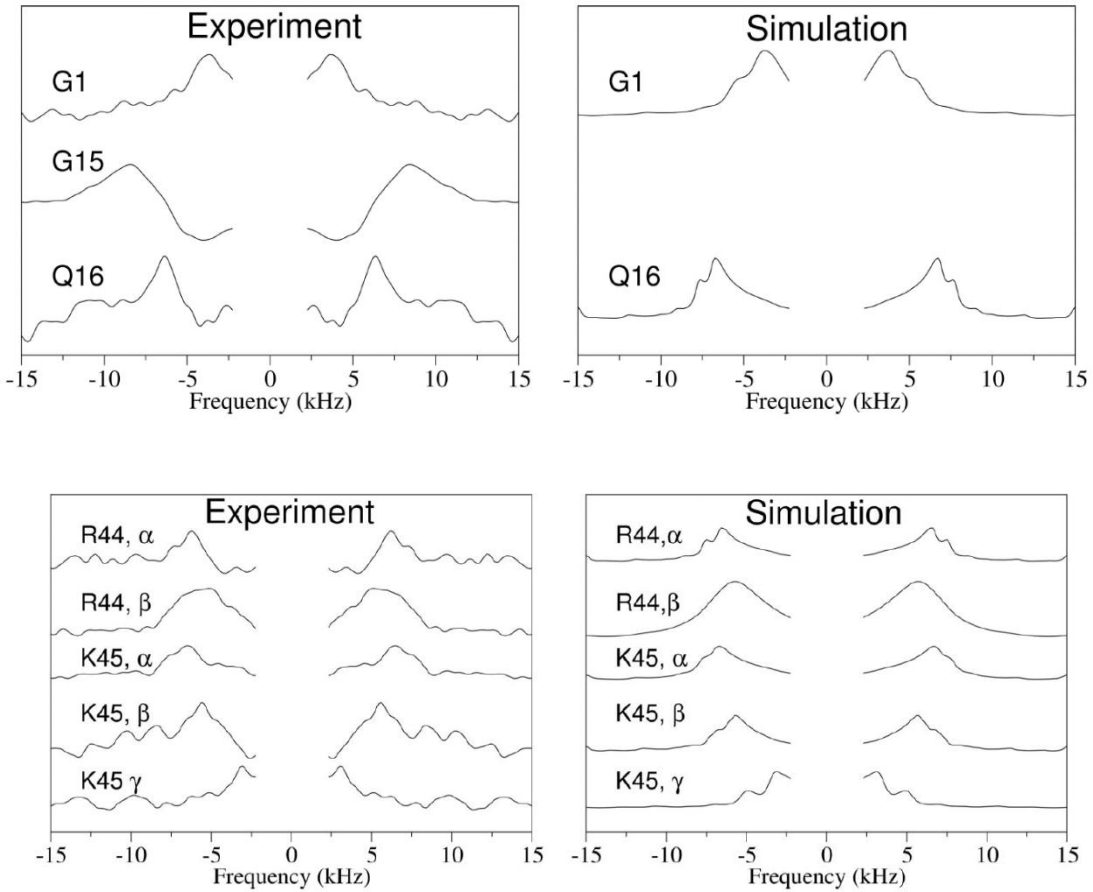

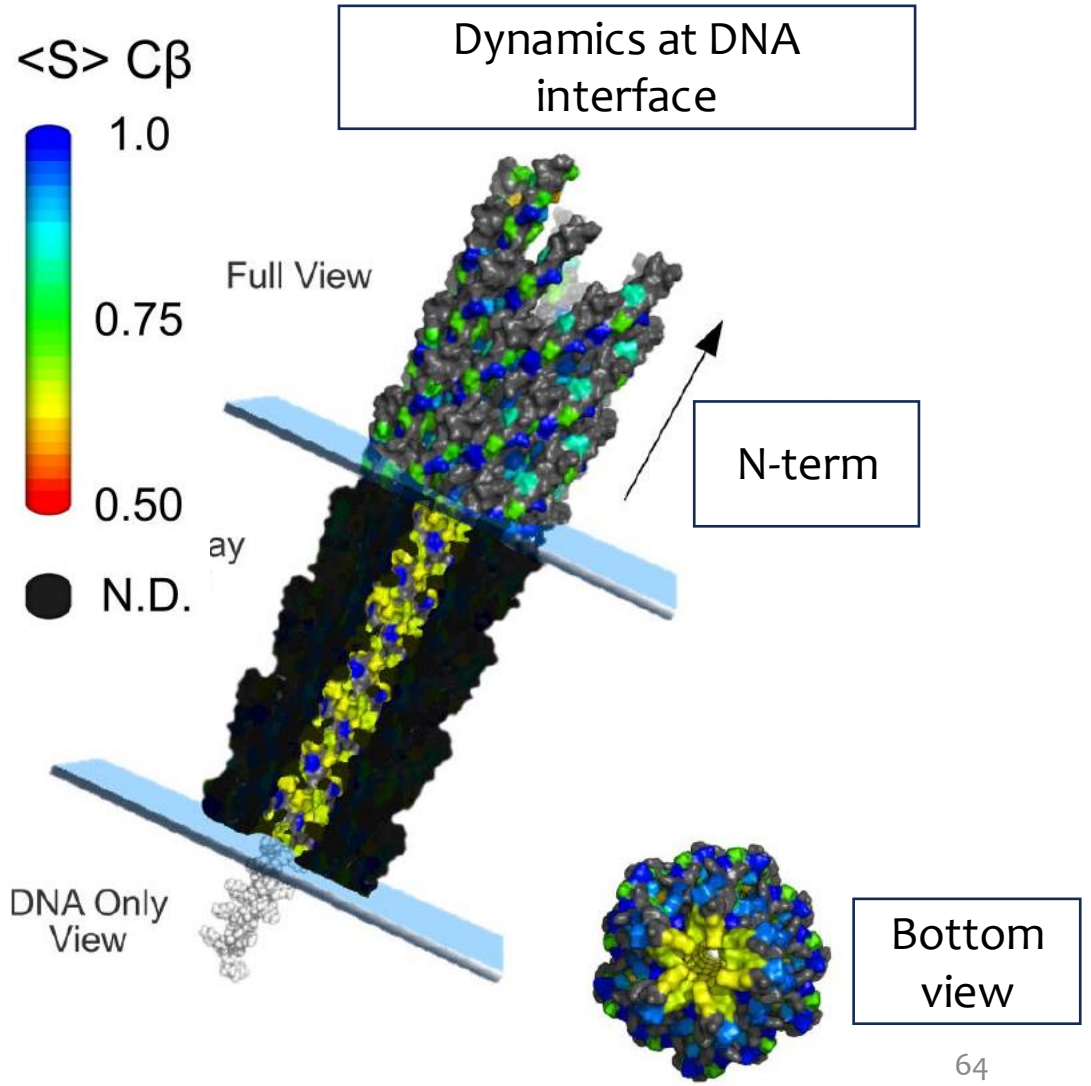

Cross-polarization at fast MAS

Analysis of local molecular motions of aromatic sidechains in proteins by 2D and 3D fast MAS NMR spectroscopy and quantum mechanical calculations†

Phys. Chem. Chem. Phys., 2015, **17**, 28789–28801

Piotr Paluch,[a] Tomasz Pawlak,[a] Agata Jeziorna,[a] Julien Trébosc,[b] Guangjin Hou,[c] Alexander J. Vega,[c] Jean-Paul Amoureux,[bd] Martin Dracinsky,*[e] Tatyana Polenova*[c] and Marek J. Potrzebowski*[a]

Cross-polarization at fast MAS

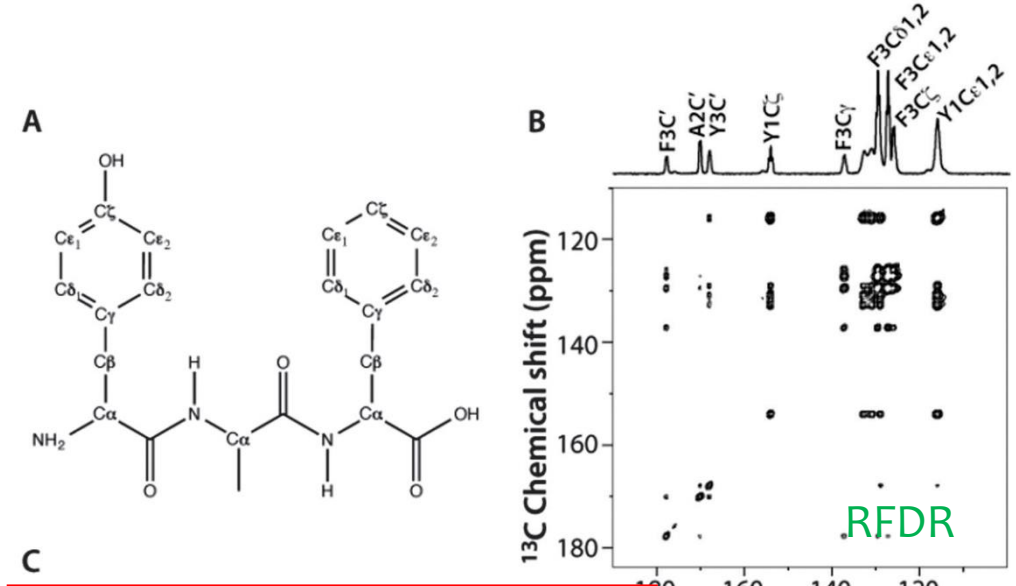

The dipolar tensor has assymetry due to motion

Ring flips of Phe but not Tyr

^{1}H-detected CP-based dipolar recoupling

Accurate Determination of Motional Amplitudes in Biomolecules by Solid-State NMR *ACS Phys. Chem Au* 2023, 3, 199–206

Veniamin Chevelkov, Sascha Lange, Henry Sawczyc, and Adam Lange*

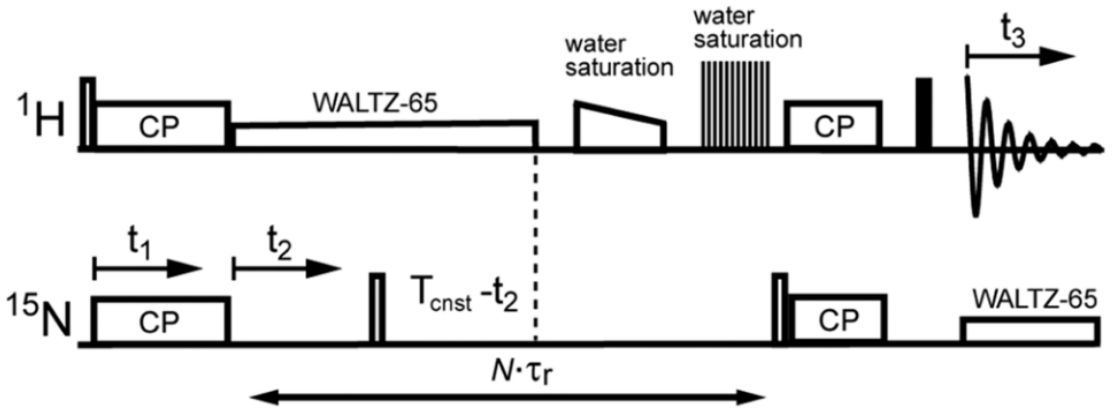

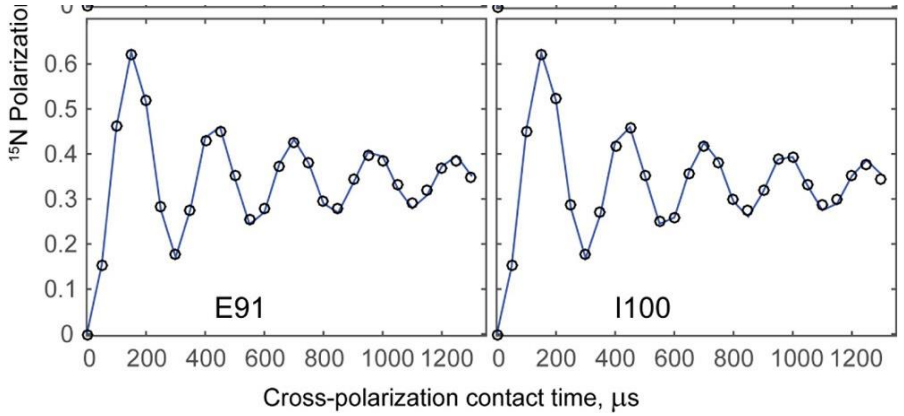

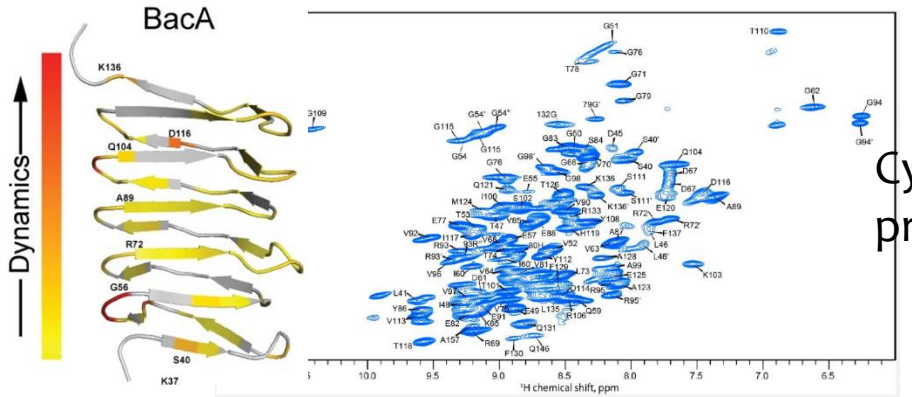

Cytoskeleton protein

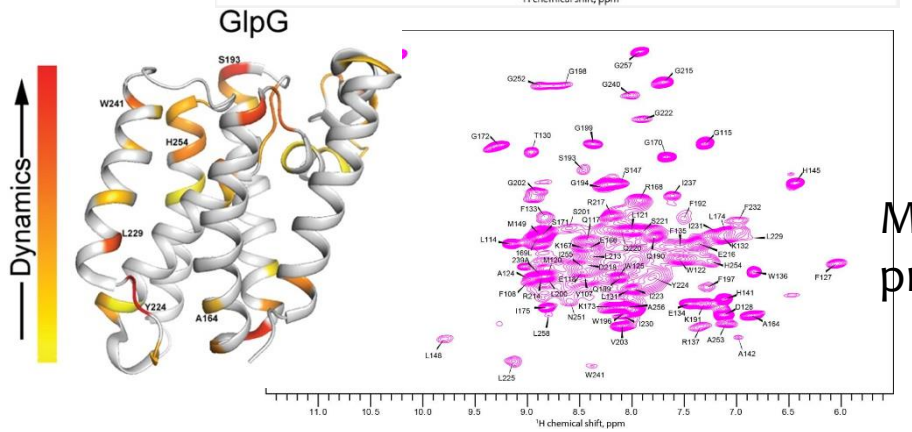

Membrane protein

Order parameters in diffusion cone angle

BacA

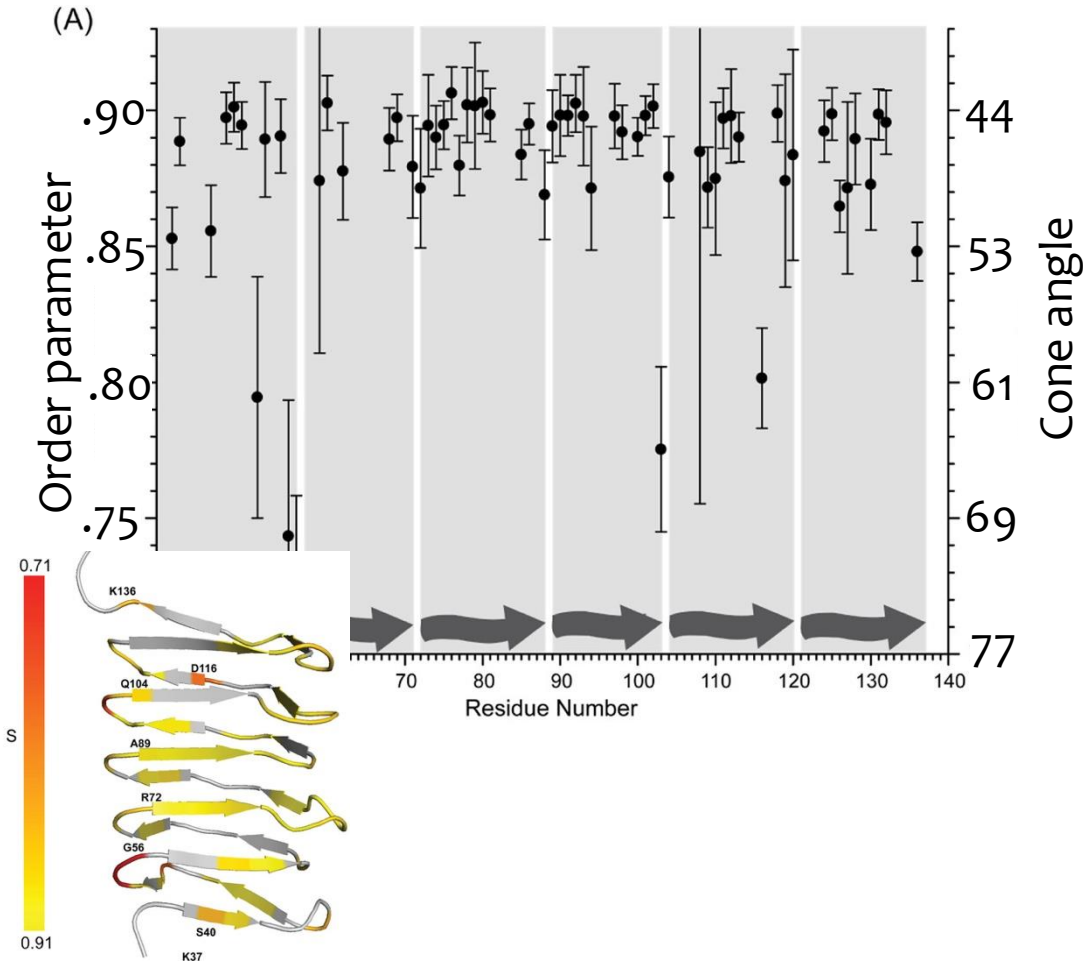

Carefull considertion of RF inhomogeniety

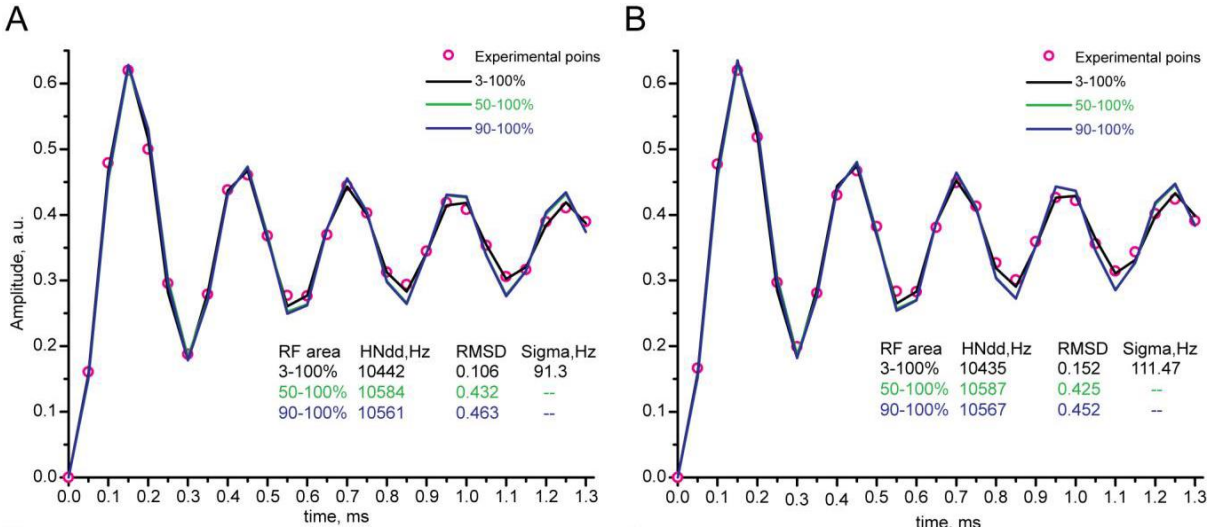

REDOR – C-N + H-X for fast spinning

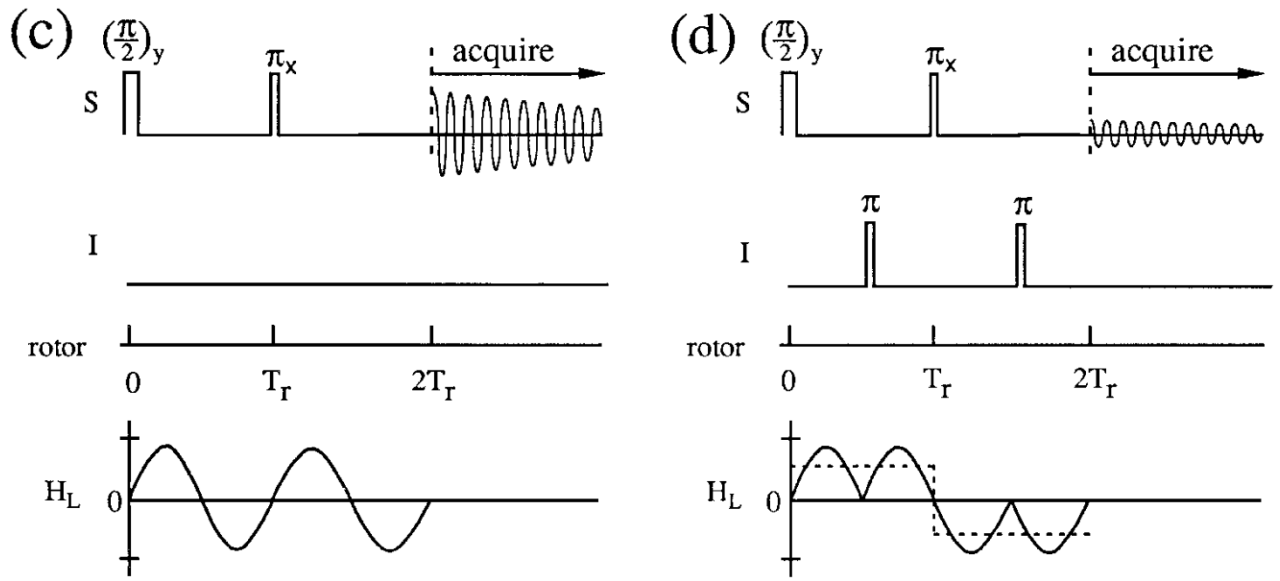

Concepts in Magnetic Resonance, Vol. 10(5) 277–289 (1998)

Terry Gullion

So: Run an experiment without I-spin pulse

S: Run an experiment with I-spin pulse

Repeat for N X TR cycles

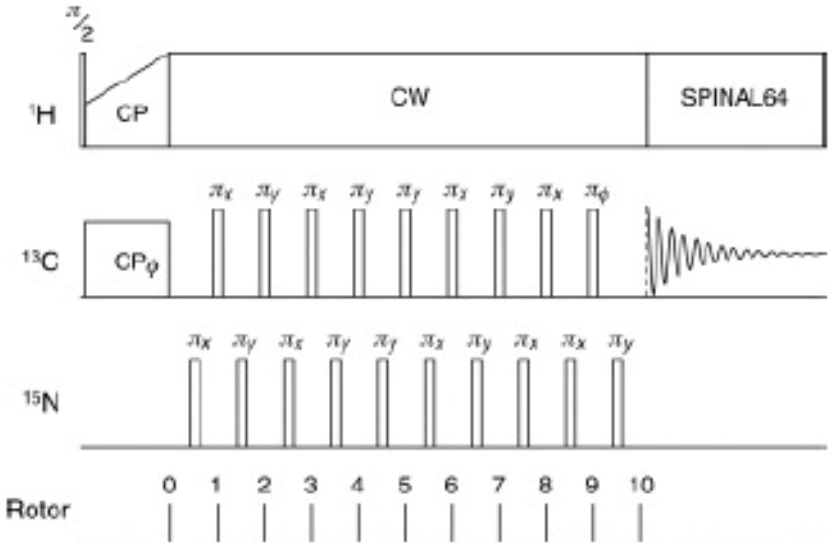

Measuring the dipolar interaction ‘d’ with REDOR

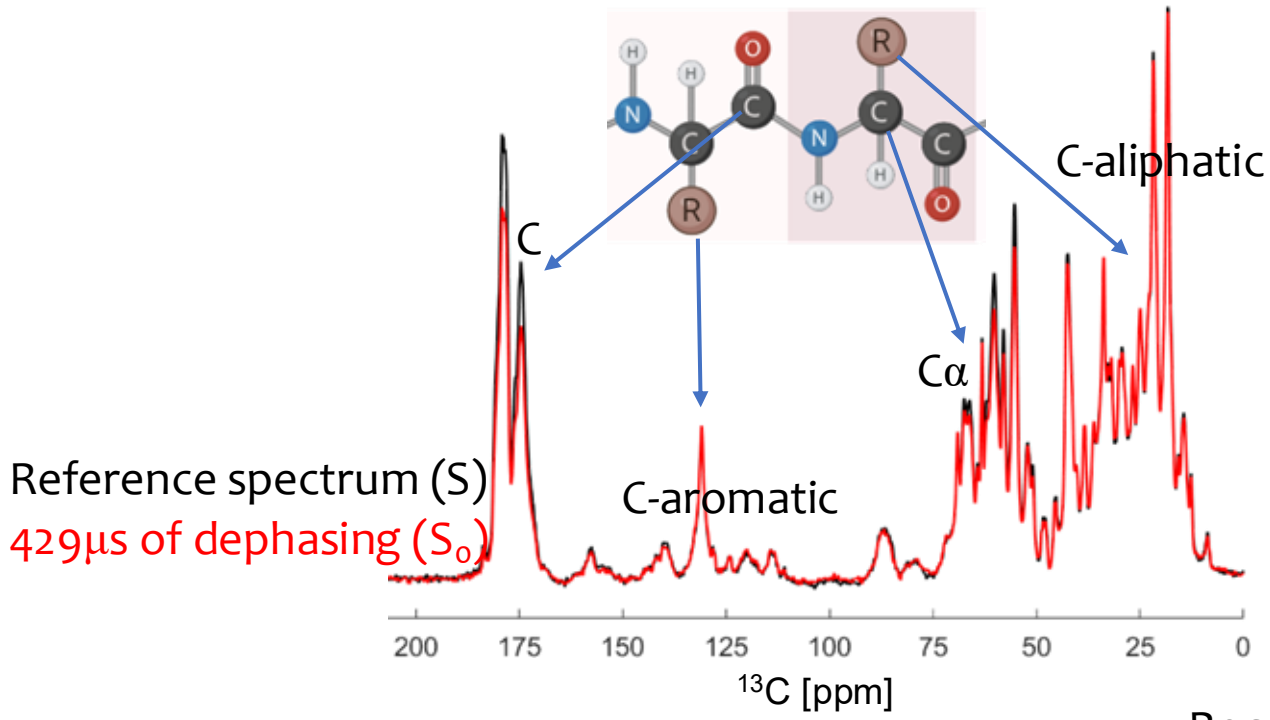

Reference spectrum (S)

429µs of dephasing (S_0)

$\frac{S}{S_0}$ | $1 - \frac{S}{S_0}$

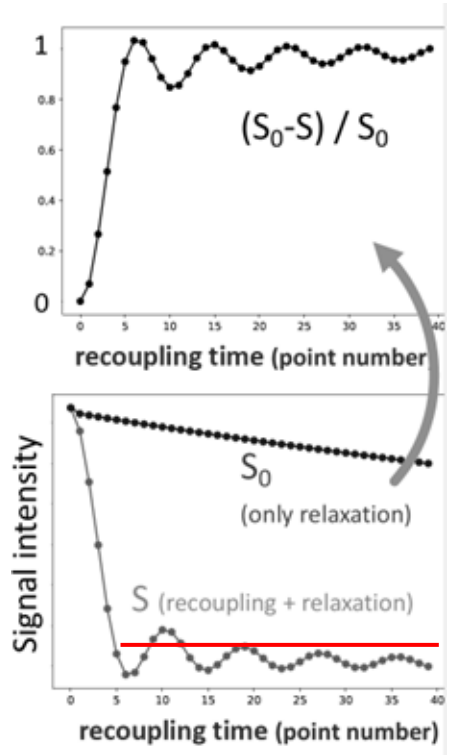

$$1 - \frac{S}{S_0} = 1 - \frac{\pi\sqrt{2}}{4} J_{1/4}(\sqrt{2}d\tilde{t}) J_{-1/4}(\sqrt{2}d\tilde{t})$$

Recoupling time

Effective Dipolar Constant

* T. Gullion, J. Schaefer; JMR (1989); 81 196-200; **K. T. Mueller; JMR (1995); 113 81-93

Averaged REDOR curves

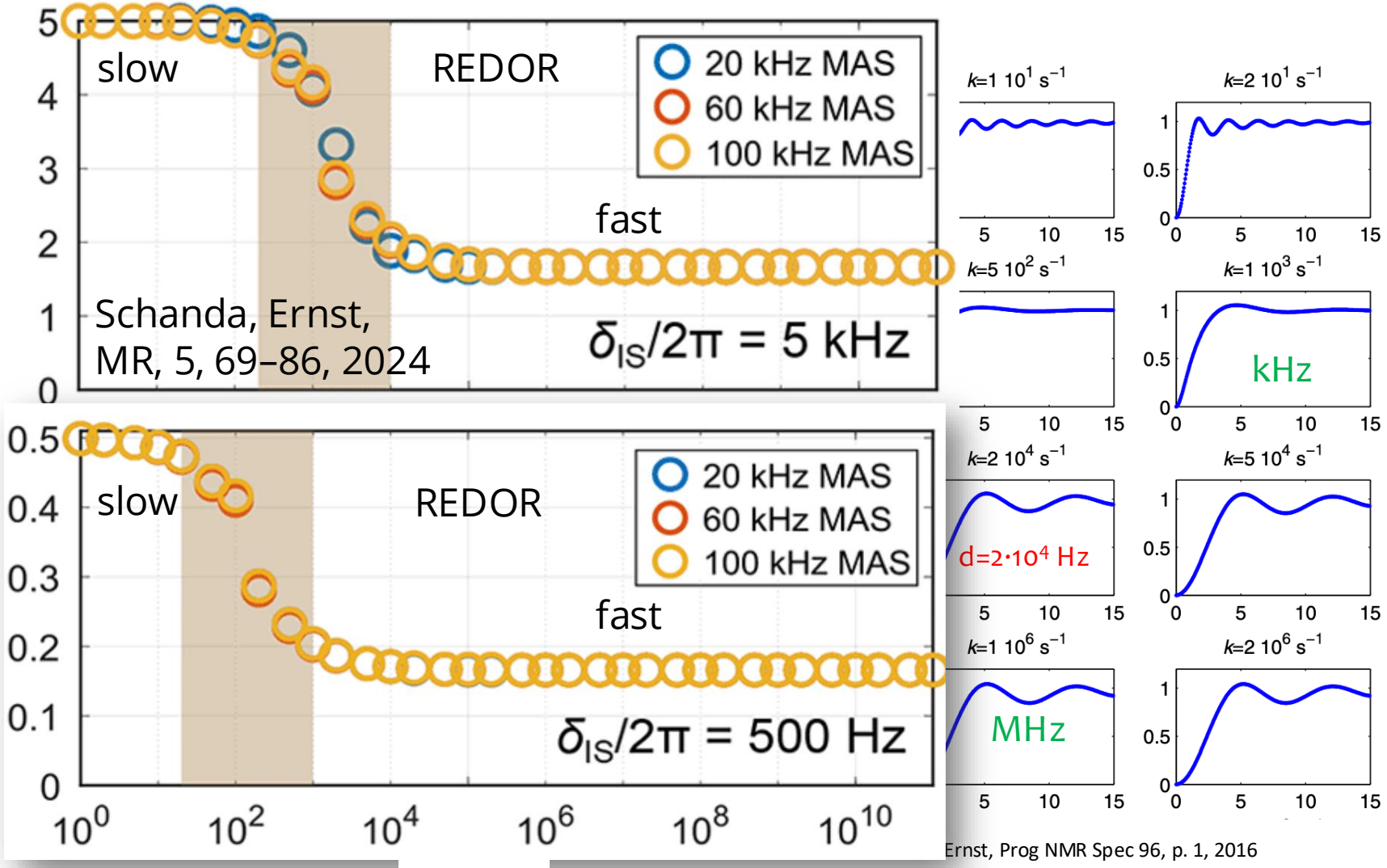

Assume 3-site jump
at rate k.
Interaction 20 kHz

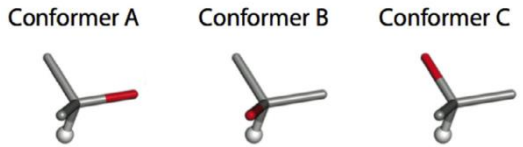

fast

Ernst, Prog NMR Spec 96, p. 1, 2016

Backbone dynamics via Psuedo-3D $^{13}C\{^{15}N\}$ REDOR

Dipolar-based (rigid-dynamic residues) Scalar-based (most dynamic residues)

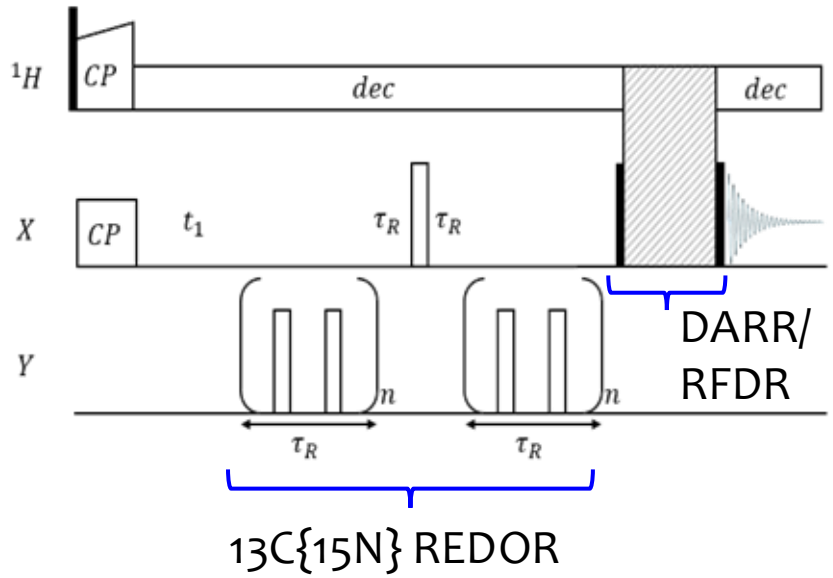

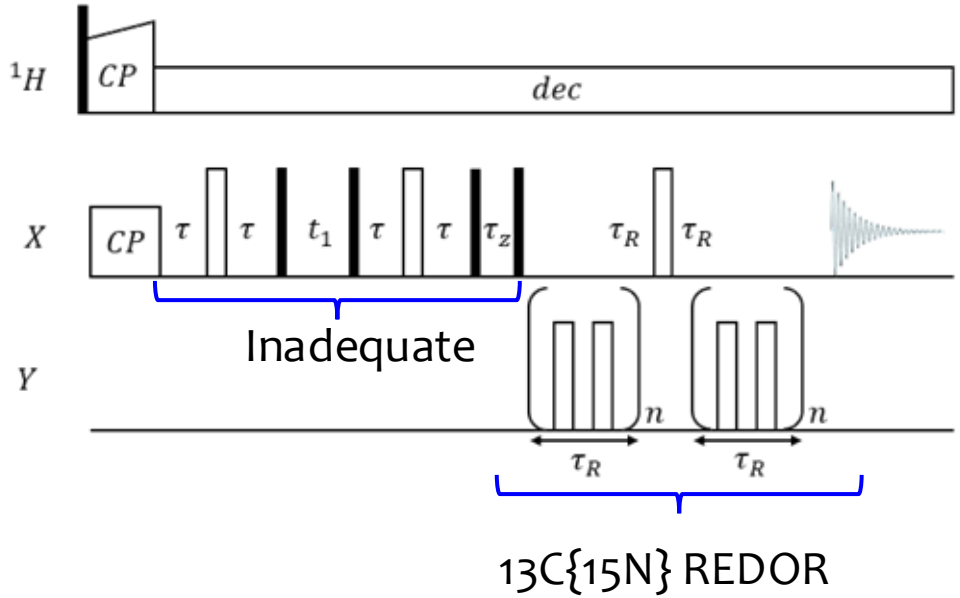

Time scale ~ 1 kHz

* O. S. Lusky, D. Sherer, A. Goldbourt; JACS AU, 4, 3619, 2024.

Homonuclear Recoupling techniques

- DARR (and variants) - Dipolar
- RFDR – Dipolar + scalar
- J-INADEQUATE – scalar, DQ-based

All start with CP – ensuring residues with S>0 are detected

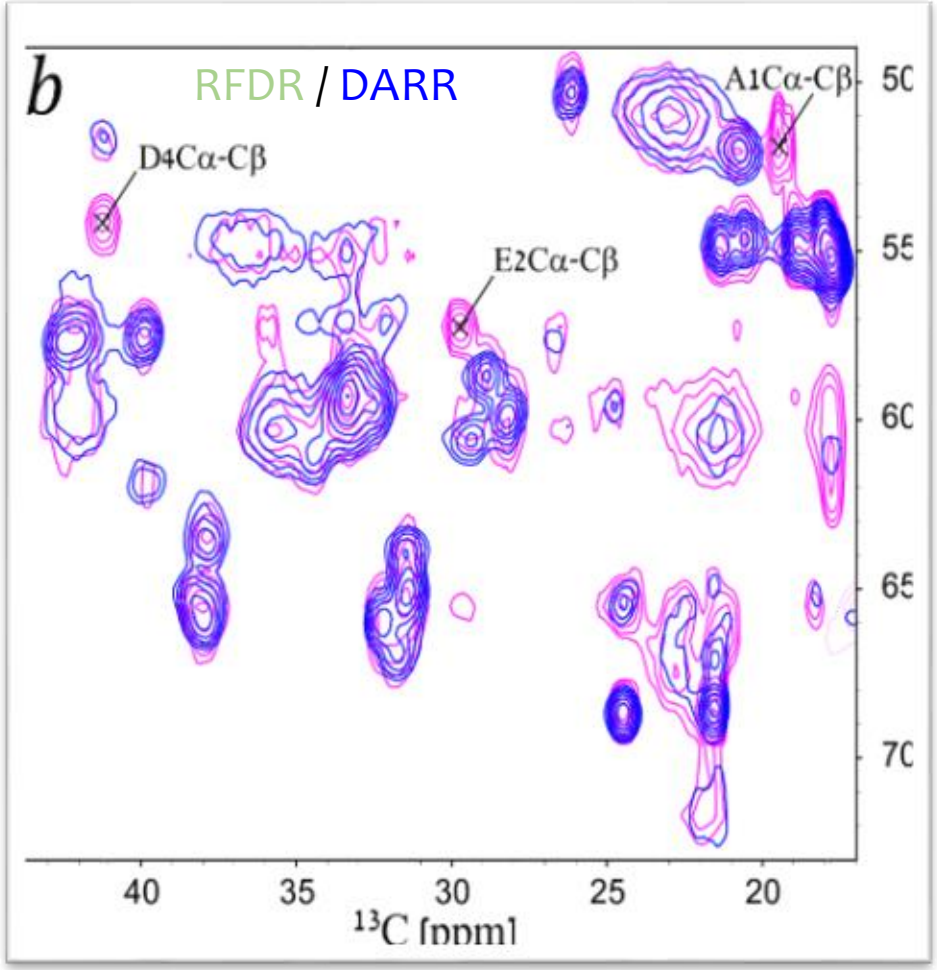

2D-REDOR-Dephased DARR and RFDR

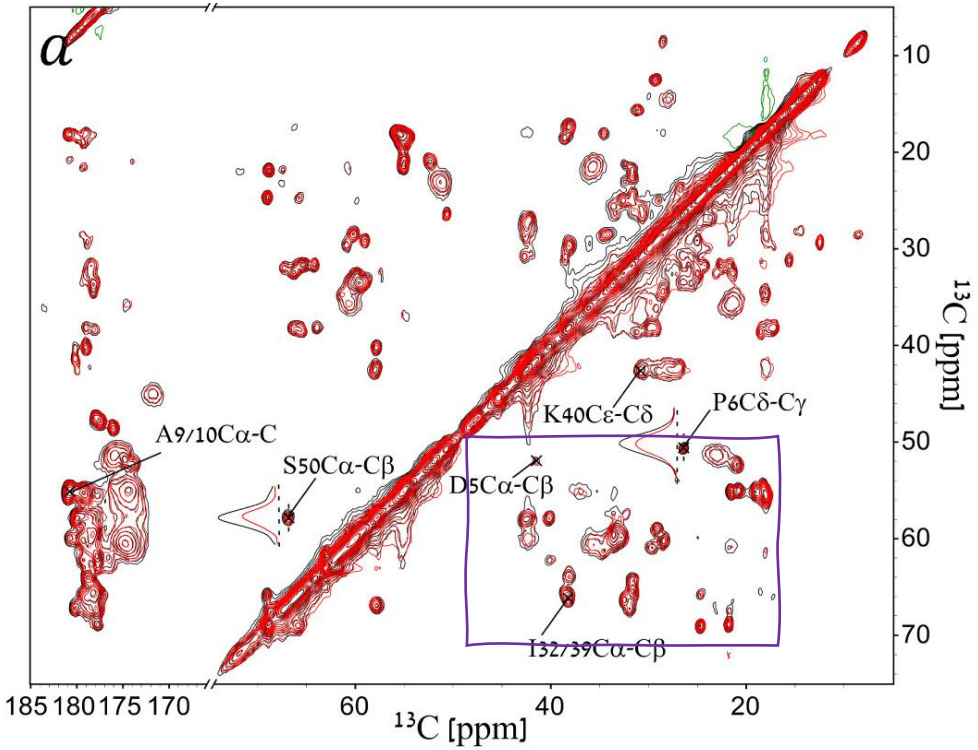

DARR-REDOR
S and So
429µs dephasing

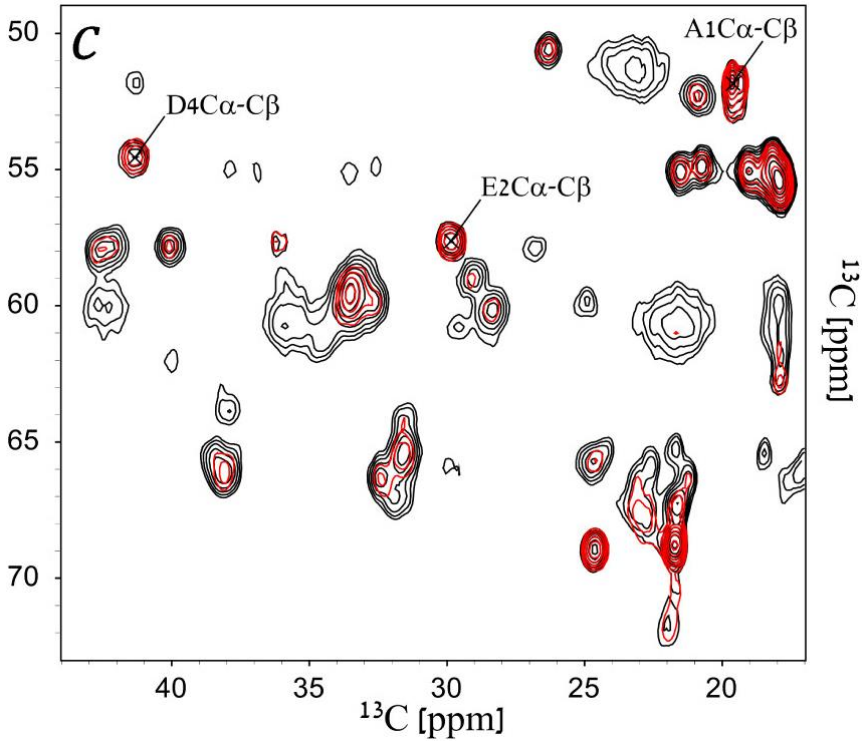

DARR-RFDR
S and So
1143µs dephasing

Example of phage REDOR data

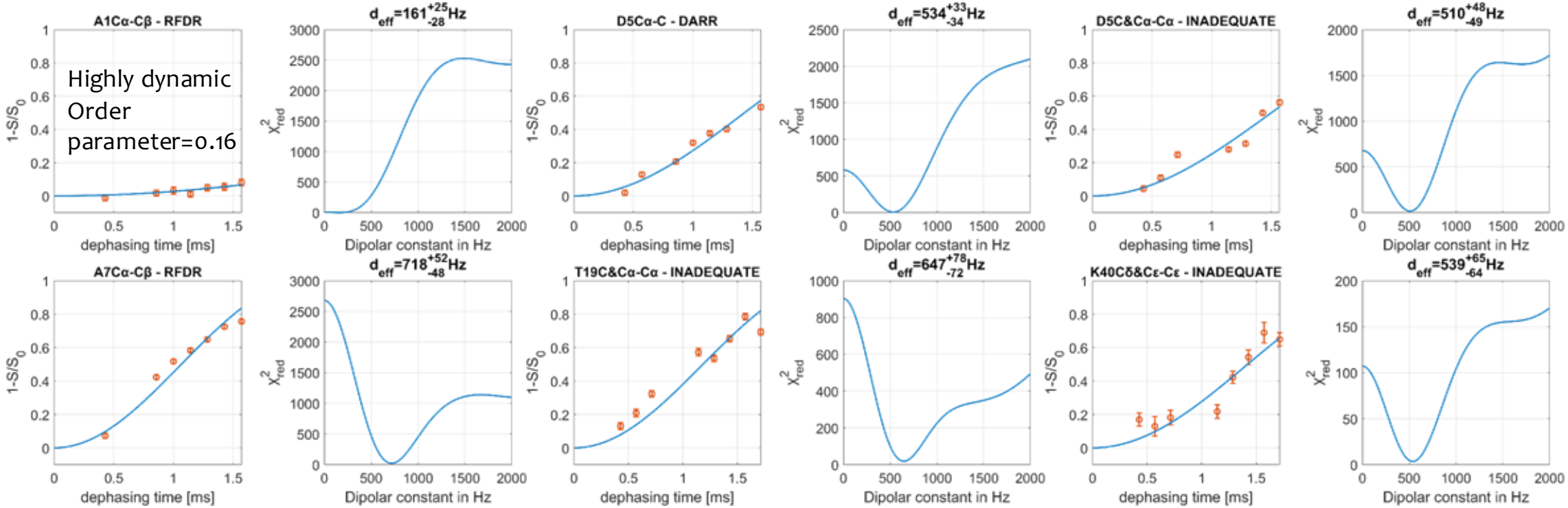

Results

Sequence:
AEGDDPAKAAFDSL
QASATEMIGYAWAM
VVVIVGATIGIKLFKKF
TSKAS

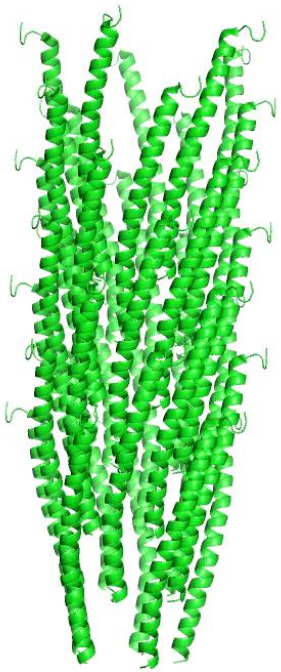

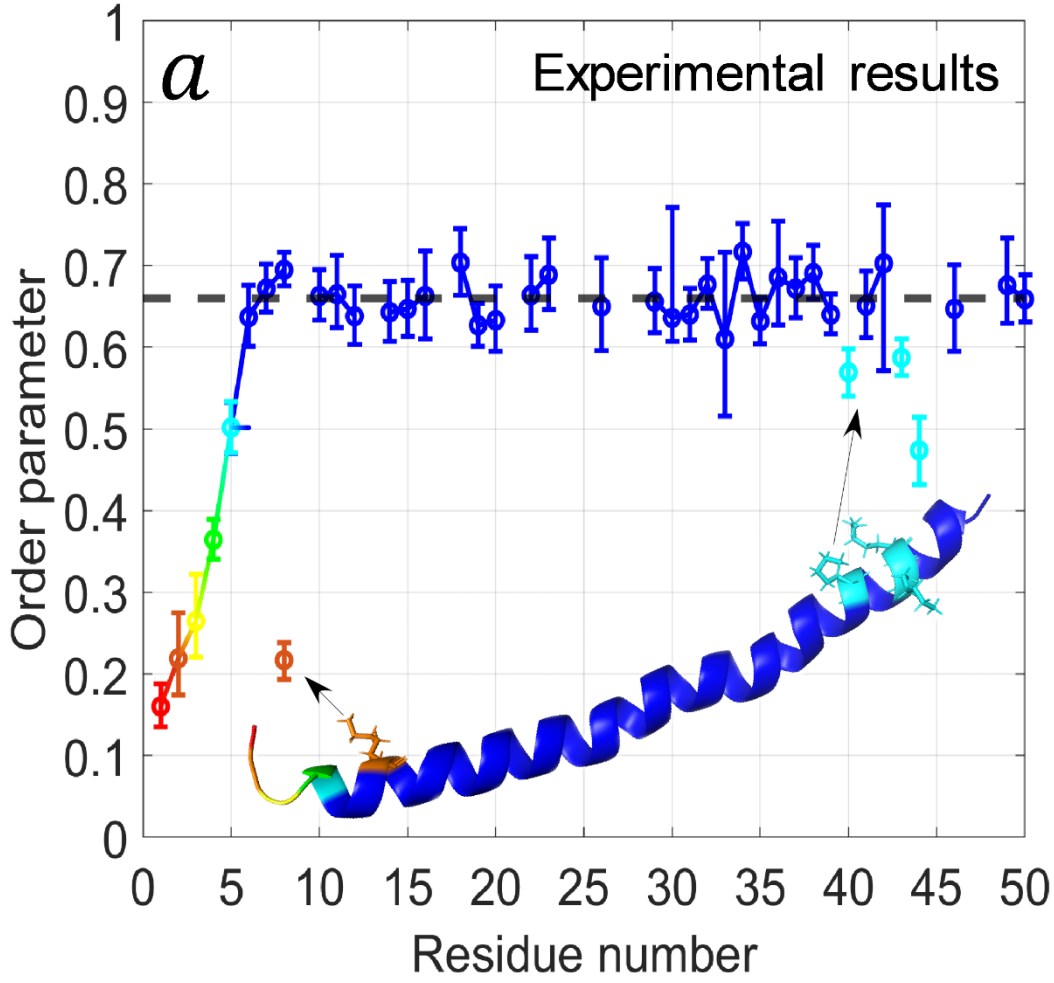

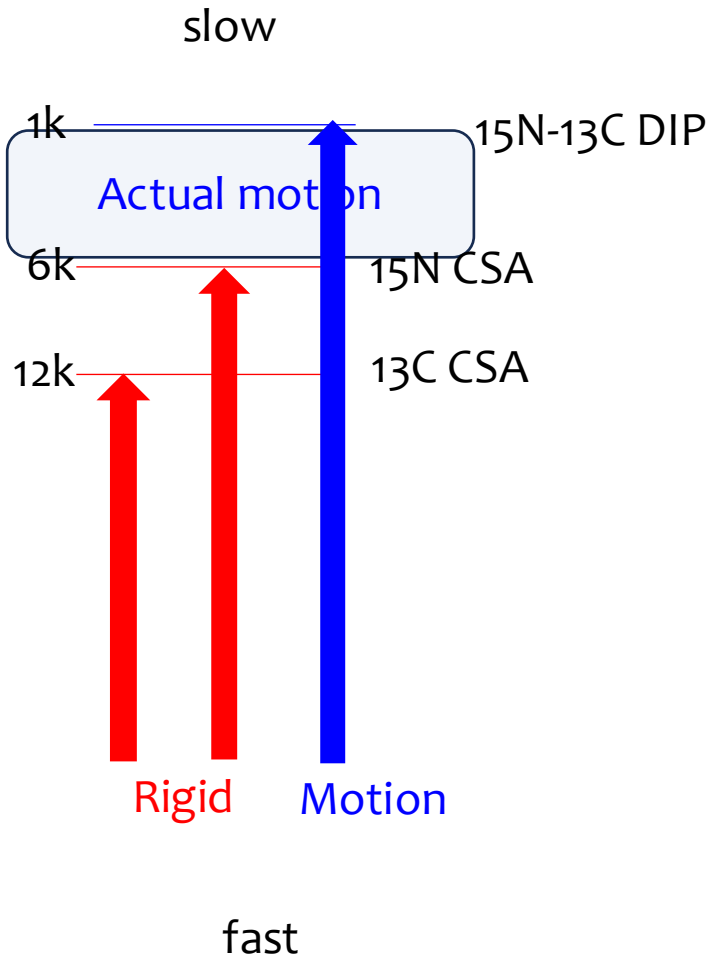

^{1}H-detected NH order parameters - ubiquitin

Time scale ~ 10 kHz

Requires fast MAS or deuteration

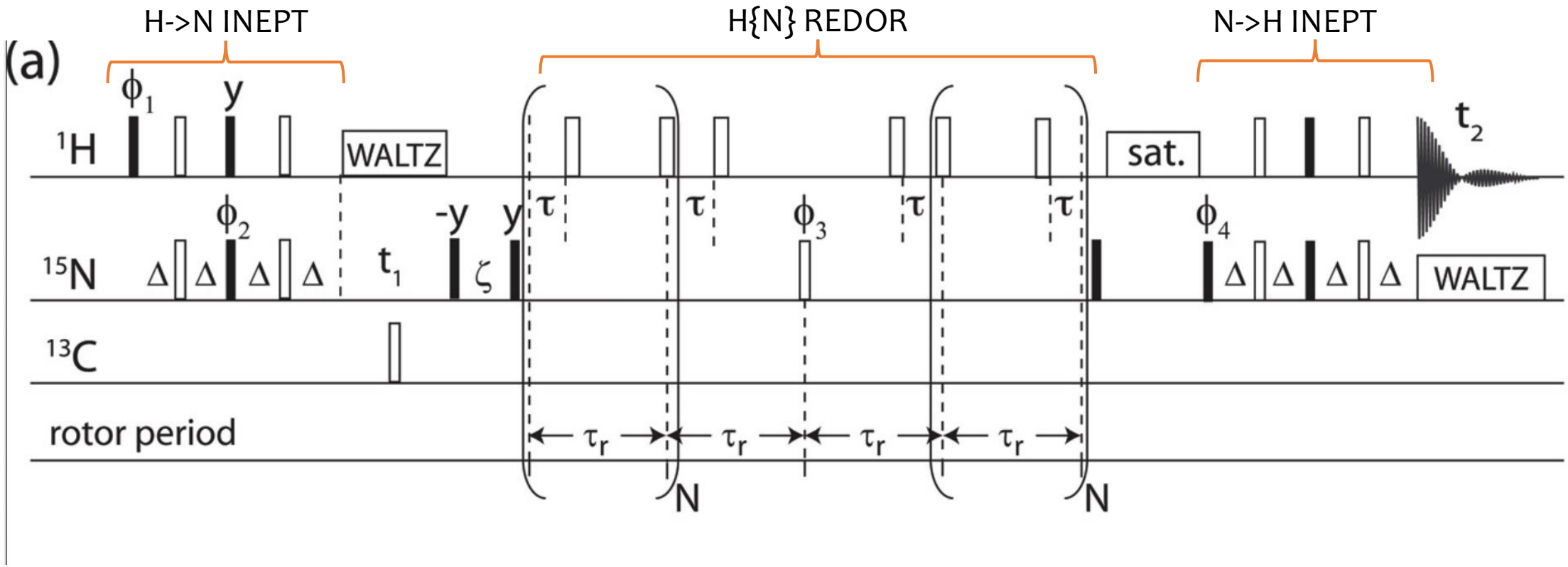

Quantitative Analysis of Protein Backbone Dynamics in Microcrystalline Ubiquitin by Solid-State NMR Spectroscopy

Schanda, Meier, Ernst,
J. Am. Chem. Soc. 2010, 132, 45, 15957–15967

^{1}H-detected NH order parameters - ubiquitin

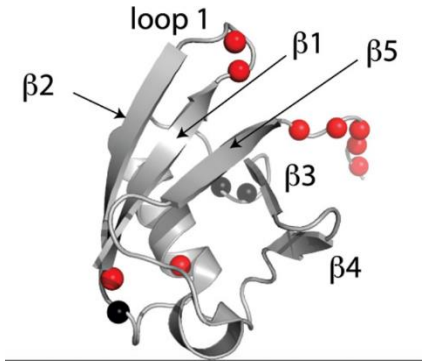

1H-15N plane –
30%-exchanged ^{2}H/^{13}C/^{15}N-labeled Ubiquitin
B=20T; MAS=45 kHz

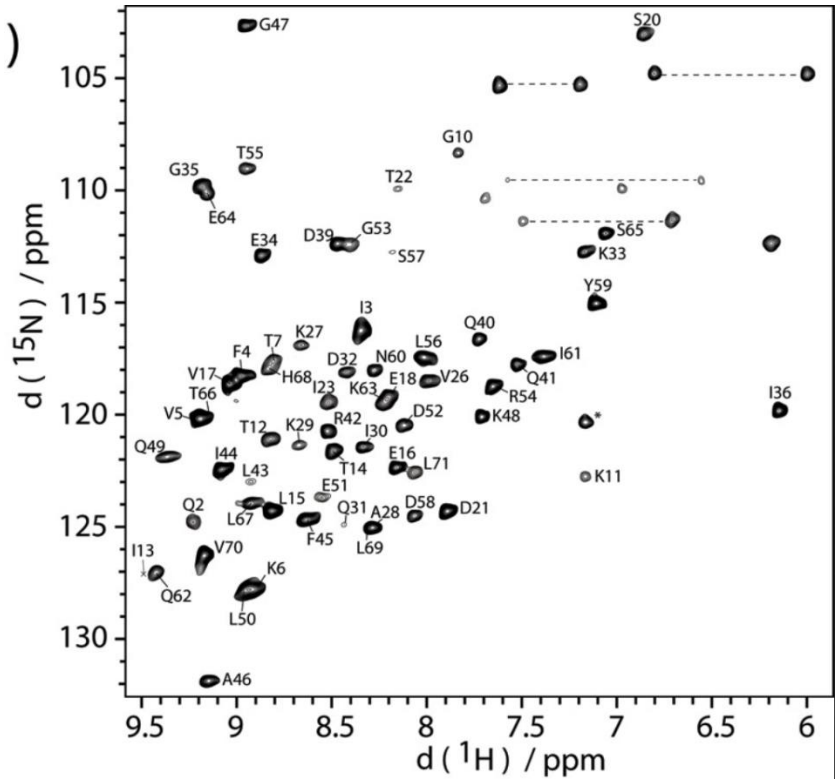

Order parameters
Model: diffusion in a cone

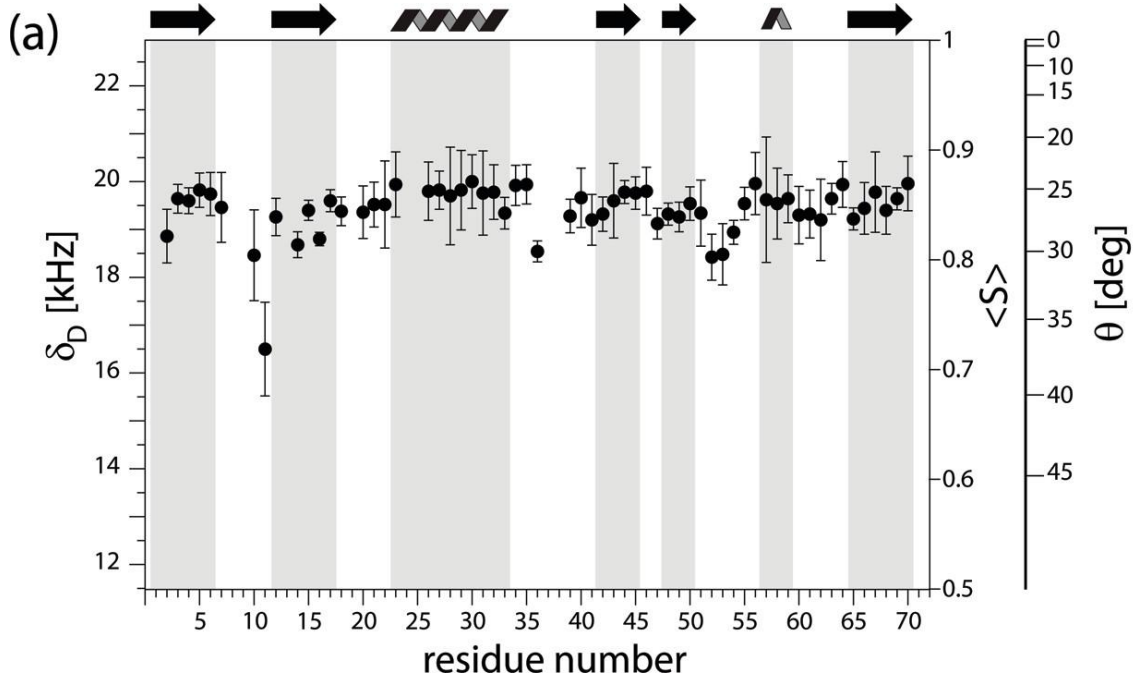

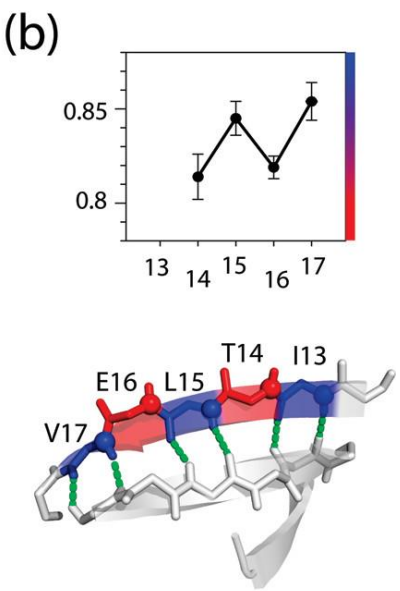

CODEX – detection of slow motions

Centerband-Only Detection of Exchange: Efficient Analysis of Dynamics in Solids by NMR

E. R. deAzevedo, W.-G. Hu, T. J. Bonagamba, and K. Schmidt-Rohr

J. Am. Chem. Soc. 1999, 121, 8411-8412

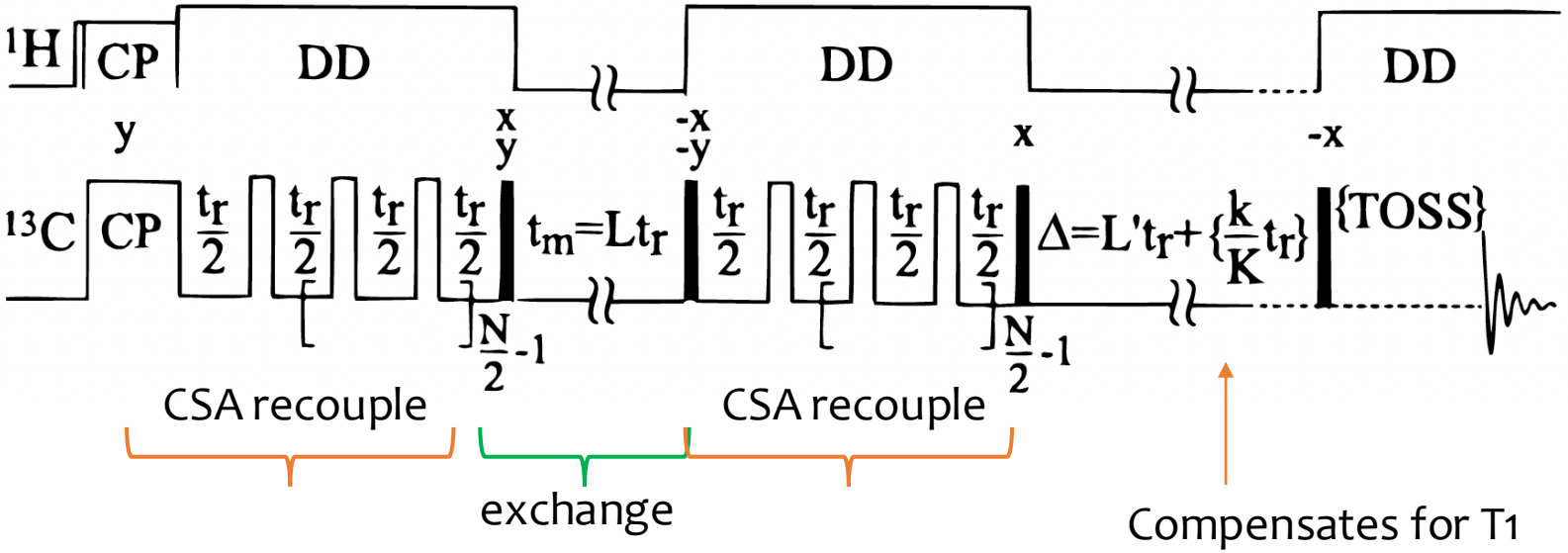

CODEX –

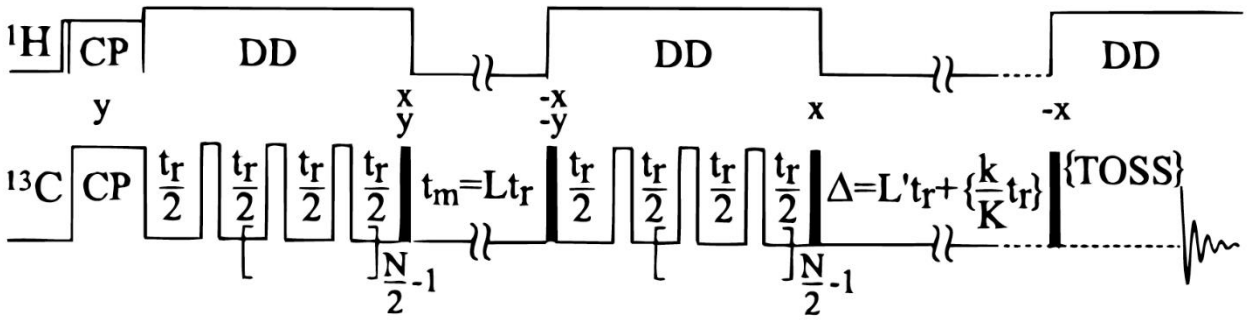

CODEX S

CODEX So reference

Difference: No motion

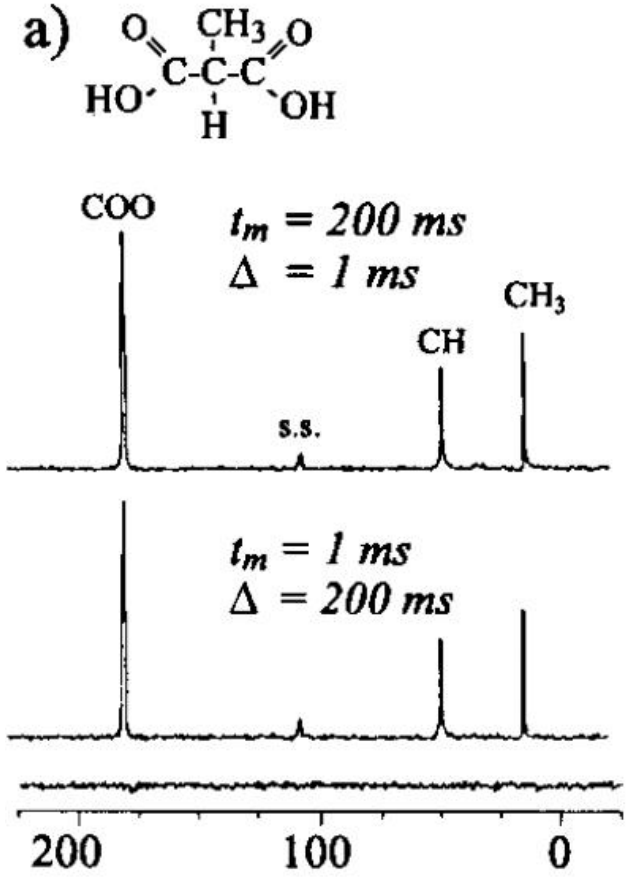

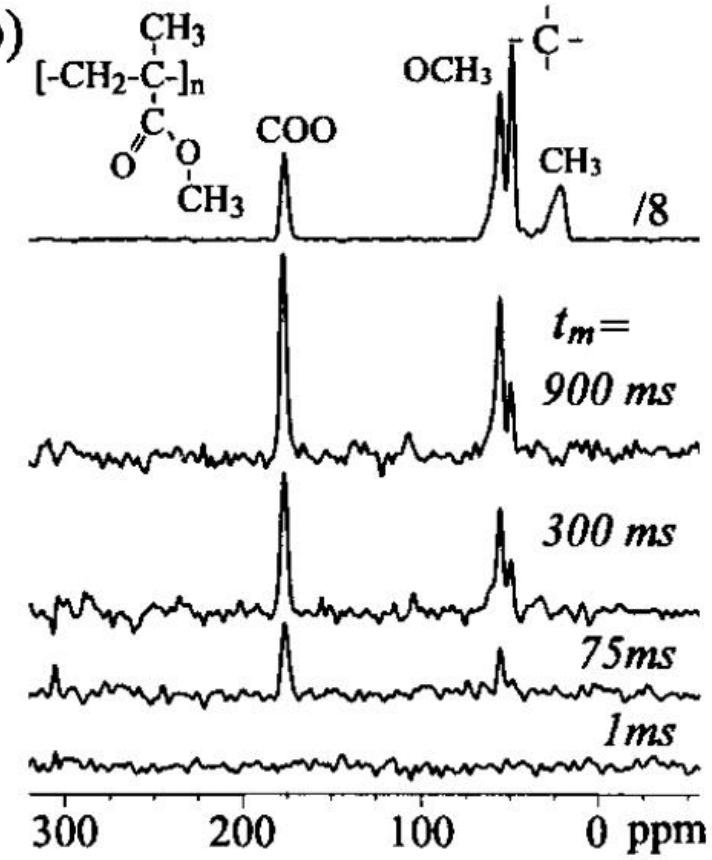

CODEX So reference

tm

CODEX in proteins

- 13C-13C spin diffusion is faster than slow motions– cannot be compensated.
- Solutions:
  - Fast MAS
  - 15N-15N CODEX
  - Sparse labeling

15N CODEX in ubiquitin

Determination of slow motions in extensively isotopically labeled proteins by magic-angle-spinning ^{13}C-detected ^{15}N exchange NMR

E.R. deAzevedo [1], S.B. Kennedy, M. Hong *

Chemical Physics Letters 321 (2000) 43–48

Also: Hong et co., Macromolecules 2001, 34, 25, 8675–8685

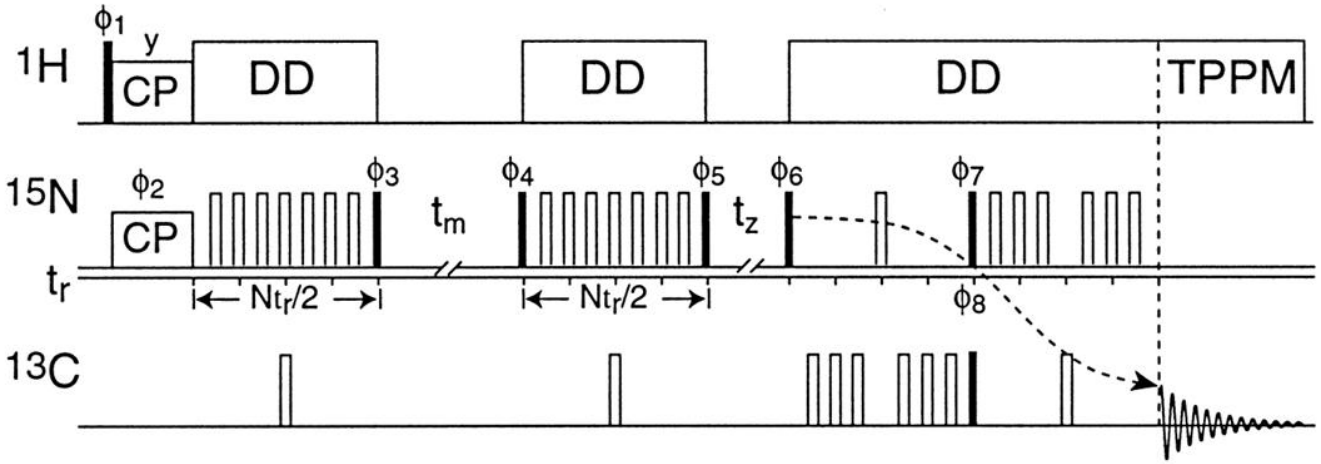

Ubiquitin – no slow motions

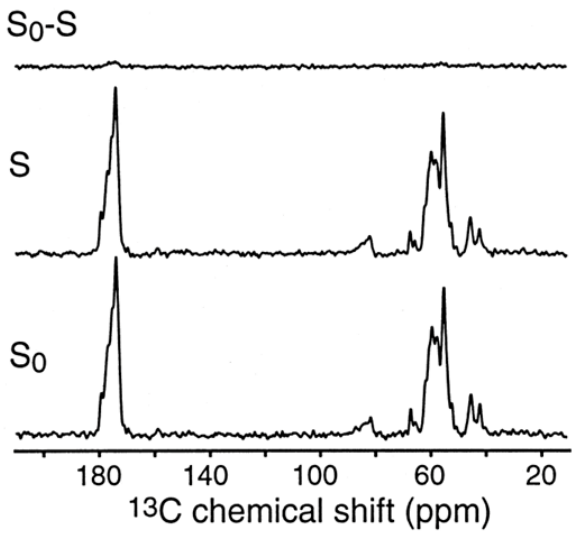

triblock – N-term motions

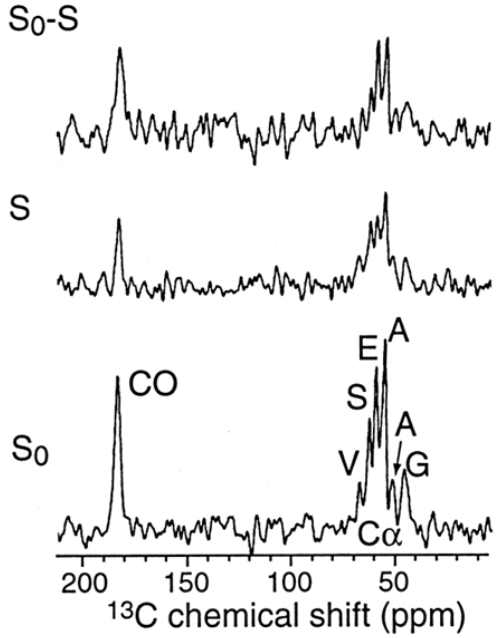

15N dipolar CODEX

Direct Observation of Millisecond to Second Motions in Proteins by Dipolar CODEX NMR Spectroscopy

Alexey Krushelnitsky[*†], Eduardo deAzevedo[‡], Rasmus Linser[§], Bernd Reif[§], Kay Saalwächter[*∥], and Detlef Reichert[*∥]

J. Am. Chem. Soc. 2009, 131, 34, 12097–12099

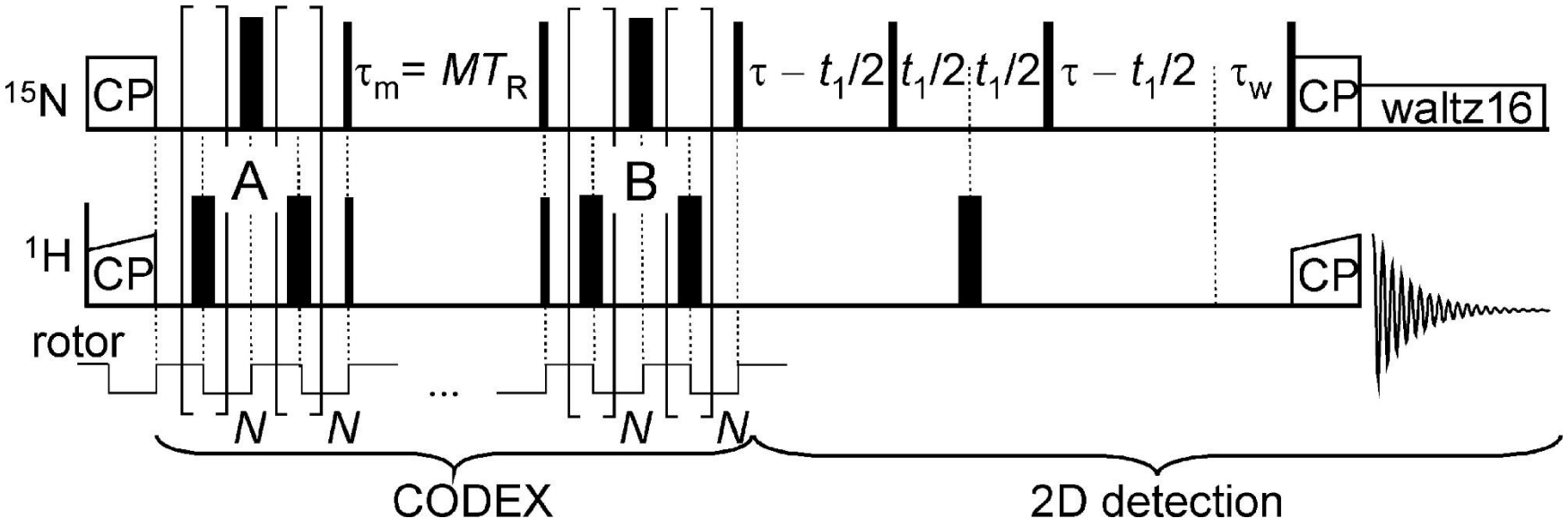

15N dipolar CODEX – results (ubiquitin)

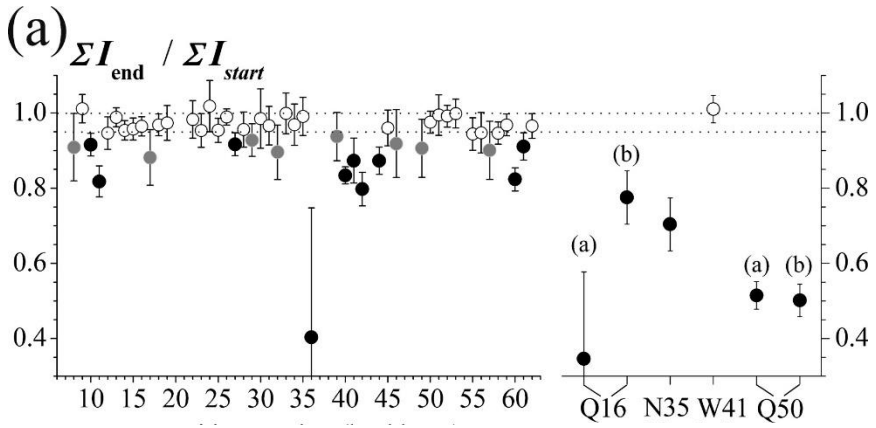

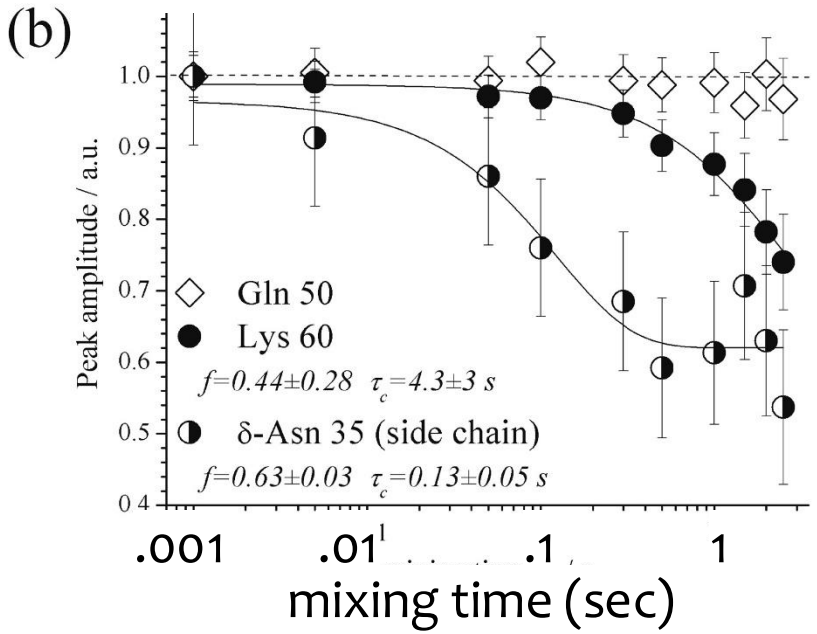

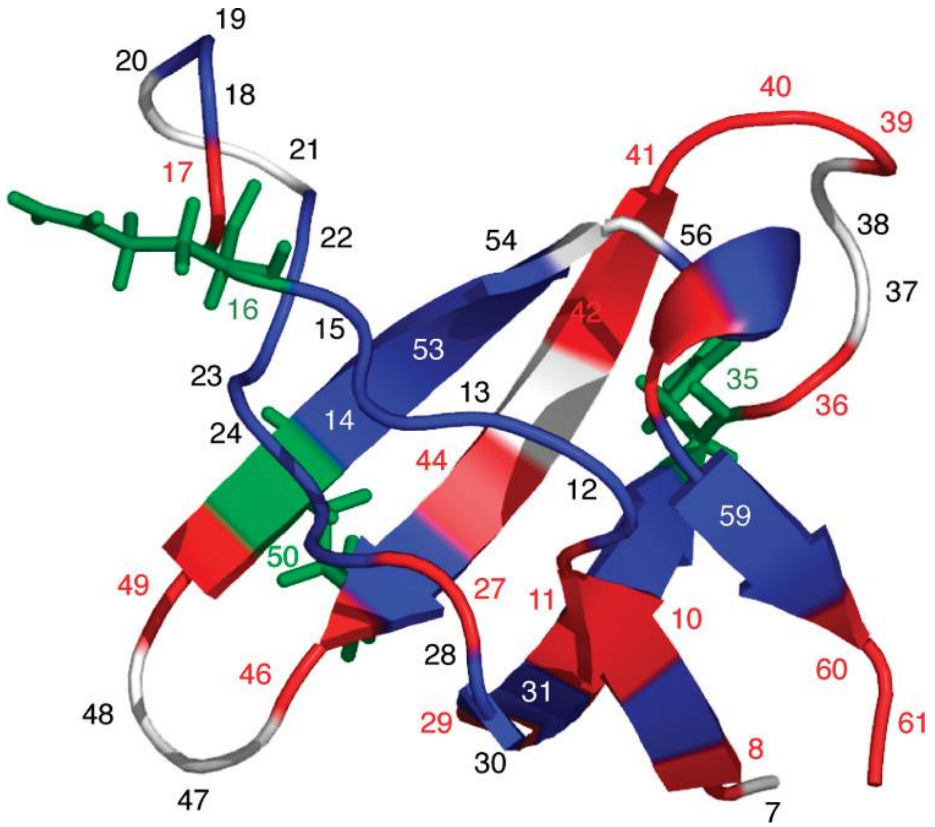

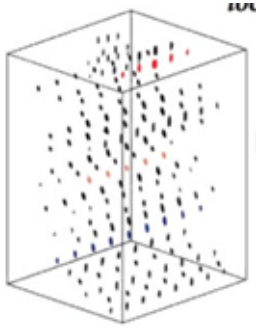

2H MAS NMR lineshapes

Characterization of dynamic processes using deuterium in uniformly 2H, 13C,15N enriched peptides by MAS solid-state NMR
Maggy Hologne, Zhongjing Chen, Bernd Reif
J Magn Reson 179, 20, 2006

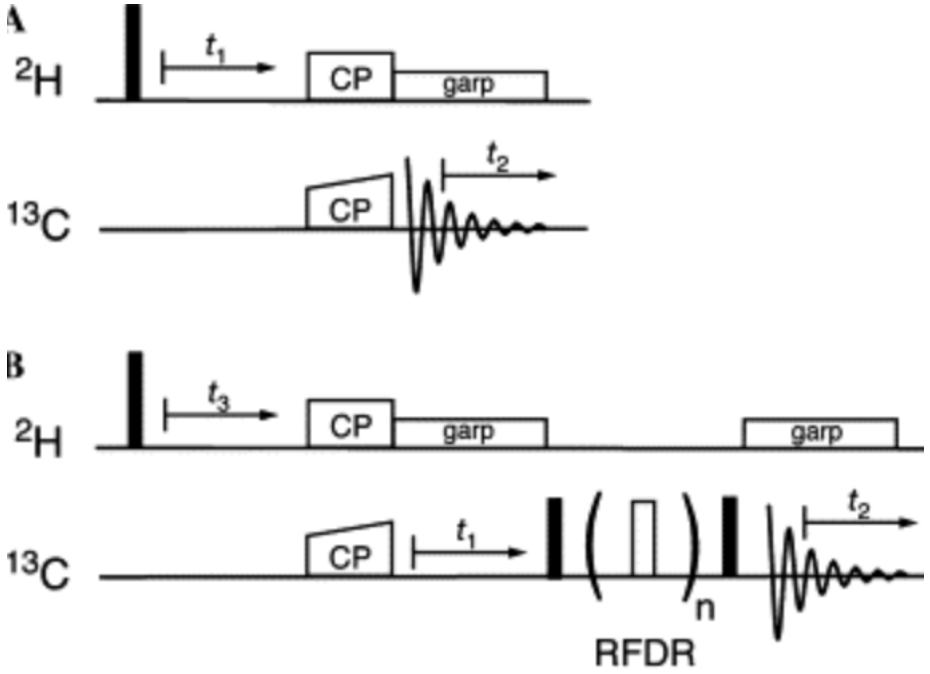

Site-Specific Internal Motions in GB1 Protein Microcrystals Revealed by 3D 2H–13C–13C Solid-State NMR Spectroscopy
Xiangyan Shi, Chad M Rienstra
JACS 138, 4105, 2016

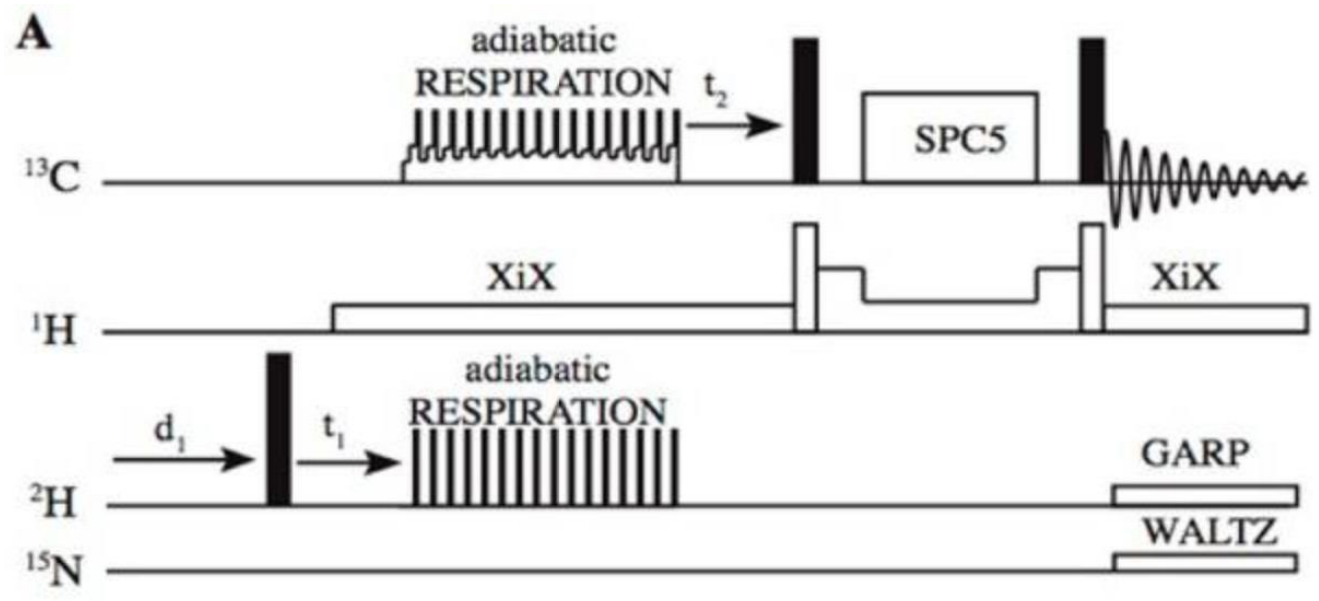

2H MAS NMR lineshapes

Sample: N-acetyl Valine

Characterization of dynamic processes using deuterium in uniformly 2H, 13C,15N enriched peptides by MAS solid-state NMR

Maggy Hologne, Zhongjing Chen, Bernd Reif

J Magn Reson 179, 20, 2006

Typical Cq ~ 170 kHz (6X10^{-6} sec)

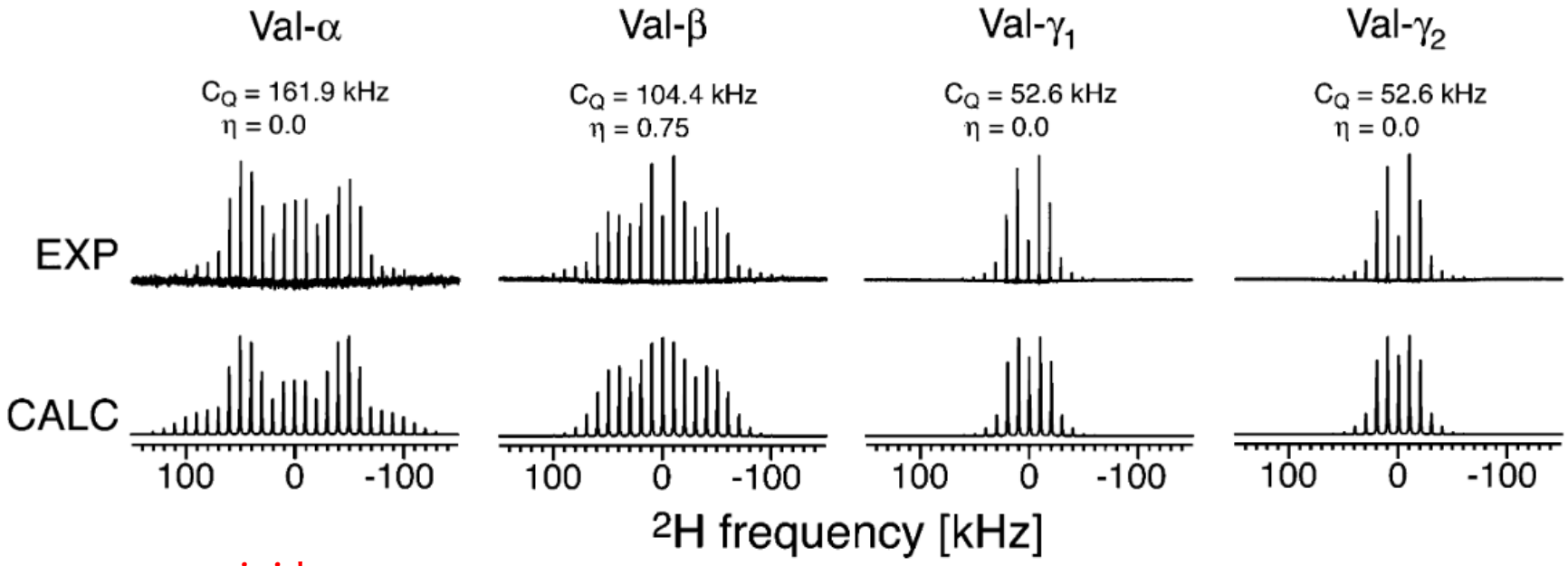

rigid

Motion in or on a cone 42 or 29 deg

Methyl group 3-site hop

Methyl group 3-site hop

2H MAS NMR lineshapes

Sample: protein GB1

Site-Specific Internal Motions in GB1 Protein Microcrystals Revealed by 3D 2H–13C–13C Solid-State NMR Spectroscopy
Xiangyan Shi, Chad M Rienstra
JACS 138, 4105, 2016

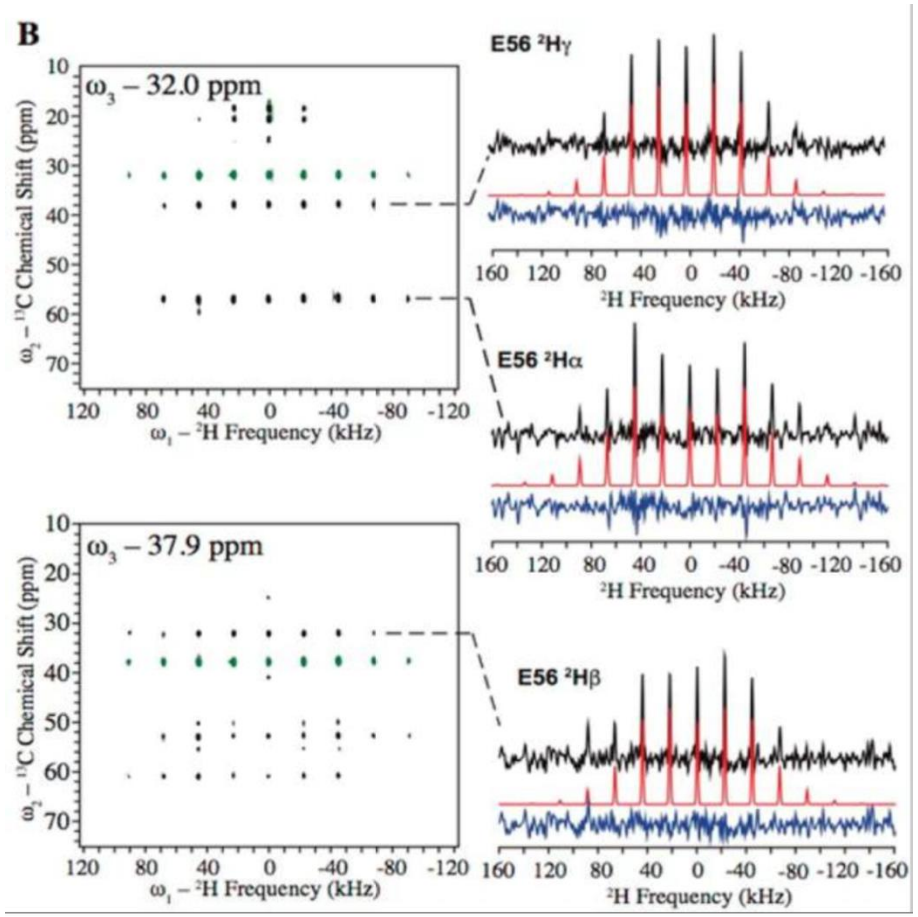

2D 2H-13C planes of 3D 2H-13C-13C

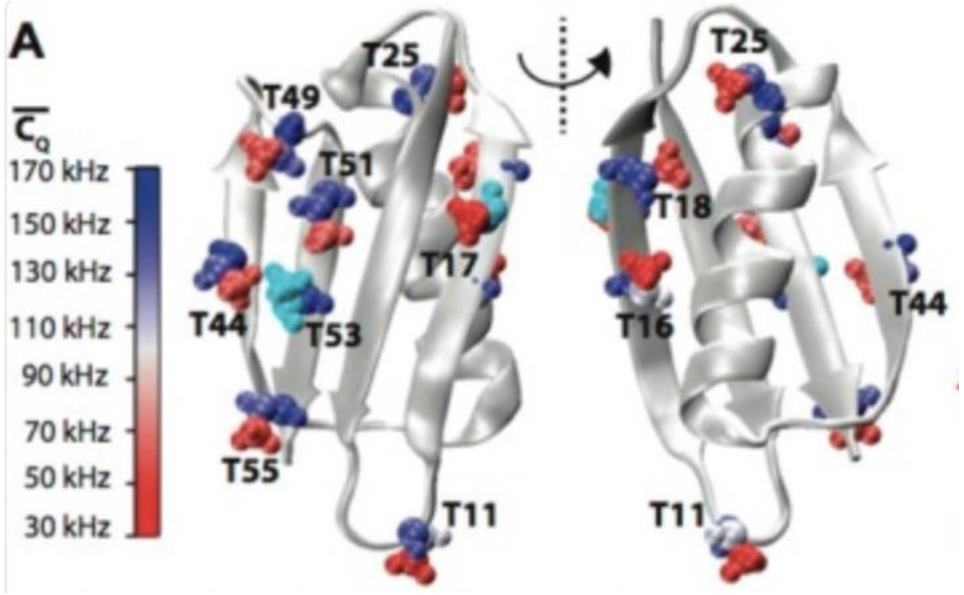

Variability in Thr dynamics, red are CH3 groups

2H lineshape sensitivie to motional model

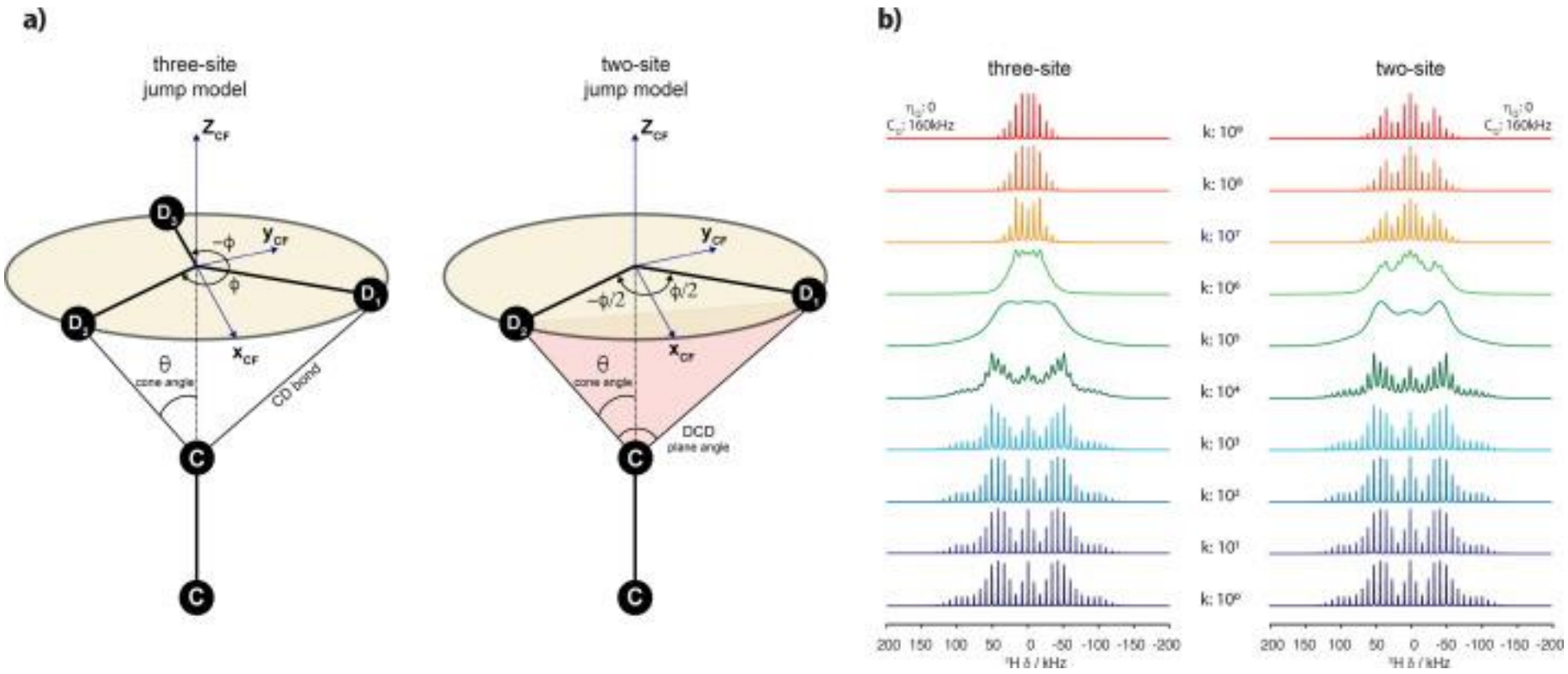

Akbey, JMR 327, 106974, 2021

2H lineshape sensitivie to temperature

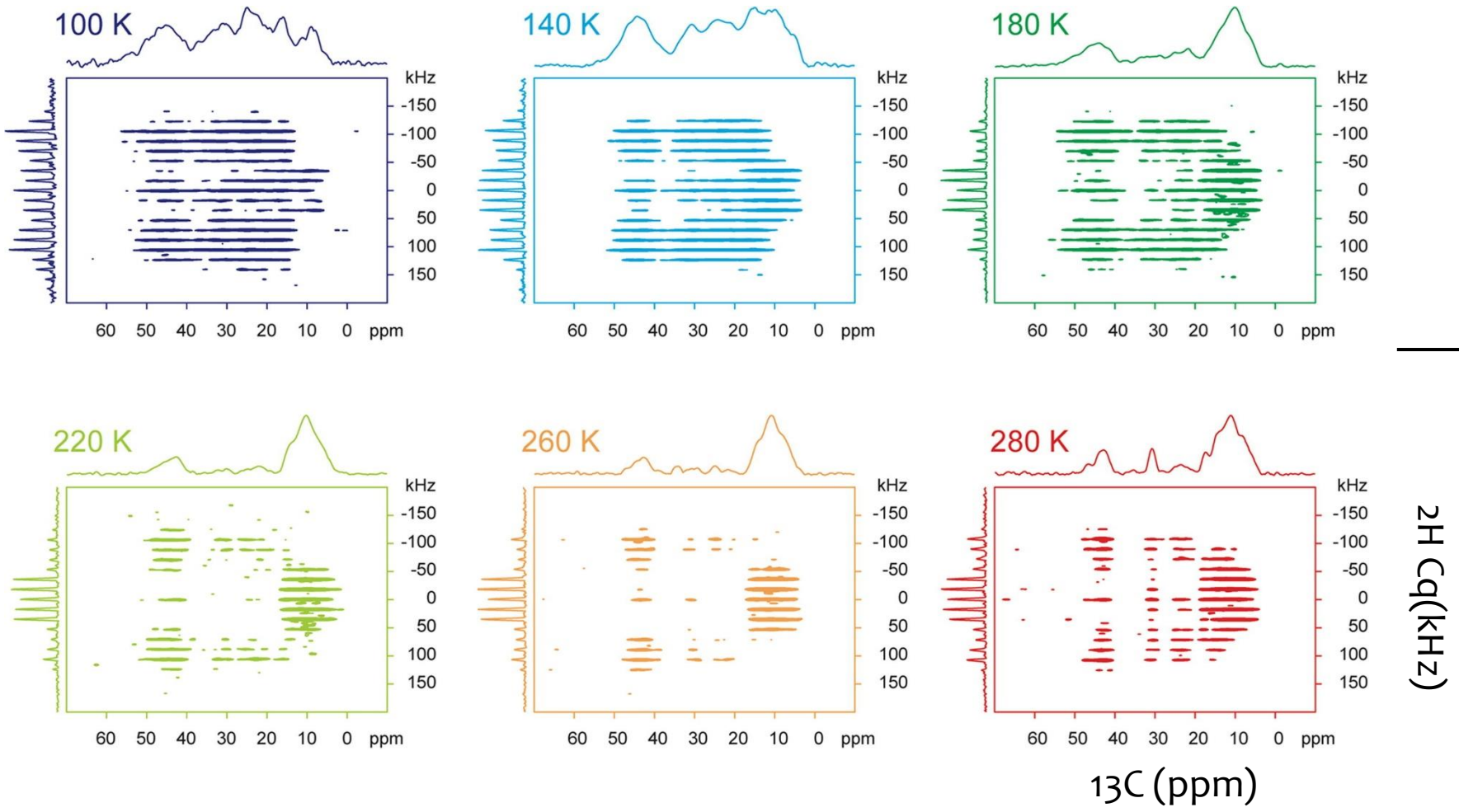

Can calculated activation energies from Ahrenius plots

Akbey, JMR 327, 106974, 2021

Summary

Anisotropic interactions are probes for dynamics in the solid state

CSA recoupling techniques,
6-12 kHz

Dipolar recoupling techniques,
1-20 kHz

CODEX – slow motions, 1 Hz

Motional models can be differentiated

Also look at fast motions via relaxation times